REVERSIBLE MOLECULAR ENCAPSULATION IN SELF-ASSEMBLED AND MECHANICALLY LOCKED CONTAINERS WITH POLAR INTERIOR

Monica Espelt Ripoll

Dipòsit Legal: T 1103-2014

UNIVERSITAT ROVIRA I VIRGILI
REVERSIBLE MOLECULAR ENCAPSULATION IN SELF-ASSEMBLED AND MECHANICALLY LOCKED CONTAINERS WITH POLAR INTERIOR
Monica Espelt Ripoll
DL: T 1103-2014

UNIVERSITAT ROVIRA I VIRGILI
REVERSIBLE MOLECULAR ENCAPSULATION IN SELF-ASSEMBLED AND MECHANICALLY LOCKED CONTAINERS WITH POLAR INTERIOR
Monica Espelt Ripoll
DL: T 1103-2014

UNIVERSITAT ROVIRA I VIRGILI
REVERSIBLE MOLECULAR ENCAPSULATION IN SELF-ASSEMBLED AND MECHANICALLY LOCKED CONTAINERS WITH POLAR INTERIOR
Monica Espelt Ripoll
DL: T 1103-2014

UNIVERSITAT ROVIRA I VIRGILI
REVERSIBLE MOLECULAR ENCAPSULATION IN SELF-ASSEMBLED AND MECHANICALLY LOCKED CONTAINERS WITH POLAR INTERIOR
Monica Espelt Ripoll
DL: T 1103-2014

PhD Thesis

REVERSIBLE MOLECULAR ENCAPSULATION IN SELF-ASSEMBLED AND MECHANICALLY LOCKED CONTAINERS WITH POLAR INTERIOR

Mónica Espelt Ripoll

Supervised by Prof. Pablo Ballester Balaguer

Tarragona, July 2013

UNIVERSITAT ROVIRA I VIRGILI

UNIVERSITAT ROVIRA I VIRGILI
REVERSIBLE MOLECULAR ENCAPSULATION IN SELF-ASSEMBLED AND MECHANICALLY LOCKED CONTAINERS WITH POLAR INTERIOR
Monica Espelt Ripoll
DL: T 1103-2014

UNIVERSITAT ROVIRA I VIRGILI
REVERSIBLE MOLECULAR ENCAPSULATION IN SELF-ASSEMBLED AND MECHANICALLY LOCKED CONTAINERS WITH POLAR INTERIOR
Monica Espelt Ripoll
DL: T 1103-2014

UNIVERSITAT ROVIRA I VIRGILI

DEPARTAMENT DE QUIMICA ANALITICA I QUIMICA ORGANICA

C/ Marcel.lí Domingo s/n
Campus Sescelades
43007 Tarragona
Tel. 34 977 55 97 69
Fax 34 977 55 84 46
e-mail: secqaqo@urv.net

Prof. Pablo Ballester Balaguer, Group Leader of the Institute of Chemical Research of Catalonia (ICIQ) and Research Professor of the Catalan Institution for Research and Advanced Studies (ICREA),

CERTIFIES that the present work entitled "Reversible Molecular Encapsulation in Self-Assembled and Mechanically Locked Containers with Polar Interior" that Mónica Espelt Ripoll presents to obtain the PhD degree in Chemistry, has been carried out under his supervision in his research group at ICIQ and fulfills all the requirements to be awarded with the Doctor Mention.

Tarragona, July 2013

Prof. Pablo Ballester Balaguer

UNIVERSITAT ROVIRA I VIRGILI
REVERSIBLE MOLECULAR ENCAPSULATION IN SELF-ASSEMBLED AND MECHANICALLY LOCKED CONTAINERS WITH POLAR INTERIOR
Monica Espelt Ripoll
DL: T 1103-2014

UNIVERSITAT ROVIRA I VIRGILI
REVERSIBLE MOLECULAR ENCAPSULATION IN SELF-ASSEMBLED AND MECHANICALLY LOCKED CONTAINERS WITH POLAR INTERIOR
Monica Espelt Ripoll
DL: T 1103-2014

ACKNOWLEDGEMENTS

Tota aventura, vivència o experiència arriba a la seua fi algun dia. I passa el mateix amb una tesi doctoral. Després de quatre anys molt intensos, per fi veig el fruit del meu esforç recompensat amb aquesta tesi doctoral que teniu a les vostres mans. Els quatre anys passats a l'ICIQ han sigut un temps molt profitós en el que he crescut com a persona i he aprés molt com a química. Encara que no sempre ha estat fàcil, penso que finalment n'he eixit reforçada.

El meu especial agraïment li dedico al meu director de tesi, Pau Ballester. A ell li dec l'oportunitat que em va presentar el setembre de l'any 2009 de començar una tesi doctoral en el camp de la Química Orgànica Supramolecular, un camp d'investigació no massa conegut quan un/a està a la facultat, que m'ha fascinat durant aquests anys. Moltes gràcies per compartir el teu saber químic amb mi i per formar-me com a investigadora.

Molts han sigut els companys amb qui he compartit laboratori durant aquests anys. El primer a qui vull recordar és **Marcos Chas**. Ell em va obrir el camí, em va ensenyar el seu saber fer i va fer que la transició entre la química de la llicenciatura i el treball del dia a dia al laboratori fóra més portadora. A ell li dec els meus primers passos químics i moltes discussions químiques fructíferes. Moitas grazas, *galegiño*!! A **Virginia Valderrey**, mi compañera de fatigas. Hemos hecho todo a la vez desde que llegaste a Tarragona y hasta hemos acabado viviendo juntas. Lo más admirable es que hayamos sobrevivido. ¡Dos doctorandas de último año juntas son como dos bombas a punto de estallar! Como no, no me podía olvidar de **Moira Ciardi**, nuestra auténtica italiana, con la que tan buenos momentos de risas, de cenas, de piscina, etc. he compartido. Aún nos quedan muchas cosas por vivir y mucho mundo que ver. *Non ti preoccupare!* El meu més sincer agraïment a **Gemma Aragay**, una de les persones més treballadores i efectives/eficients que conec. Moltes gràcies per llegir i rellegir la tesi les vegades que ha sigut necessari. I gràcies també per la teua continua presència i recolzament sempre que ha sigut necessari. A todos los miembros actuales del grupo como **Nelson Giménez**

(l'altre valencianet), **Albano Galán** (mi compañero en el sufrir de los catenanos), **Dani Hernández** (quién nos enseñó los mil tipos distintos de café), **Ramón Romero** (¿para dónde cuándo ese pulpo?), **Louis Adriaenssens**, **Sasa Korom**, **Frank Arroyave**… y a los anteriores como **Eddy Martin** (the party animal), **Laura Hernández**, **Bego Verdejo**, **Guzmán Gil**, **Muñiz**, **Inma Pintre**, **Carmela Molinaro**, **Carol Estarellas**, y los Summer Fellows, visitantes de verano y visitantes en general. De todos y cada uno de ellos he aprendido algo. Y a Beatriz Martin, sempre disposta a ajudar en tot allò que ha fet falta. A special mention goes to **Heather Kitto** who had read one chapter of the thesis manuscript and corrected my English. Y a toda la gente de las unidades de soporte a la investigación por hacer nuestro trabajo más sencillo. Thanks to all!!

També voldria agrair alguns dels meus professors de llicenciatura de la Universitat Jaume I que em van descobrir, d'una o altra manera, el món de la investigació i també em van animar a iniciar una tesi doctoral. Sense ells/elles, mai hagués seguit aquest camí.

Finalment, el meu agraïment més profund és per a la meua família, la meua parella i els amics i amigues que, malgrat la distància geogràfica, han estat sempre al meu costat. Moltíssimes gràcies pel vostre suport incondicional i els ànims que m'heu transmés amb llargues converses telefòniques i per correu electrònic, que m'han ajudat a seguir endavant. Sense la vostra força, mai hagués arribat tant lluny.

El treball desenvolupat en aquesta tesi doctoral ha estat finançat econòmicament per l'Institut Català d'Investigació Química (beca 13/09), el Ministerio de Economía y Competitividad (contrato FPU, AP2010/1943), la Universitat Rovira i Virgili i la Institució Catalana de Recerca i Estudis Avançats, ICREA.

UNIVERSITAT ROVIRA I VIRGILI
REVERSIBLE MOLECULAR ENCAPSULATION IN SELF-ASSEMBLED AND MECHANICALLY LOCKED CONTAINERS WITH POLAR INTERIOR
Monica Espelt Ripoll
DL: T 1103-2014

A les persones que sempre han cregut en mi,

UNIVERSITAT ROVIRA I VIRGILI
REVERSIBLE MOLECULAR ENCAPSULATION IN SELF-ASSEMBLED AND MECHANICALLY LOCKED CONTAINERS WITH POLAR INTERIOR
Monica Espelt Ripoll
DL: T 1103-2014

TABLE OF CONTENTS

CHAPTER 5. Synthesis and Binding Studies of a Calix[4]pyrrole-Calix[4]pyrrole Bis[2]catenane Molecular Capsule.

UNIVERSITAT ROVIRA I VIRGILI
REVERSIBLE MOLECULAR ENCAPSULATION IN SELF-ASSEMBLED AND MECHANICALLY LOCKED CONTAINERS WITH POLAR INTERIOR
Monica Espelt Ripoll
DL: T 1103-2014

UNIVERSITAT ROVIRA I VIRGILI
REVERSIBLE MOLECULAR ENCAPSULATION IN SELF-ASSEMBLED AND MECHANICALLY LOCKED CONTAINERS WITH POLAR INTERIOR
Monica Espelt Ripoll
DL: T 1103-2014

CHAPTER 1

INTRODUCTION

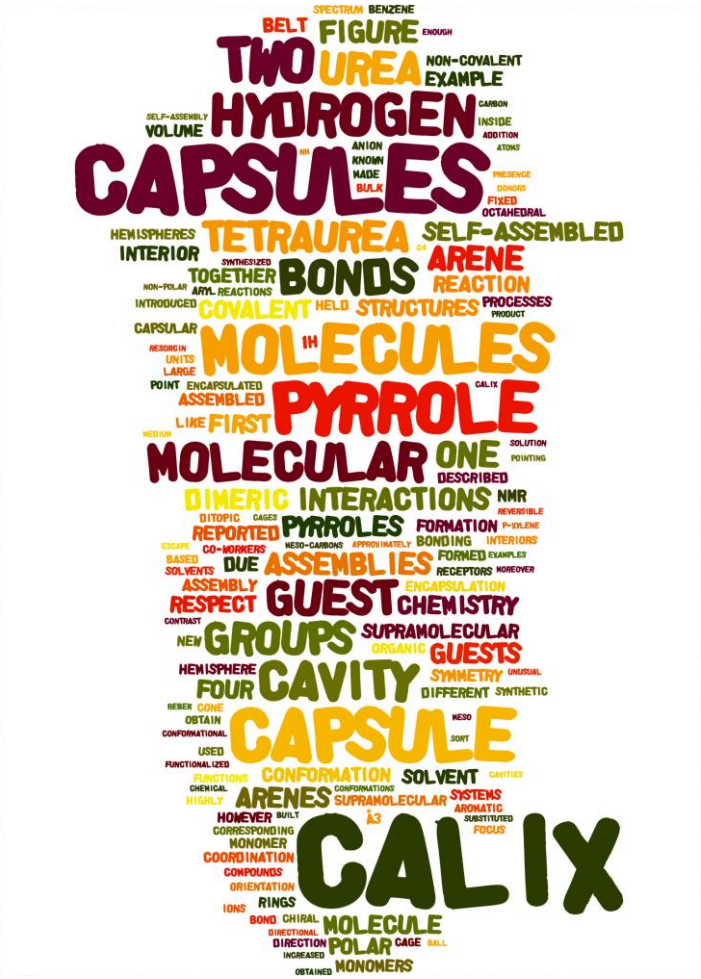

UNIVERSITAT ROVIRA I VIRGILI
REVERSIBLE MOLECULAR ENCAPSULATION IN SELF-ASSEMBLED AND MECHANICALLY LOCKED CONTAINERS WITH POLAR INTERIOR
Monica Espelt Ripoll
DL: T 1103-2014

1.1.General Introduction

In this chapter the concept of Supramolecular Chemistry is introduced, a relatively young field of chemistry research, parallel to the traditional covalent chemistry. The importance of the microenvironments created by different types of cavities is highlighted. Several examples of capsular assemblies, held by covalent or non-covalent interactions are described. Even though our interest lies on the non-covalent assemblies, it is important to mention covalently-built capsules as their authors were pioneers and for the first time it was said that cavities comprise "a new phase of matter".[1]

Among the many supramolecular systems reported in literature, we select and describe several examples of assemblies formed by coordination and hydrogen bonds. We focus our attention on capsular assemblies made of two hemispheres which are held together by different arrays of hydrogen bonds. Next, we introduce the molecular capsules built from monomers bearing urea functions. The interdigitation of two monomers form capsules connected by the so-called urea belt. Subsequently, capsules with functionalized interiors are described. We are interested in the use of calix[4]pyrrole scaffolds for self-assembled capsules formation.

1.2.Supramolecular chemistry

Supramolecular chemistry was defined by Jean-Marie Lehn as the "chemistry beyond the molecule".[2,3] The aims of supramolecular chemistry are the design and construction of complex and functional chemical systems held together by intermolecular (non-covalent) forces and the study of the selective interactions between a substrate and a molecular receptor.[4]

Supramolecular chemistry is an interdisciplinary field of science in which Chemistry, Physics and Biology converge: synthetic organic chemistry to build the receptors, physical chemistry for quantifying the interactions, and biochemistry and biological processes related to the substrate binding and recognition. Supramolecular systems have

been synthesized and used for molecular recognition, selective transport processes and supramolecular catalysis among other applications.[5]

The sort of supramolecular systems we are interested in are the molecular capsules and we will focus on them in this introductory chapter.

1.3. Molecular Capsules

Molecular capsules are of increasing interest for the scientific community since they display very interesting features. The microenvironment created in their interior is able to modify the chemical properties of captured molecules.

On one hand, molecular capsules can act as *containers* which can protect and stabilize molecules or reactive intermediates, preventing its reactivity in the bulk medium.[6,7] They can deliver encapsulated molecules across membranes being involved in drug delivery processes. On the other hand, self-assembled molecular flasks were proved to operate as *reaction vessels* in different ways: accelerating the rate of reactions,[8,9] obtaining of atypical products of reactions by stabilizing unusual conformations of the guests (preorganization) and changing the regio- or stereoselectivity of reactions[10,11] or stabilizing unusual conformations and transition states, undergoing new reactivity due to the enforced proximity of two molecules.[12,13,14] They can facilitate the reaction of encapsulated molecules that otherwise would not occur. The isolation of the molecules from the bulk solution and the increased local concentration results in an acceleration of the reaction rate. They can also entrap a molecule synthesized inside the cavity allowing the starting materials to escape.[15] Furthermore, molecular containers can lead to a better understanding of the recognition phenomena that takes place in biological receptors. The chemical conversions that take place in enzymes are mimicked in these synthetic reaction confined spaces. The release of the product formed in a catalyzed reaction inside a molecular flask results a difficult task and it is the key point in the design of capsular assemblies functioning in catalysis. Sometimes the product cannot escape from the molecular flask due to the increased size respect to the starting materials,[16] better fit in the cavity and increased association constant. If this is the case the turnover of the catalysis is prevented and the reaction stops. This problem can be overcome if the

product of the reaction has a significantly smaller association constant compared to the reactants. [17]

Covalent molecular capsules

The first molecular capsules were achieved by Cram[18,19] nearly 30 years ago. These types of capsules were gathered by covalent bonds. The studies of Cram and co-workers were based on carcerands, a closed-surface and globe-shaped compounds with hollow interiors large enough to incarcerate simple compounds (**Figure 1**). They concluded that carceplexes, carcerand compounds whose interiors imprison simple molecules, were a sort of molecular cells whose interiors were a new and unique phase of matter able to stabilize unstable guests by preventing reactions with molecules of the bulk solution. The studies in the field of covalent hosts continued with cyclodextrins,[20] carcerands,[21] hemi-carcerands, [22] micelle- and vesicle-based systems and protein cages.[23]

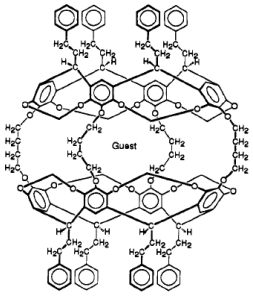

Figure 1: Example of a carceplex reported by Cram.[24] *Copyright 1993 American Chemical Society*.

Capsules assembled by non-covalent interactions

The design and preparation of a capsule in a covalent manner turns into a difficult task from the synthetic point of view. In the last decades, capsules were assembled by using weaker and reversible intermolecular interactions between complementary building blocks which provide synthetic advantages with respect to the covalent counterparts. These interactions mainly cover hydrogen bonds and metal-ligand coordination bonds.[25] Hydrogen-bonding interactions are highly directional, whereas metal-ligand bonds also high directional are generally much stronger, yielding more robust self-assembled structures. The capsules assembled by non-covalent interactions allow the guest

molecules to get in and out of the cavity to the bulk medium in a dynamic process, in striking contrast with the covalent capsules, where the molecules or ions contained were prisoner molecules that cannot escape without breaking covalent bonds (permanent guests). The reversible encapsulation processes enables the exchange of constituents, a new feature respect to the covalent capsules.

Coordinative bonds offer a diversity of bond strengths and geometries due to the variety of potential metal ions, ligands, and coordination geometries. Several examples of coordination cages have been described by Fujita. One of the approaches used to obtain these assemblies was the so-called "*molecular paneling*". This is a highly efficient approach for building large 3D structures and it consists of linking two-dimensional planar organic components *via* metal-coordination. The first example of using the "*molecular paneling*" approach to obtain a 3D discrete structure is an M_6L_4 octahedral assembly, reported in 1995.[26] The octahedral cage (**Figure 2a**) self-assembles in the presence of Pd^{II} and Pt^{II} ions coordinated to a diamine in a square-planar geometry and a tridentate, triangular ligand (1,3,5-tris-(4-pyridyl)triazine), which acts as a molecular panel. Another example of coordination cage was developed by Raymond and co-workers.[27] It was a tetrahedral capsule (**Figure 2b**) assembled with octahedral metal ions like Fe^{3+} or Ga^{3+} and naphthalene-linked bidentate ligands. Both three-dimensional structures contain large hydrophobic cavities capable of encapsulating organic molecules (octahedral cage) and monocationic guests (tetrahedral cage). In addition, these cages are highly soluble in water which enables the encapsulation of organic molecules in aqueous medium.

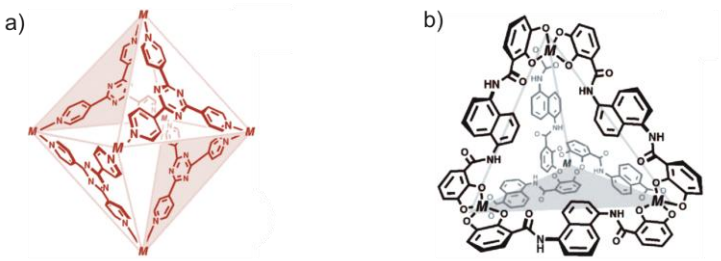

Figure 2: a) Octahedral coordination cage of Fujita and co-workers, b) Tetrahedral coordination capsule of Raymond and co-workers. *Copyright 2009 Wiley-VCH Verlag GmbH & Co.*

The use of hydrogen bonds for the self-assembly of three-dimensional capsules was introduced by Rebek and co-workers 20 years ago, with the reversible molecular capsule named "tennis ball".[28] The monomer consisted of two glycoluril subunits appended to a central aromatic skeleton. The tennis ball was based on the dimerization of the seven-membered ring monomers (**Figure 3**) that were self-complementary in hydrogen bonding. The capsule was held together by a seam of eight hydrogen bonds surrounding a cavity of approximately 60 $Å^3$, able to reversibly entrap small molecules like methane, ethane, and ethylene.

The degree of occupancy was shown to be a key factor[29] for the encapsulation of one or another guest(s) molecule(s). A proper guest is the one that has a suitable shape to fit within the cavity and presents the correct packing coefficient, which was found to be around 55% (ratio of the guest volume to the host's cavity volume) in the liquid state.

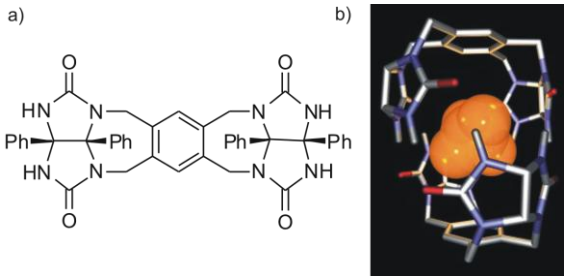

Figure 3: a) Monomer of the tennis ball, b) Molecular model of the self-assembled tennis ball. *Molecular model Copyright 2001 Arash Rebek and Lubomir Sebo, The Scripps Research Institute webpage.*

Calix[4]arenes and resorcin[4]arenes are standard subunits for self-assembled molecular capsules. Although there is multitude of capsules published in the literature with two, three, four, or six components,[30] we will focus on the capsules made of two hemispheres which are the most common assemblies.

One representative example of dimeric capsule is the one that Rebek and co-workers obtained and called the cylindrical capsule[31] (**Figure 4**). This capsule was obtained from the self-assembly of a bowl-shaped resorcin[4]arene elaborated with aromatic panels and containing terminal hydrogen-bond donors and acceptors groups. These type of cavitands are usually in dynamic equilibrium between kite and vase conformations.[32,33]

In this particular case, however, the fact of maximizing the number of hydrogen bond interactions brought two units together in vase conformation to give a dimeric capsule.[34] The dimerization process takes place in a rim-to-rim manner and it is stabilized through eight bifurcated hydrogen bonds at its edges, between the imide hydrogens of one molecule and the two carbonyls oxygens of another. The cyclic pattern of hydrogen bonding between the imides had no precedent.

The cylindrical capsule reached an internal volume of 420 $Å^3$, an appreciable increase with respect to the previously assembled tennis ball. This deeper cavity was large enough to accommodate two molecules of solvent like benzene or toluene which could be easily replaced by adamantane or ferrocene carboxylic acid. Moreover, it presented a size and shape selectivity for hetero-guest pair encapsulation processes: one molecule of benzene and one of *p*-xylene were encapsulated. While two molecules of benzene leave too much free space in the cavity, two *p*-xylene molecules make it too packed. Thus, one benzene and one p-xylene molecule yield the best packing coefficient.

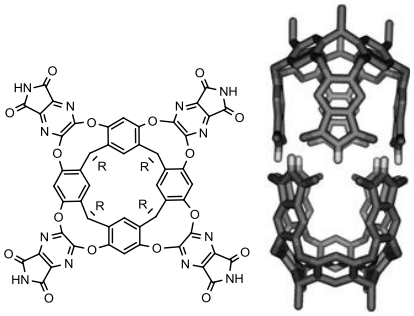

Figure 4: Cylindrical capsule based resorcin[4]arenes prepared by Rebek and co-workers. *Copyright of the molecular model 2007 The Royal Society of Chemistry and the Centre National de la Recherche Scientifique 2007*.

Calixarenes capsules. The urea belt.

Many authors have worked with calix[4]arenes derivatives, for example, Böhmer,[35,36] Reinhoudt,[37,38] etc., however the first example of self-assembled capsules made of two interdigitated and self-complementary calix[4]arenes derivatives was reported by Rebek in 1995.[39] The calix[4]arene monomer was decorated with urea groups which are both

donors and acceptors of hydrogen bonds. Urea functions were formerly used in supramolecular assemblies due to their capability to create highly ordered hydrogen bonding networks.[40,41] In the presence of an adequate guest (solvent molecule), the self-complementary tetraurea calix[4]arenes organized a directional array of 16 hydrogen bonds with a head-to-tail topology of the 8 urea functions, which are all oriented in the same direction. Four of the interlocking ureas come from the top hemisphere, and four from the bottom hemisphere. In each urea function, both NH groups of one urea are hydrogen bonded to the carbonyl oxygen of the neighboring urea (opposite hemisphere) and the oxygen atom of the CO group acts as hydrogen bond acceptor with the adjacent NH groups. This cyclic arrangement of hydrogen bonds is known as "urea belt".

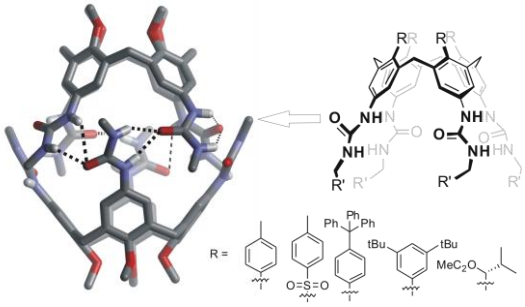

Figure 5: Tetraurea calix[4]arene self-assembled dimeric capsule. It is the first example of self-assembled capsule with hydrogen-bonded urea belt.

A "cone conformation" of the tetraurea calix[4]arenes was a necessary condition to obtain a cavity and this conformation can be maintained by attaching sizable groups at the lower rim. Different evidence of the existence of the tetraurea calix[4]arene self-assembled capsule was derived from ^{1}H NMR spectroscopy, mass spectrometry and through the detection of guest molecules included inside the cavity. The ^{1}H NMR spectra of the tetraurea calix[4]arene in non-polar solvents was reported to be different from the spectra in polar and hydrogen-bonding competitive solvents, such as dimethyl sulfoxide. In a polar solvent, the ^{1}H NMR spectrum is in agreement with a C_4 symmetry compound, which corresponds to the tetraurea calix[4]arene monomer fixed in the cone conformation. In a non-polar solvent, however, the tetraurea calix[4]arene displayed an unusual symmetry. This unfamiliar spectrum was ascribed to the different symmetries of the dimeric complex versus the single calix[4]arene monomer. From these results, the

authors deduced that the octaurea dimer possessed an S_8 symmetry in contrast to the C_4 symmetry of the calix[4]arene. An S_8 symmetry means that each individual calixarene of the assembly is chiral, although the overall capsule is *meso* and achiral. The cavity interior encloses a volume of approximately 200 $Å^3$. The molecules encapsulated in this assembly were solvent molecules like toluene or chloroform.

Self-assembled capsules with polar interior

The importance of the structures enclosing polar groups in its interior lies on the possibility to determine the position and orientation of the guest molecules, a difference with respect to the previous assemblies in which the guests display no order. Hexameric capsular assemblies with interior directed polar groups were reported earlier by Atwood[42] and Ballester.[43] Atwood described an hexameric assembly made of resorcin[4]arenes and pyrogallol[4]arenes where the internal order of the guests was brought by hydrogen bond donors (hydroxyl groups) not involved in the framework or the capsule; while Ballester reported an hexameric capsule of a calix[4]pyrrole-resorcinarene hybrid monomer where the guests were fixed by the NH groups of the calix[4]pyrrole core. Furthermore, two-wall calix[4]pyrrole dimeric capsules were described by Kohnke.[44] Nevertheless, we will focus here exclusively on dimeric assemblies built from four-wall tetraurea calix[4]pyrroles.

Calixpyrroles

Calix[4]pyrroles are known since the 19th century when Baeyer[45] first synthesized them by an acid-catalyzed condensation of pyrrole and acetone. These compounds were first named as porphyrinogens. Porphyrinogens are macrocyclic species formed by four pyrrole rings linked by the alpha or *meso*-position via sp^3-hybridized carbon atoms (**Figure 6**). When the *meso*-carbons substituents are hydrogens, the compound is susceptible to oxidation to the corresponding porphyrin. Nevertheless, the total substitution at their *meso* positions avoids its oxidation and leads to stable structures. Thus, they are not porphyrin precursors anymore. The name calixpyrrole was coined by Sessler[46] due to their structural and conformational similarity to calixarenes, in which the four aryl rings were substituted by four pyrrole rings. In non-polar solvents

calix[4]pyrroles adopt the least polar 1,3-alternate conformation (**Figure 6**). In the presence of a hydrogen-bond acceptor, like anions or polar molecules, calix[4]pyrroles undergo a conformational change in which all four pyrrole moieties point inwardly. This is known as cone conformation where all the pyrrolic N-H groups contribute to the hydrogen bonding.

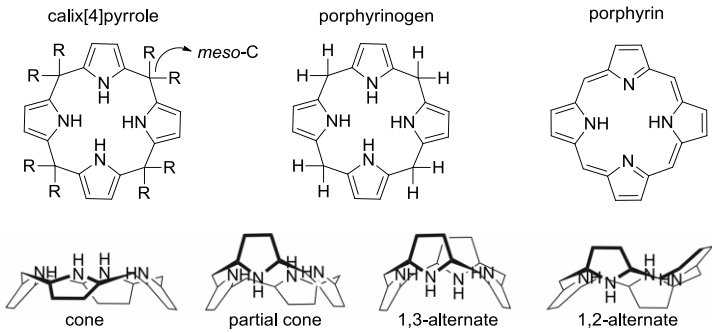

Figure 6: Top) Calix[4]pyrroles, porphyrinogen and porphyrin structures, bottom) Schematic representation of the conformational behavior of calix[4]pyrroles.

It is worth noting that when *meso*-carbons are non-symmetrically substituted configurational isomerism arises (**Figure 7**). The configurational notation is based on the orientation of the *meso*-aryl groups: alpha for the aryl ring pointing to the same direction as the pyrrole rings and beta when it is pointing in opposite direction. The aryl substitution on the calix[4]pyrrole upper rim opened the possibility to create a cavity.[47] The α,α,α,α isomer of a calix[4]pyrrole bearing axially substituted aryl groups in each of the four *meso*-carbons forms a bowl-shape, deep aromatic cavity.

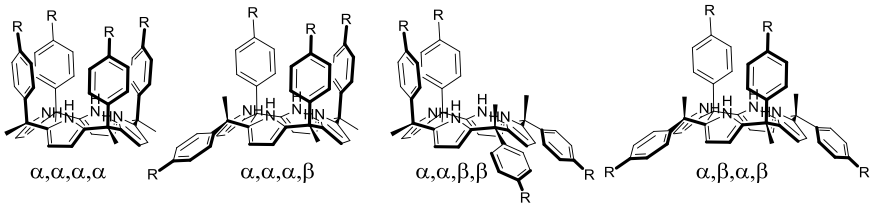

Figure 7: Schematic representation of the configurational isomers of an aryl-extended calix[4]pyrrole in the cone conformation.

A century after its discovery, the ability of calixpyrroles as anion receptors was widely studied by Sessler.[46,48] Octamethyl calix[4]pyrrole was found to be an effective receptor for anions in organic solvents (**Figure 8a**). Four hydrogen bonds between the anion and the pyrrolic NHs are established. Moreover, they are known to act as ion pair receptors, holding the anion into the calix[4]pyrrole cavity and the cation in the external shallow cavity formed by the four pyrrole rings after the anion complexation (**Figure 8b**).[49]

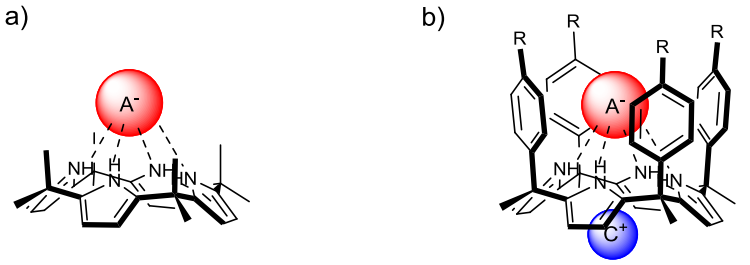

Figure 8: Schematic representation of: a) an anion complexation in the octamethyl calix[4]pyrrole and b) ion-pair complexation in an aryl-extended calix[4]pyrrole.

Self-assembly in calix[4]pyrroles

In the previous section the dimeric tetraurea-calix[4]arene capsules held together by a cyclic array of 16 hydrogen bonds were introduced. In close analogy and later on, in 2009, urea functions were inserted in the aryl-extended calix[4]pyrrole structures in order to obtain the same kind of structural arrangement of hydrogen bonds present in the calix[4]arene capsules. Calix[4]pyrroles were selected for this purpose due to their isostructural analogy with calix[4]arenes scaffolds. Apart from calixarenes, cucurbiturils and cyclodextrines, there are very few molecules which present an intrinsic cavity.

The first dimeric capsule based on tetraurea calix[4]pyrrole scaffolds functionalized with four ureas in the *para* position of their *meso* phenyl substituents and fixed together by an urea belt (**Figure 9**) was reported by our group[50] (**Figure 10**). The capsule was obtained after mixing the corresponding tetraurea calix[4]pyrrole with the adequate guest in a non-hydrogen-bonding competitive solvent. In contrast to their calixarene analogs this sort of capsules require the extra addition of a guest(s) molecule(s) owing that the solvent encapsulation is not enough to induce the assembly of the capsule.

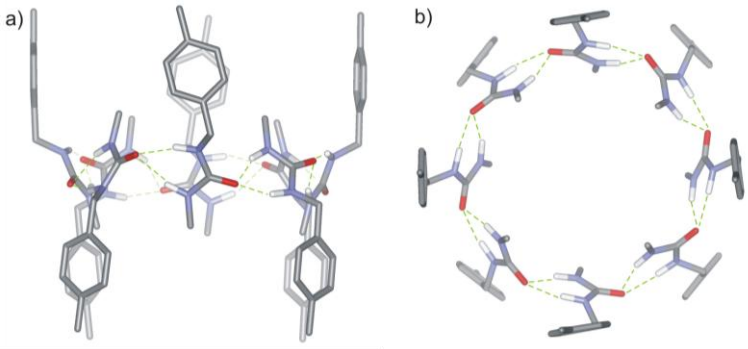

Figure 9: Hydrogen bonded urea belt of a self-assembled calix[4]pyrrole capsule: a) side view and b) top view.

Figure 10 represents an example of endo-functionalized capsule with polar groups in its interior, a great difference (and a new feature) respect to the calix[4]arene capsules in which the guests were freely tumbling inside the cavity with no preorganization. The calix[4]pyrrole units oriented the guests in a permanent direction by establishing 4 hydrogen bonding interactions in each hemisphere, allowing to determine the exact position of guest molecules. The functionalized interior of the calix[4]pyrrole capsules exhibits guest selectivity beyond the control of size or shape exclusion. Moreover, the calix[4]pyrrole capsules displayed a deeper aromatic cavity than its calix[4]arenes equivalents and, as a consequence, a bigger cavity volume when two units are assembled. The enclosed volume, calculated from the crystal structure, was approximately 312 $Å^3$ a substantial increase with respect to the calix[4]arene capsules (200 $Å^3$).

The formation of the self-assembled dimeric capsules derived from tetraurea calix[4]pyrrole was confirmed by ^1H and 2D NMR spectroscopy, GPC chromatography, ESI-MS spectrometry and, finally, by X-ray analysis. The ^1H NMR of the tetraurea calix[4]pyrrole in DMSO revealed well resolved signals corresponding to the C_4 symmetry of the monomeric compound. The spectrum in dichloromethane, however, showed ill-defined signals corresponding to the formation of aggregates of unknown stoichiometry probably due to the hydrogen-bonding interactions between monomers. A dramatic change was observed in the ^1H NMR spectrum of the tetraurea calix[4]pyrrole in dichloromethane solution after the addition of the ditopic guest 4,4'-dipirydil bis-

N,N'-oxide pointing out to the formation of a discrete and well-defined supramolecular species instead of the previous aggregates.

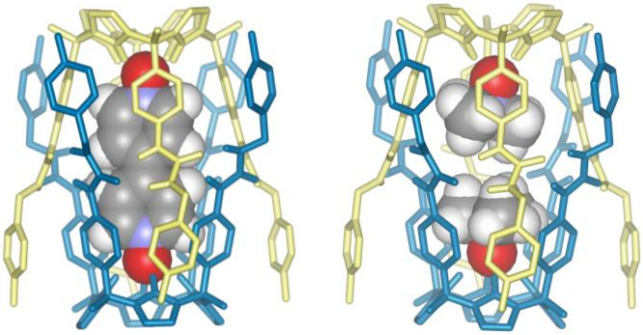

Figure 10: Graphical representations of tetraurea extended calix[4]pyrrole assemblies energy minimized structures containing: left) one molecule of 4,4'-bipyridine bis-*N*-*N'*-oxide and right) two molecules of trimethylamine *N*-oxide.

The first molecule used to template the capsule formation was a ditopic guest, 4,4'-dipirydil bis-*N,N'*-oxide. This guest had a double function: the induction of the cone conformation in the calix[4]pyrrole scaffold and the perfect length to bring together the two endohedral binding sites of the tetraurea calix[4]pyrrole capsule. This means that it fixed the two monomers at the exact distance to form the urea belt. At this point, it was thought that the ditopic guest was necessary to template the capsule formation, however, one year later the induced self-assembly of tetraurea capsule's by monotopic guest was explored (**Figure 10**) and successfully achieved.[51] It was confirmed then that a ditopic guest was not a necessary condition for the capsule construction. The pairwise encapsulation of two monotopic guests (homo- or hetero-pair) within the molecular capsule was relevant for a possible future application of these capsules as reaction vessels.

Chirality was introduced to the calix[4]pyrrole dimeric capsules by assembling two units of chiral tetraurea calix[4]pyrroles.[52] Those chiral calix[4]pyrroles were decorated with methyl groups at the benzylic carbons, hence these carbon atoms became stereogenic. It was observed that the two hemispheres of a capsular assembly built from two enantiopure chiral tetraurea calix[4]pyrroles with the same absolute configuration (*R* or *S*) at each stereogenic carbon atoms were cyclodiastereomers. Even though the

two monomers were identical, when the capsule is formed the unidirectional orientation of the urea groups forming the urea belt transformed the two hemispheres in two disteromeric halves. With respect to the orientation of the urea groups, one of the hemispheres must be *M* (anticlockwise turn of ureas when viewed from the top of the hemisphere) and the other one must be *P* (clockwise turn).

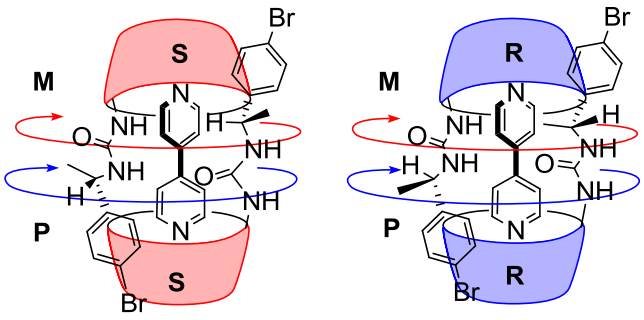

Figure 11: Schematic representation of the homocapsules assembled from enatiomerically pure tetraurea calix[4]pyrrole monomers.

1.4.Aims of the Thesis

Our research group is currently interested in extending the size and the volume of the internal cavity provided by molecular capsules assembled by dimerization of calix[4]pyrrole scaffolds. Our final goal is the use of these supramolecular structures as molecular vessels in which chemical reactions can be performed. To this end, the incorporation of polar groups in the interior of the cavity is a must. Our expectations involve the pair-wise encapsulation of polar guest, the control of their relative orientation and positioning with geometries close to those required for the transition state of the reaction, that we would like to mediate within the capsular assembly.

In line with these general objectives, the present thesis work deals with the study of the polar interiors of self-assembled homocapsules based on calix[4]pyrrole scaffolds, as well as the anisotropic polar interior of a mechanically locked calix[4]arene-calix[4]pyrrole heterocapsule. The properties of the internal cavities of the receptors will be probed through the inclusion of different guests. Moreover, the extension of the internal volume of the calix[4]pyrrole components of dimeric capsules and the preparation of an unprecedented mechanically linked calix[4]pyrrole – calix[4]pyrrole molecular container will also constitute final goals of this work.

In order to study the interior of self-assembled calix[4]pyrrole capsules, a series of bis-*N*-oxides were designed to be used as "molecular rulers". The aims of this project were:

- The evaluation of the range of molecules able to be included in the capsule.
- The study of the modulation of the cavity depending on the included guest and the adaptation of the guest to the dimensions of the capsule.
- The study of the capsule's symmetry based on the complexity of the NMR proton spectra of both the bound host and the encapsulated guest.

Regarding the study of the polar interior of the mechanically locked calix[4]arene – calix[4]pyrrole capsule the following objectives were pursued:

- The improvement of synthetic steps and purification strategies previously reported for its synthesis.

- The evaluation of the binding properties of a homologous series of linear mono *N*-oxides with the mechanically locked container.
- The comparison between the binding results obtained with the mechanically locked container and an analogous supramolecular capsule having one calix[4]arene and one calix[4]pyrrole hemisphere.
- The evaluation of the binding properties of the mechanically locked capsule towards ion pairs, metalocenes and biologically active molecules

The extension of the size and volume of the cavity of aryl extended calix[4]pyrroles by elongation of their four aromatic walls. This process leads to the preparation of unprecedented super-extended calix[4]pyrroles. The following goals were pursued within this sub-project:

- Synthesis of super-extended calix[4]pyrroles.
- Studies of the binding properties of super-extended calix[4]pyrroles.
- Synthesis of tetraurea super-extended calix[4]pyrroles.
- Study of the self-assembly process of tetraurea super-extended calix[4]pyrroles into dimeric capsules.

Finally, in the project related to the synthesis of an unprecedented calix[4]pyrrole - calix[4]pyrrole mechanically locked capsule, we set up for the achievement of the following aims:

- The synthesis of a novel calix[4]pyrrole - calix[4]pyrrole capsule having the two hemispheres covalently linked with mechanical bonds.
- The study of the encapsulation properties of the container using different molecules of guests.

1.5.Outline of the Thesis

Chapter 2 describes the study of the polar interior of non-chiral self-assembled dimeric molecular capsules based on tetraurea calix[4]pyrroles and the adaptability of its dimensions to the size of the encapsulated substrates. To this end, we used the results obtained in the encapsulation studies using a homologous series of aliphatic bis-*N*-oxides functioning as molecular rulers, with the dimeric capsules. Unexpectedly, we observed the appearance of diasterotopic signals for some of the protons of the encapsulated guest in the ^{1}H NMR spectra of the capsular assemblies. This interesting phenomenon was further investigated using chiral dimeric capsules.

In **Chapter 3** the extension of the cavity of a calix[4]pyrrole by means of the elongation of the walls of an aryl-extended tetrahalogenated calix[4]pyrrole is described. The elaboration of the cavity of the aryl extended calix[4]pyrrole was done through the introduction of additional phenyl rings at the upper rim making use of the Sonogashira reaction. The results obtained in the complexation experiments performed with the super-extended calix[4]pyrroles encouraged us to synthesize super-extended tetraurea calix[4]pyrroles. The dimerization process of super-extended tetraureas should provide self-assembled dimeric capsules featuring a significant increase in their internal cavity volume compare to the simple aryl-extended counterparts. The results obtained in the synthesis and the binding experiments of the novel super-extended tetraurea calix[4]pyrroles can be found in this chapter.

The studies performed to evaluate the size modification and adaptability exhibited by the aromatic cavity enclosed in the hybrid molecular capsule calix[4]arene – calix[4]pyrrole in which both hemispheres are linked by a mechanical bond are discussed in **Chapter 4**. These studies involve the analysis of the results obtained for the encapsulation processes of a homologous series of aliphatic *N*-oxides with the mechanically locked container. The obtained results are compared to the ones we obtained using a the same series of *N*-oxides and a supramolecular capsule analog, assembled by dimerization of two different tetraureas with calix[4]arene and calix[4]pyrrole scaffolds, respectively. Additionally, the binding studies of other types

of substrates, i.e., ion pairs, metalocenes and biologically relevant molecules, are also covered in this chapter.

Lastly, **Chapter 5** describes the synthesis of a novel mechanically locked calix[4]pyrrole – calix[4]pyrrole capsule featuring a sizeable increase of its internal volume when compared to the previous structure described in Chapter 4 also displaying bis-[2]-catenane topology. The mechanically locked homo-dimer possesses polar functionalization at the closed ends of both hemispheres. Preliminary binding experiments of the homo-dimer with bis-*N*-oxides, mono-*N*-oxides and metalocenes are also described.

References and notes

[1] Sherman, J. C.; Cram, D. J. *J. Am. Chem. Soc.* **1989**, *111*, 4527-4528.

[2] Lehn, J. M. *Angew. Chem.-Int. Edit.* **1988**, *27*, 89-112.

[3] Lehn, J. M. *Angew. Chem.-Int. Edit.* **1990**, *29*, 1304-1319.

[4] Lehn, J. M. *Science* **1993**, *260*, 1762-1763.

[5] Lehn, J. M. *Chem. Soc. Rev.* **2007**, *36*, 151-160.

[6] Ziegler, M.; Brumaghim, J. L.; Raymond, K. N. *Angew. Chem.- Int. Ed* **2000**, *39*, 4119-4121.

[7] Dong, V. M.; Fiedler, D.; Carl, B.; Bergman, R. G.; Raymond, K. N. *J. Am. Chem. Soc.* **2006**, *128*, 14464-14465.

[8] Kang, J. M.; Rebeck, J. *Nature* **1997**, *385*, 50-52.

[9] Kusukawa, T.; Nakai, T.; Okano, T.; Fujita, M. *Chem. Lett.* **2003**, *32*, 284-285.

[10] Yoshizawa, M.; Tamura, M.; Fujita, M. *Science* **2006**, *312*, 251-254.

[11] Chen, J.; Rebek, J. *Organic Letters* **2002**, *4*, 327-329.

[12] Timmerman, P.; Verboom, W.; Vanveggel, F. C. J. M.; Vanduynhoven, J. P. M.; Reinhoudt, D. N. *Angew. Chem.-Int. Ed.* **1994**, *33*, 2345-2348.

[13] Shivanyuk, A.; Rebek, J. *J. Am. Chem. Soc.* **2002**, *124*, 12074-12075.

[14] Nishioka, Y.; Yamaguchi, T.; Yoshizawa, M.; Fujita, M. *J. Am. Chem. Soc.* **2007**, *129*, 7000-7001.

[15] Yoshizawa, M.; Kusukawa, T.; Fujita, M.; Yamaguchi, K. *J. Am. Chem. Soc.* **2000**, *122*, 6311-6312.

[16] Yoshizawa, M.; Kusukawa, T.; Fujita, M.; Yamaguchi, K. *J. Am. Chem. Soc.* **2000**, *122*, 6311-6312.

[17] Kang, J. M.; Hilmersson, G.; Santamaria, J.; Rebek, J. *J. Am. Chem. Soc.* **1998**, *120*, 3650-3656.

[18] Cram, D. J.; Karbach, S.; Kim, Y. H.; Baczynskyj, L.; Kalleymeyn, G. W. *J. Am. Chem. Soc.* **1985**, *107*, 2575-2576.

[19] Sherman, J. C.; Knobler, C. B.; Cram, D. J. *J. Am. Chem. Soc.* **1991**, *113*, 2194-2204.

[20] Breslow, R.; Dong, S. D. *Chem. Rev.* **1998**, *98*, 1997-2011.

[21] Cram, D. J. *Science* **1983**, *219*, 1177-1183.

[22] Cram, D. J. *Nature* **1992**, *356*, 29-36.

[23] Vriezema, D. M.; Aragones, M. C.; Elemans, J. A. A. W.; Cornelissen, J. J. L. M.; Rowan, A. E.; Nolte, R. J. M. *Chem. Rev.* **2005**, *105*, 1445-1489.

[24] Robbins, T. A.; Cram, D. J. *J. Am. Chem. Soc.* **1993**, *115*, 12199-12199.

[25] Yoshizawa, M.; Klosterman, J. K.; Fujita, M. *Angew. Chem.- Int. Ed* **2009**, *48*, 3418-3438.

[26] Fujita, M.; Oguro, D.; Miyazawa, M.; Oka, H.; Yamaguchi, K.; Ogura, K. *Nature* **1995**, *378*, 469-471.

[27] Caulder, D. L.; Powers, R. E.; Parac, T. N.; Raymond, K. N. *Angew. Chem.-Int. Edit.* **1998**, *37*, 1840-1843.

[28] Wyler, R.; de Mendoza, J.; Rebek, J. *Angew. Chem.-Int. Edit.* **1993**, *32*, 1699-1701.; Branda, N.; Wyler, R.; Rebek, J. *Science* **1994**, *263*, 1267-1268.

[29] Mecozzi, S.; Rebek, J. *Chem.-Eur. J.* **1998**, *4*, 1016-1022.

[30] MacGillivray, L. R.; Atwood, J. L. *Nature* **1997**, *389*, 469-472.

[31] Heinz, T.; Rudkevich, D. M.; Rebek, J. *Nature* **1998**, *394*, 764-766.

[32] Moran, J. R.; Karbach, S.; Cram, D. J. *J. Am. Chem. Soc.* **1982**, *104*, 5826-5828.

[33] Moran, J. R.; Ericson, J. L.; Dalcanale, E.; Bryant, J. A.; Knobler, C. B.; Cram, D. J. *J. Am. Chem. Soc.* **1991**, *113*, 5707-5714.

[34] Rebek, J. *Accounts Chem. Res.* **2009**, *42*, 1660-1668.

[35] X-ray crystal structure of a tetraurea calix[4]pyrrole dimeric capsule: Mogck, O.; Bohmer, V.; Vogt, W. *Tetrahedron* **1996**, *52*, 8489-8496.

[36] Mogck, O.; Paulus, E. F.; Bohmer, V.; Thondorf, I.; Vogt, W. *Chem. Commun.* **1996**, 2533-2534.

[37] Scheerder, J.; Vreekamp, R. H.; Engbersen, J. F. J.; Verboom, W.; vanDuynhoven, J. P. M.; Reinhoudt, D. N. *J. Org. Chem.* **1996**, *61*, 3476-3481.

[38] Scheerder, J.; vanDuynhoven, J. P. M.; Engbersen, J. F. J.; Reinhoudt, D. N. *Angew. Chem.-Int. Edit.* **1996**, *35*, 1090-1093.

[39] Shimizu, K. D.; Rebek, J. *Proc. Natl. Acad. Sci. U.S.A.* **1995**, *92*, 12403-12407.

[40] Zhao, X. Q.; Chang, Y. L.; Fowler, F. W.; Lauher, J. W. *J. Am. Chem. Soc.* **1990**, *112*, 6627-6634.

[41] Etter, M. C.; Urbanczyklipkowska, Z.; Ziaebrahimi, M.; Panunto, T. W. *J. Am. Chem. Soc.* **1990**, *112*, 8415-8426.

[42] Atwood, J. L.; Barbour, L. J.; Jerga, A. *Proc. Natl. Acad. Sci. U.S.A.* **2002**, *99*, 4837-4841.

[43] Gil-Ramirez, G.; Benet-Buchholz, J.; Escudero-Adan, E. C.; Ballester, P. *J. Am. Chem. Soc.* **2007**, *129*, 3820-3821.

[44] Cafeo, G.; Kohnke, F. H.; Valenti, L.; White, A. J. P. *Chem.-Eur. J.* **2008**, *14*, 11593-11600.

[45] Baeyer, A. *Ber. Dtsch. Chem. Ges.* **1886**, 2184-2185.

[46] Gale, P. A.; Sessler, J. L.; Kral, V.; Lynch, V. *J. Am. Chem. Soc.* **1996**, *118*, 5140-5141.

[47] Anzenbacher, P.; Jursikova, K.; Lynch, V. M.; Gale, P. A.; Sessler, J. L. *J. Am. Chem. Soc.* **1999**, *121*, 11020-11021.

[48] Gale, P. A.; Sessler, J. L.; Kral, V. *Chem. Commun.* **1998**, 1-8.

[49] Custelcean, R.; Delmau, L. H.; Moyer, B. A.; Sessler, J. L.; Cho, W. S.; Gross, D.; Bates, G. W.; Brooks, S. J.; Light, M. E.; Gale, P. A. *Angew. Chem.- Int. Ed* **2005**, *44*, 2537-2542.

[50] Ballester, P.; Gil-Ramirez, G. *Proc. Natl. Acad. Sci. U.S.A.* **2009**, *106*, 10455-10459.

[51] Gil-Ramirez, G.; Chas, M.; Ballester, P. *J. Am. Chem. Soc.* **2010**, *132*, 2520-2521.

[52] Chas, M.; Gil-Ramirez, G.; Escudero-Adan, E. C.; Benet-Buchholz, J.; Ballester, P. *Organic Letters* **2010**, *12*, 1740-1743.

CHAPTER 2

BINDING STUDIES OF A CALIX[4]PYRROLE SELF-ASSEMBLED MOLECULAR CAPSULE

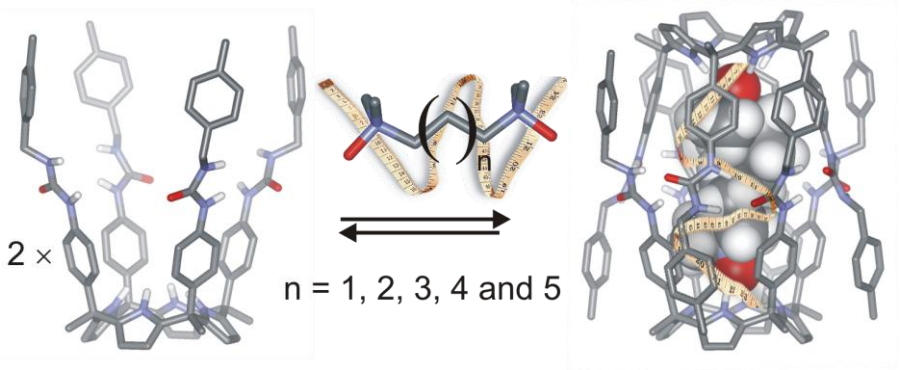

Part of this Chapter has been published in:

M. Espelt, P. Ballester. *Org. Lett.*, **2012**, *14*, 5708-5711.

UNIVERSITAT ROVIRA I VIRGILI
REVERSIBLE MOLECULAR ENCAPSULATION IN SELF-ASSEMBLED AND MECHANICALLY LOCKED CONTAINERS WITH POLAR INTERIOR
Monica Espelt Ripoll
DL: T 1103-2014

1. Introduction

In solution, the emergence of self-assembled molecular capsules stabilized by hydrogen bonding interactions requires the appropriate filling of their inner spaces. Mecozzi and Rebek formulated the 55% packing coefficient rule, which is the ratio of the guest volume to the cavity of the host volume, to explain and predict efficient encapsulation processes.[1] Molecular modeling studies and X-ray crystallography data are useful for producing estimates of available volumes in the internal cavity of molecular containers.[2] However, variable results can be obtained depending on the parameters used to determine empty spaces, i.e. probe radii and grid spacing. The use of a homologous series of molecules, so-called molecular rulers, constitutes an experimental approach to probe the available space inside a molecular container.[3]

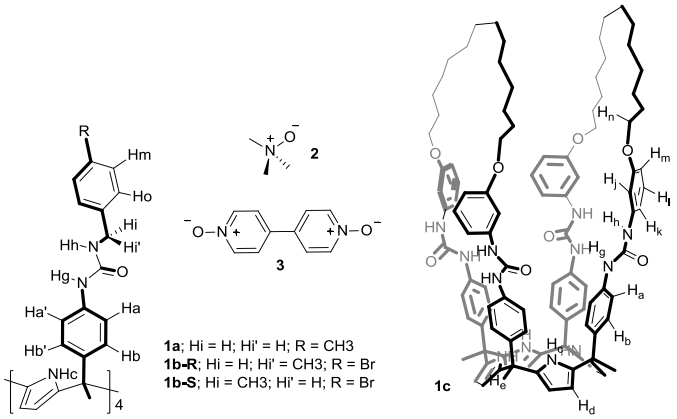

Figure 1: Tetraurea calix[4]pyrroles **1**, trimethylamino *N*-oxide **2** and dipyridyl bis-*N*-oxide **3**.

In our group it was recently described the dimerization of tetraurea calix[4]pyrrole **1a** induced by the pairwise encapsulation of trimethyl-*N*-oxide **2** (**Figure 1**).[4] The oxygen atom of each of the two included *N*-oxides **2** is hydrogen bonded to the four pyrrole NHs located at opposite ends of the capsule. The capsular assembly is stabilized by the formation of a belt of 16 hydrogen bonds between the eight urea functions, which are all oriented in the same direction. Previously, the self-assembly of **1** was also achieved using just one molecule of 4,4'-bipyridine-*N,N'*-dioxide **3** as a template.[5] We observed a significant variation in the estimated volumes for the empty internal cavities of

1a•1a⊃2$_2$ (MM3 minimized structure, 359 Å^3) and **1a•1a⊃3** (X-ray structure, 312 Å^3), which suggested to us the existence of cavity size modulation through guest-induced fit. In the work described in this chapter, we determine the level of guest induced fit achievable by the cavity of the capsular assembly **1a•1a**. To this end, we selected a homologous series of *N,N,N',N'*-tetramethylalkyl-*N,N'*-dioxides **4** as potential encapsulation guests.

2. Results and Discussion

2.1. Synthesis

The synthesis and characterization of the tetraurea calix[4]pyrroles **1a, *S*-1b** and ***R*-1b** has been described in detail by our group[5,6] and will not be discussed here. Bisloop tetraurea calix[4]pyrrole **1c** was synthesized following a similar literature procedure[7] applied in the synthesis of a closely related tetraurea calix[4]arene. *N,N'*-dioxides **4a**, **4b**, and **4d** were obtained by oxidation of the corresponding commercially available diamines. Using literature procedures, the diamine that leads to **4c** was obtained by $LiAlH_4$ reduction of *N,N',N'',N'''*-tetramethylglutaramide. This tetramethylglutaramide was prepared by reacting dimethyl glutarate with dimethylamine and sodium methoxide. Whereas the diamine that leads to **4e** was obtained by double nucleophilic substitution of 1,7-dibromoheptane with dimethylamine.

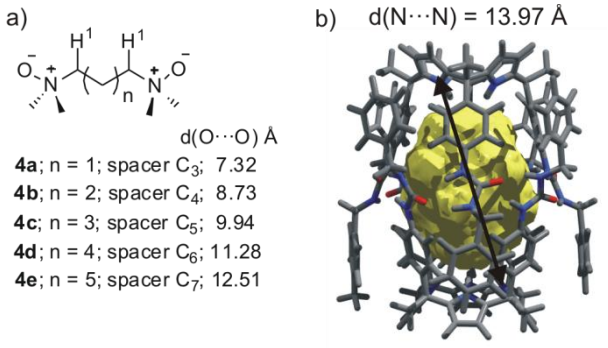

Figure 2: a) Series of bis-*N*-oxides **4** used as molecular rulers; b) Rendering of the MM3 minimized structure of the **1a•1a⊃2$_2$** complex with the shape of the inner space calculated using Swiss-Pdb Viewer (˜359 Å^3) after guest deletion.

2.2. Bis-*N*-oxides as Molecular Rulers

Guest series **4** represents a set of molecular rulers because, although its components are conformationally flexible, they possess easily measurable oxygen-oxygen distances that can be progressively varied by a single methylene unit. The dimethyl-*N*-oxide knobs placed at both termini of the rulers provide an ideal fit in terms of size, shape, and function for interacting with the inner functionalized cavities (poles) defined by the *meso*-phenyl calix[4]pyrrole units in **1a•1a**. From these studies, we expected to gain additional information on the conformational malleability of the bis-*N*-oxide series **4** caused by encapsulation in **1a•1a**. The induced fit of the host's cavity and the guest adaptability seem to be inevitably linked.[8,9,10]

Initial encapsulation experiments were performed by simply adding 0.5 equivalents of bis-*N*-oxide **4a-e** to individual NMR tubes containing 1-2 mM suspensions of tetraurea **1a** in $CDCl_3$. Only the addition of bis-*N*-oxides **4b**, **4c**, and **4d** (C_4-C_6) resulted in the rapid dissolution of the mixtures. Analyzing the resulting solutions by ^{1}H-NMR spectroscopy revealed the existence of sharp and well resolved proton signals having the earmarks for the formation of the capsules **1a•1a⊃4b-d** with S_8 symmetry (**Figure 3**).[4]

Guest **4a** is too short to establish a simultaneous ditopic interaction with the two endohedral calix[4]pyrrole binding sites in **1a•1a**. Assuming a typical hydrogen bonding distance of 3.0 Å, the sum of the distance between the oxygen atoms in **4a** plus two hydrogen bonds (7.32 + 6.0 = 13.32 Å) is not enough to bridge the gap between the two binding sites (d(N··N) ≈ 14 Å, **Figure 2b**). Similar calculations suggest that **4b** and **4c** are suitable fits because, in their fully extended conformation, the sum of their O-O distance plus two hydrogen bonds matches the capsule's dimensions. The other two bis-*N*-oxides **4d-e** must adopt some folded conformation to fit into the capsule. Capsular assembly **1a•1a⊃4e** is not observed by experiment. The folding required for **4e** to adapt to the capsule's dimensions is probably too energetically costly and cannot be compensated by the gain in host-guest interactions provided by the self-assembly.

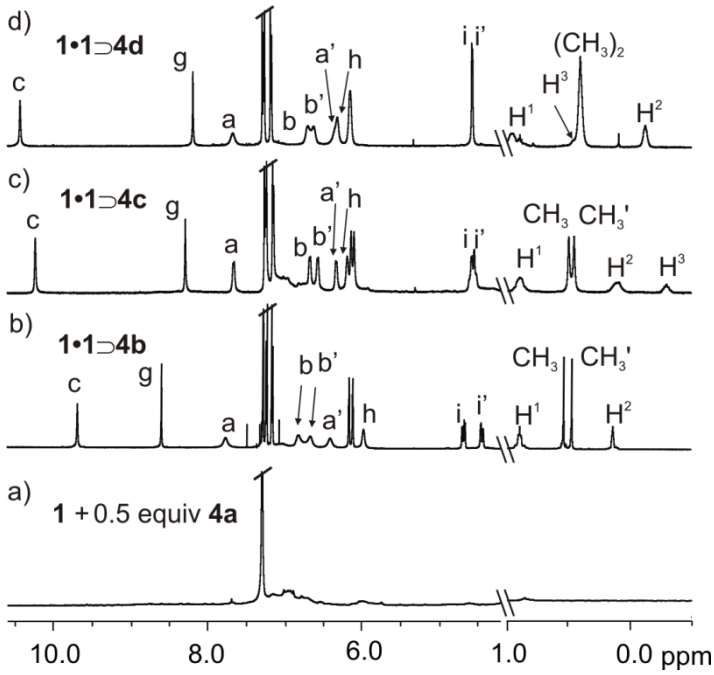

Figure 3: Selected upfield and downfield regions of the ^{1}HNMR spectra acquired from the $CDCl_3$ solutions obtained by mixing: (a) urea **1a** and 0.5 equiv of **4a**; (b) urea **1a** and 0.5 equiv of **4b**, (c) urea **1a** and 0.5 equiv of **4c**; and (d) urea **1a** and 0.5 equiv of **4d**. See **Figure 2**a for proton assignment. H_2 and H_3 correspond to methylene protons β and γ with respect to the N-atoms of **4**.

In the formed capsular assemblies, the observation of two sets of two separated doublets for the *meso*-phenyl *ortho* (a,a') and *meta* (b,b') protons with respect to the urea group is general; it originates from the asymmetry inherent to the unidirectional orientation of the eight urea groups and the slow interconversion on the ^{1}H NMR time scale between the two possible directional senses.[11] The difference in broadening between the proton signals of the *meso* aromatic protons in the assemblies **1a•1a⊃4b-d** is due to slightly different rate constant values for interconverting the sense of direction of the capsules' urea belts. By means of EXSY experiments (see *Experimental Section*) we determined $k_{ex} = 20 \pm 2\ s^{-1}$ ($\Delta G^{\#} = 15.6$ kcal/mol) for **1a•1a⊃4b**, $k_{ex}=10 \pm 1 s^{-1}$ ($\Delta G^{\#} = 16.0$ kcal/mol) for **1a•1a⊃4c**, and $k_{ex}=14 \pm 1\ s^{-1}$ ($\Delta G^{\#} = 15.8$ kcal/mol) **1a•1a⊃4d**. These data suggested that the urea belt in **1a•1a⊃4c** is stabilized by slightly stronger hydrogen bonding interactions than in the other two capsules.[12]

We also noticed that, as the length of the guest was increased, the benzylic (H_h) and phenylic (H_g) NH protons of the urea groups in the **1a•1a** capsules shifted in opposite directions (**Figure 3** and **Table 1**).

	1a•1a⊃4b	**1a•1a⊃4c**	**1a•1a⊃4d**
∂ (H_h)	5.91	6.20	6.29
d (C=O··H_hN)[a]	2.97 ± 0.01	2.95 ± 0.01	2.96 ± 0.01
angle (O··H_hN)[a]	160.0 ± 0.2	162.4 ± 0.4	162.2 ± 0.4
∂ (H_g)	8.57	8.28	8.15
d (C=O··H_gN)[a]	2.99 ± 0.01	3.02 ± 0.01	3.01 ± 0.01
angle (O··H_gN)[a]	159.0 ± 2.3	157.4 ± 0.9	158.3 ± 0.6
d(Cent-Cent)[b]	13.54	13.54	13.67

[a] Measured in the MM3 energy minimized structures. [b] Distance between the two centroids defined by the four C_{meso} of each calixpyrrole.

Table 1: Chemical shift values (ppm) of hydrogen bonded protons in the urea belt of the assemblies and averaged geometric parameters (distance, Å; angle, deg).

This fact can be explained by analyzing the folding of the guests inside the cavity. Molecular modeling (MM3) showed that longer guests must fold in order to fit into the **1a•1a** capsular assembly and bridge the gap between the two binding sites. This folding must somehow apply pressure to the ends and sides of the self-assembly forcing the two tetraurea units to slip partially in order to increase the dimensions of the capsule.[13] The separation of the urea units shortens and enhances the linearity of the hydrogen bonds between the carbonyl oxygens and the benzylic NHs but has the opposite effect for the hydrogen bonds with the phenylic NHs (**Figure 4** and **Table 1**). Based on the energy barriers calculated for the interconversion of the urea belt direction and taking **1a•1a⊃4b** as reference, a putative increase in the strength of the benzylic NH hydrogen bond (shorter distance and better linearity) compensates for the potential weakening of the phenylic one (longer distance) in **1a•1a⊃4c-d** assemblies.

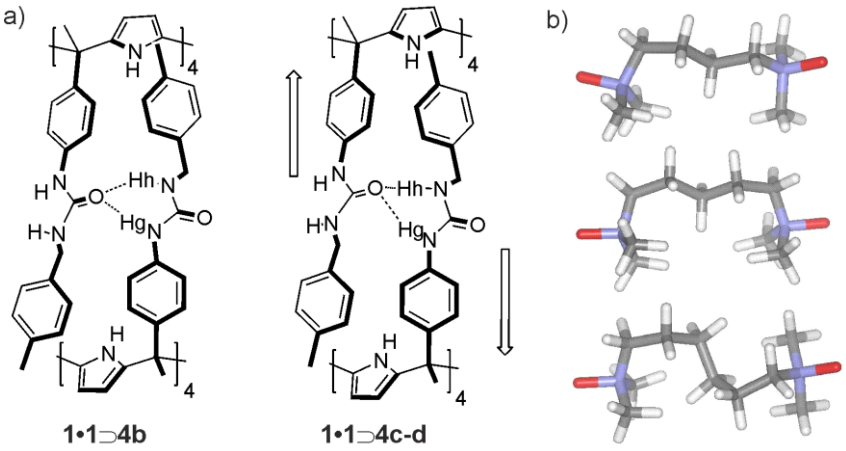

Figure 4: (a) Schematic representation of the effect caused by the capsule's enlargement on the urea belt. (b) Folded conformations adopted by the encapsulated guest in the energy minimized capsules **1a•1a⊃4b-d**, **4b**, **4c** and **4d**, from top to bottom.

Interestingly, the pyrrole NH protons (H_c) showed a monotonic trend of downfield shifts in response to the guest's length. The longer the guest's alkyl chain, the deeper the terminal *N*-oxide knobs are positioned into the aromatic cavities of the two calix[4]pyrrole poles yielding shorter NH··O hydrogen bonds.

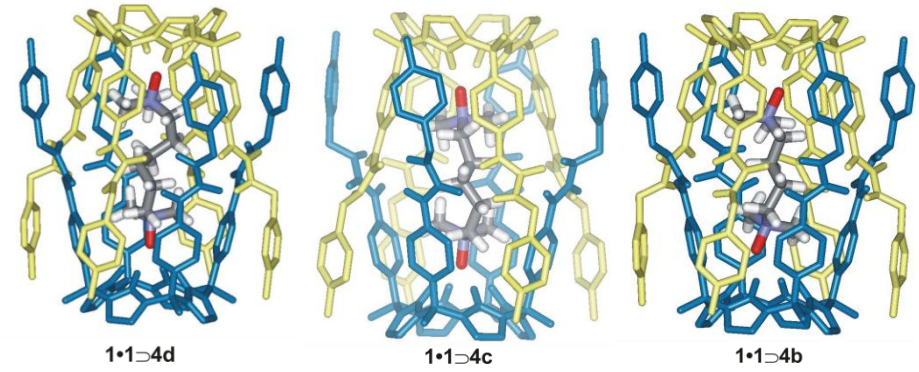

Figure 5: Energy minimized structures of the assemblies: **1a•1a⊃4b**, **1a•1a⊃4c** and **1a•1a⊃4d**.

Possible conformations for the encapsulated guests in assemblies **1a•1a⊃4b**, **1a•1a⊃4c**, and **1a•1a⊃4d** were derived from molecular modeling studies (**Figure 5**). Guest **4b** (C_4 spacer) possesses a length compatible with the capsule's dimensions and can be

accommodated in **1a•1a** in an almost fully extended conformation although a conformation with one gauche interaction also fits (**Figure 4b**).

2D COSY experiments were very useful for the assignment of the proton signals of the bound guests (*Experimental Section*, **Figure 14**). Encapsulated **4b** showed four upfield shifted signals: two multiplets, one corresponding to the methylene protons (H^1) α to the guest nitrogen (δ = 0.88 ppm; Δδ = 2.42 ppm; 4H) and another β to the methylene (H^2) protons (δ = 1.21ppm; Δδ = 1.95 ppm; 2H), and two singlets for the diastereotopic methyl protons of each *N*-oxide knob (δ = 0.45 and 0.51 ppm; Δδ = 2.8 ppm; 12H).[14] The methyl groups and the α methylene experienced the larger upfield shifts due to increased shielding by the aromatic groups at the poles of the cavity compared to its equator. The dimensions of guest **4c** are compatible with encapsulation in a fully extended conformation; however, molecular modeling suggested that the presence of one gauche interaction provides a more complementary guest conformation for hydrogen bonding with the polar ends in **1a•1a** (**Figure 4b**). Guest **4d** and **4e** are definitely too long to be encapsulated in an extended conformation and must fold in order to fit in the capsule. Coiling into a helix has been shown to be a suitable mechanism for long alkanes to decrease their length when included in cylindrical spaces related to the inner cavity of **1a•1a**.[15,16,17] The NOEs observed between the terminal methyl groups and H^3 provided a clear indication of the existence of gauche conformations in the four and five carbon atom chains of encapsulated **4c** and **4d**, respectively (**Figure 4b**). In the ^{1}H NMR spectra, the chemical shift change of the H^3 methylene protons is noticeably smaller for the longer spacer (Δδ(**4c**) = 1.8 vs Δδ(**4d**) = 1.0 ppm). This observation is in agreement with both the placement of the C_3 methylene protons (H^3) (**Figure 3**) of **4d** close to the center of the cavity, due to coiling of the alkyl spacer into a helical conformation, and the concomitant elongation and widening of the cavity induced by guest fitting.[18] It is worth noting that the induction level of diastereotopicity caused by the unidirectional orientation of the urea groups diminishes gradually with longer guests. In other words, the larger guest **4d** causes the disappearance of diastereotopic signals for both the methyl protons of the guest and the benzylic ones in the host. Most likely, the elongation and widening of the cavity are

associated with a steady reduction of the "in-line" placement of urea carbonyl groups, decreasing the induced local anisotropy.

In order to assess this modulation of cavity size induced by guest fitting, we calculated the volumes of the encapsulation complexes **1a•1a⊃4** using Swiss-Pdb Viewer. We calculated a linear increase in both volume size (354, 359, 365 $Å^3$) and the packing coefficient (PC) values (54, 60, 61) with the length of the spacer (**4b**C_4, **4c**C_5, **4d**C_6).[19] Addition of one methylene unit requires a volume increase of 5-6 $Å^3$.The calculated parameters for the **1a•1a⊃4e** complex (i.e., hydrogen bonds lengths, binding energy and PC, **Figure 6**) do not clearly exclude its experimental observation; however, we did not detect it. We surmise that the volume modulation exhibited by **1a•1a** could easily cope with the 6 $Å^3$ increase required for the encapsulation of **4e** but that the problem may be the conformation that **4e** must adopt to fit the cavity. The folding of the C_7 spacer of **4e** into a helical conformation suitable for encapsulation in **1a•1a** demanded the presence of up to five gauche interactions.

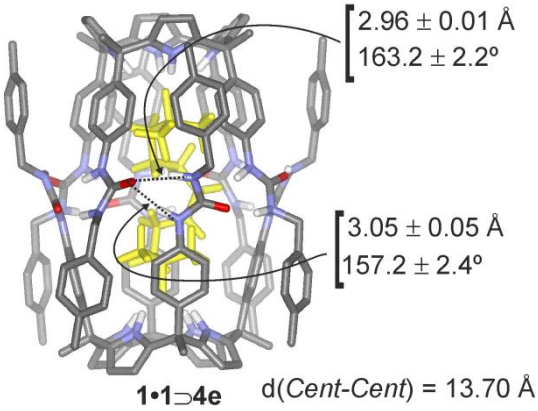

Figure 6: CAChe minimized structure of **1a•1a⊃4e**, not seen experimentally. Selected geometric parameters of the capsular assembly are indicated.

The energy cost for adopting this twisted conformation of **4e** can be estimated as 3.0 kcal/mol, considering the formation of five gauche interactions (0.6 kcal/mol per gauche interaction). Favorable interactions in **1a•1a⊃4e** should compensate for this extra cost for the species to assemble. Differences in the energies provided by the 16 hydrogen

bonds of the urea belts in the capsules **1a•1a⊃4b-c** accounts for less than 0.5 kcal/mol (*vide supra*). Other gains in binding free energy arise from hydrogen bonding each of the two oxygen atoms of the *N*-oxide knobs to the NH pyrrole protons and other favorable capsule-guest CH-π interactions.

2.3. Competitive experiments between guests

In order to rank the binding affinities of guest **4b-d** and to gain some insight into their energy differences, we performed competitive experiments. We prepared $CDCl_3$ suspensions containing 0.5 equivalents of the two competitive guests and 1 equivalent of tetraurea **1a**. To ensure that thermodynamic equilibrium had been reached and to minimize solubility problems, we heated the mixtures at 60ºC for 2.5 hours and then analyzed the solutions by ^{1}H NMR spectroscopy at room temperature (see the spectra for competitive experiments in *Experimental Section*). Integration of characteristic proton signals (pyrrolic NHs, H_c) for the two competing capsular assemblies allowed us to derive the following relationships of relative binding affinities or stabilities: 100K(**1a•1a⊃4b**) = K(**1a•1a⊃4c**) = 45K(**1a•1a⊃4d**). In terms of energy, assembly **1a•1a⊃4c** was 2.7 and 2.2 kcal/mol more stable than **1a•1a⊃4b** and **1a•1a⊃4d**, respectively. The relative strength estimated for the hydrogen bonding of the urea belt (EXSY experiments) correlates with the comparative binding affinity of guests. The drop of 2 kcal/mol in binding stability between **1a•1a⊃4c** and **1a•1a⊃4d**, after correcting for the energy difference in the hydrogen bonded belt, reflects an energetic penalty corresponding to roughly three gauche interactions for the encapsulated **4d** guest compared to **4c**. Despite the positive hints obtained from molecular modeling, the data account for why an increase in the number of gauche interactions combined with weakening of the hydrogen bonds in the urea belt effectively disrupts the formation of **1a•1a⊃4e**. In addition, the assembly encapsulating the flexible bis-*N*-oxide that is thermodynamically more stable (i.e., **1a•1a⊃4c**) was observed to be 84% of the equilibrium species in competition with trimethyl *N*-oxide **2**. However, it was not detected when bis-pyridyl-*N*-oxide **3** was used as a competitor. The fact that the four-

particle aggregate **1a•1a⊃2$_2$** is still assembled in competition with **4c** provided additional support for the presence of gauche interactions in this encapsulated guest.

2.4. Exploring the magnetic anisotropy of the capsule's interior through the induced diastereotopicity of the protons in the encapsulated guest

Previously in this chapter, we have observed that in the ^{1}H NMR spectra of the assemblies **1a•1a⊃4c** and **1a•1a⊃4b** (**Figure 3**) the methyl protons of the included guest split in two different singlets while for the free guest the same protons resonate as a unique singlet. In other words, the methyl protons of the guest become diastereotopic when encapsulated. In order to clarify this fact, other capsules were assembled using the benzyl tetraurea calix[4]pyrrole **1a**, the enantiomerically pure tetraurea calix[4]pyrrole ***R*-1b** and tetraurea bisloop calix[4]pyrrole **1c** (depicted in **Figure 1**). *N*-oxide **4c** (**Figure 2**) was the guest of choice to perform these experiments. The chiral tetraurea calix[4]pyrrole ***R*-1b** diverges from the non-chiral tetraurea calix[4]pyrrole **1a** on the substitution of one of the hydrogen atoms at the four benzylic carbons by a methyl group. This structure contains four stereogenic carbon centers with the same absolute configuration.[6] The tetraurea bisloop calix[4]pyrrole **1c** consists of a calix[4]pyrrole core but differs in structure from the previous ones, **1a** and **1b**, in having covalently linked two adjacent urea arms and the impossibility of self-assemble a capsule by dimerization due to steric hindrance between the loops.

The assembly experiments were performed by adding one equivalent of the ditopic guest **4c** to separate chloroform suspensions containing two equivalents of the enantiomerically pure tetraurea ***R*-1b** or mixture of one equivalent of each one of the two tetraureas: **1a** + ***R*-1b** and **1a** + **1c**. The resulting solutions were analyzed by ^{1}H NMR spectroscopy (**Figure 7**).

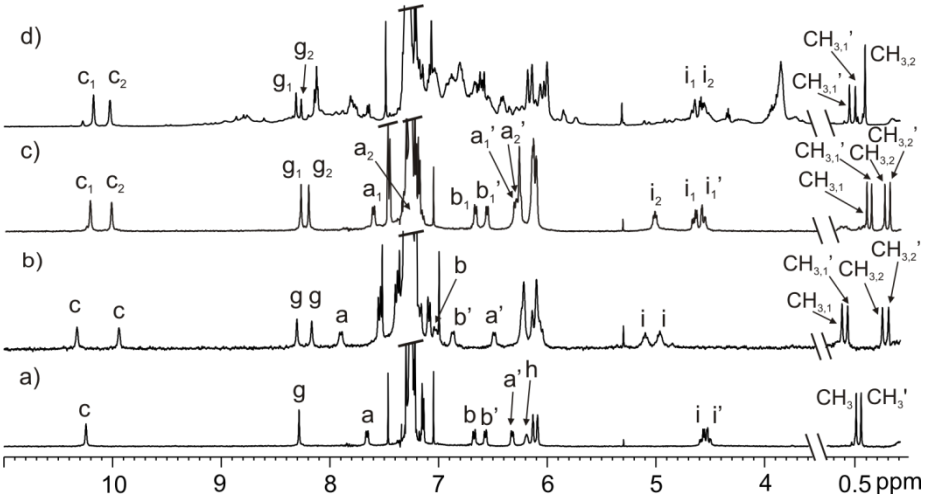

Figure 7: Selected upfield and downfield regions of the ^{1}H-NMR spectra in $CDCl_3$ of: a) homocapsule **1a•1a⊃4c**, b) homocapsule *R*-**1b•***R*-**1b⊃4c**, c) heterocapsule **1a•1b⊃4c,** and d) pseudo-rotaxane **1a•1c⊃4c**.

The splitting of the signal for the methyl protons of the guest when included in the assembly **1a•1a⊃4c** is due to the asymmetry provided by the unidirectional orientation of the urea groups provoking that the two hemispheres become enantiomeric (the local magnetic anisotropy of the chiral container influences differently the diastereotopic protons resonances of the encapsulated guest) although the whole assembly is *meso* and features an overall S_8 (C_4+S_2) symmetry. Moreover, we calculated the energy barrier for the interconversion process between the diastereotopic methyl protons of the guest **4c**, by means of an EXSY experiment, and we obtained the same value than the energy barrier required for the rotation that produces the change in the sense of the unidirectional orientation of the urea groups in the hydrogen-bonding belt ($\Delta G^{\ddagger}$ = 16.0 kcal/mol) of the capsule's equator. This result confirmed that the diastereotopicity induced in the methyl protons of the guest is due to the asymmetry provided by the unidirectional of orientation of the urea groups.

The ^{1}H-NMR spectrum of the ***R*-1b•*R*-1b⊃4c** encapsulation complex derived from the enantiomerically pure chiral tetraurea ***R*-1b** (**Figure 7b**) shows the expected number of proton signals for an assembly with two disterotopic hemispheres, each one having an apparent C_4 symmetry. As it was previously described by our group,[6] even though all

carbon stereogenic centers of the assembly have the same absolute configuration, the tetraurea monomers are cyclochiral diastereoisomers. This is due to the complementary relationships that exists between the sense of rotation of the two tetraurea calixpyrroles ***R*,M-1b•*R*,P-1b**. The notation of each cyclochiral monomer is *P* (clockwise turn) or *M* (counter clockwise turn) and it is defined from a position above the cavity (**Figure 8**). In addition, this complementarity forces a different spatial orientation of the H and $-CH_3$ benzylic substituents, with respect to the urea carbonyl group, in each cyclodiastereoconformer.

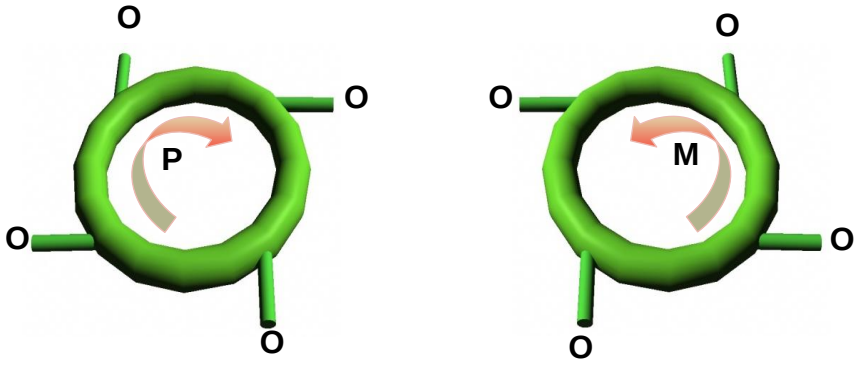

Figure 8: Senses of rotation of the urea belt: clockwise (*P*) and counter clockwise (*M*).

Two different signals are observed in the downfield region of the ^{1}H NMR spectrum corresponding to the pyrrolic NH protons (H_c) of the north and the south hemispheres that are diastereomeric. The benzylic methyne proton (H_i) and one of the urea NH protons (H_g) are also observed as two set of separated signals. Each signal in the set corresponds to the proton in a different diastereomeric hemisphere. The aromatic protons *ortho* to the urea group (H_a) appeared as two separate signals not four, probably due to a coincidence in chemical shift values. In this case, the asymmetry of the *ortho* aromatic protons is provoked by the slow rotation on the NMR time scale of both the urea belt direction and the phenyl rotation through the C_{meso}-C_{phenyl} single bond. This latter rotation has a high energy barrier when three-dimensional guests are included in the cavity of the tetraurea calix[4]pyrroles due to steric clashes with the *meso* phenyl

substituents. Our group previously reported that the encapsulation of 4,4'-dipyridyl-*N,N'*-dioxide **3** did not produce the splitting of the aromatic protons *ortho* to the urea groups at room temperature.[6] The explanation provided for this observation was that although the inclusion of bidimensional guest like **3** provokes that the change in direction of the urea belt is slow on the ^{1}H NMR timescale, as evidenced by the appearance of diasteropic signals for the benzylic protons in **1a•1a**, the rotation of the phenyl group through the C_{meso}-C_{phenyl} single bond is fast.

The protons of the methyl groups of the included guest **4c** in the chiral assembly ***R*,M-1b•*R*,P-1b⊃4c** appeared as four separate singlets, in contrast to just the two signals observed for the same protons of the guest encapsulated in the assembly **1a•1a⊃4c.** The observation of four separated singlets is the expected result for the inclusion of the two terminal –dimetylalkyl *N*-oxide knobs of **4c** in hemispheres that are diastereomeric. The coincidence in the values of the energy barriers, calculated from an EXSY experiment, for the change in direction of the urea belt (calculated from the integration of the pyrrolic NH protons cross-peaks, see **Figure 19b** in *Experimental Section*) and the chemical exchange process that occurs between the diastereotopic methyl protons of the guest encapsulated in the diastereomeric hemispheres ($\Delta G^{\ddagger}$ = 17.0 kcal/mol and $\Delta G^{\ddagger}$ = 16.5 kcal/mol, respectively) supports this hypothesis.

The chemical exchange process of methyl groups for the encapsulated guest in ***R*-1b• *R*-1b⊃4c** occurs between signals that correspond to protons included in the two diastereomeric hemispheres (see **Figure 19a** in *Experimental Section*). That is, when the urea belt rotates and changes its sense of direction, the *P* hemisphere is transformed into the *M* and vice versa, meaning that one hemisphere turns into its diastereomer. An indistinguishable assembly is obtained but the diastereomeric hemispheres have been interconverted: **(*R,M*·*R,P*)-1b$_2$⊃4c** to **(*R,P*·*R,M*)-1b$_2$⊃4c.** This hypothesis explains the existence of a chemical exchange process between the guest's methyl groups located in the two diasteromeric hemispheres of the capsule without having to invoke other dynamic processes like capsule disassembly and guest tumbling that can be associated with significantly higher energy barriers.

The equimolar combinations of tetraurea calix[4]pyrroles **1a** + enantiomerically pure ***R*-1b** (**Figure 7c**) and **1a** + bis-loop **1c** (**Figure 7d**) produced mainly the corresponding heteroassemblies **1a•*R*-1b⊃4c** or **1a•1c⊃4c**, respectively. In the assembly of **1a•1c⊃4c**, the ^{1}H NMR analysis of the mixture reveals the presence of small signals in the downfiled region corresponding to the pyrrolic NHs homoassembly **1a•1a⊃4c**. The process to obtain exclusively the heterocapsule **1a•*R*-1b⊃4c** as the major assembly in solution was very fast (minutes). On the contrary, the obtainment of the **1a•1c⊃4c** heterocapsule as the major assembly was achieved after heating the NMR tube and adding an excess of the bisloop **1c** (1.2 eq of **1c** vs 1.0 eq of **1a**).

Not surprisingly, in both heteroassemblies **1a•*R*-1b⊃4c** and **1a•1c⊃4c**, the pyrrole NH protons and urea NH protons of each hemisphere resonate as two separate signals as expected for chemically non-equivalent hydrogens. The two signals of each set are not involved in chemical exchange confirming their chemical non-equivalency. Interestingly, the 2D NOE experiment revealed the existence of cross peaks (close spatial proximity) between the signals of the NHs of the pyrroles and ureas and signals of the protons of the encapsulated guest.

The ^{1}H NMR spectrum of the heteroassembly containing the non-chiral tetraurea and the enantiomerically pure tetraurea, **1a•*R*-1b⊃4c** shows 4 signals (two sets of two signals) for the methyl protons of the included guest. Upon capsule formation **1a** adopts a cyclochiral conformation (M or P) due to the complementarity relationships that exist between the senses of direction of the urea groups in each hemisphere. Consequently, the protons of the encapsulated guest become diastereotopic. The tetraurea ***R*-1b** is already chiral and adopts a cyclodiasteromeric conformation that complements with that of **1a**. The protons of the guest included in the hemisphere of ***R*-1b** are also diasterotopic. Because the hemispheres of **1a** and ***R*-1b** are chemically non-equivalent four different signals are observed for the methyl protons of encapsulated **4c**. One might expect the formation of two diastereomeric capsules from the combination of **1a** and ***R*-1b: M-1a•*R*,P-1b** and **P-1a•*R*,M-1b**. If this was the case, we should observe eight separate signals for the methyl proton of the encapsulated **4c**, four signals for each guest included in a different diastereomeric assembly.

Our group reported that the self-assembly of the achiral tetraurea **1a** and the enantiomerically pure tetraurea **1b** experiences chirality induction from the carbon stereogenic center to a preferred sense of direction of the urea groups in **1b**. Thus, it has been demonstrated that tetraurea ***R*-1b** induces an *M* sense of direction and tetraurea ***S*-1b** prefers a *P* sense of direction of urea groups.[6] One of the two possible cyclo-diastereomeric conformations that can be adopted by ***R*-1b** on capsule formation is significantly higher in energy. This property induces the assembly of the heterocapsule between **1a** and ***R*-1b** as a single diastereomer: **P-1a•*R*,M-1b**. In other words, the change in the sense of rotation of the urea belt is energetically not allowed for **P-1a•*R*,M-1b**. In complete agreement with this observation we did not detect the existence of chemical exchange between the two different sets of two signals corresponding to the methyl proton of encapsulated **4c** in **P-1a•*R*,M-1b** (**Figure 21** in *Experimental Section*).

In the ^{1}H NMR spectrum of the capsular assembly with pseudo-rotaxane topology **1a•1c⊃4c** we expected to observe 4 separate signals (two sets of two singlets) for the methyl protons of the included guest. Surprisingly, only three signals are evident in the upfield region of the spectrum (**Figure 7d**). These three signals are consistent with the placement of the methyl groups of **4c** in two chemically non-equivalent hemispheres, because one of them integrates for six protons and the other two for three protons. Unexpectedly, two signals of diastereotopic methyl groups resonate at the same chemical shift and appear as a singlet that integrates for six protons.

EXSY experiments (**Figure 22**) revealed the existence of cross-peaks between the signals integrating for three protons each. This observation indicates the existence of a chemical exchange process between them and that they correspond to two diastereotopic methyl groups included in one of two hemispheres of **1a•1c⊃4c**. The barrier of the chemical exchange process was calculated to be 17.3 kcal/mol, a value that coincides well with the energy barrier for the rotation of the sense of direction of the urea belt, that interconverts the capsule into its enantiomer **M-1a• P-1c** to **P-1a•M-1c**.

2.5. Dynamics of the exchange of capsules' hemispheres

We became interested in to investigating the dynamics of the exchange process involving capsules' hemispheres when homocapsules containing the same or different guests are mixed.

The ^{1}H NMR analysis of a close to equimolar mixture of preformed capsules homocapsules **1a•1a⊃4c** and ***R*-1b•*R*-1b⊃4c** in chloroform solution resulted in the observation of the heterocapsule **1a•1b⊃4c** (**Figure 9**) as the major component after 30 minutes elapsed (the heterocapsule is the major assembly but it coexists with the homocapsule **1a•1a ⊃4c** that was in slight excess at t=0). This result indicates that the self-sorting process of the homocapsules into the heterocapsule is almost exclusive $K_{ss} > 10^3$ and translates into a significant energy bias towards the heterocapsule. The statistically estimated self-sorting equilibrium constant for the isoenergetic dimeric assemblies is $K_{ss} = 4$, due to the energetic degeneracy of the heterocapsule.

Conversely, when 0.5 equivalents of **4c** are added to an equimolar suspension of the two tetraureas, the immediate ^{1}H NMR analysis of the resulting solution shows the exclusive assembly of the heterocapsule (*vide supra*). Taken together, these results indicate that the thermodynamic equilibrium of the self-sorting process is reached much faster when the suspension of tetraurea is used instead of pre-formed capsules. Most likely, the heterocapsule **1a•1b⊃4c** is more soluble than the homocapsules and the kinetics of the solubilization process are responsible for the different composition of the mixtures at t=0 for the two methodologies. The fact that the equilibrium for the self-sorting process using preformed capsules is reached after more than 30 minutes demonstrates that the exchange process of capsules' halves has a high energy barrier due to the elevated number of hydrogen bonds (16) that must be broken for the disassembly of the capsular aggregates into halves. It is worthy to note, that the study of these exchange processes is very sensitive to concentration and to the relative stoichiometric amounts of tetraureas and capsules employed, which are not always mixed in the precise amounts due to the technical difficulty when weighting.

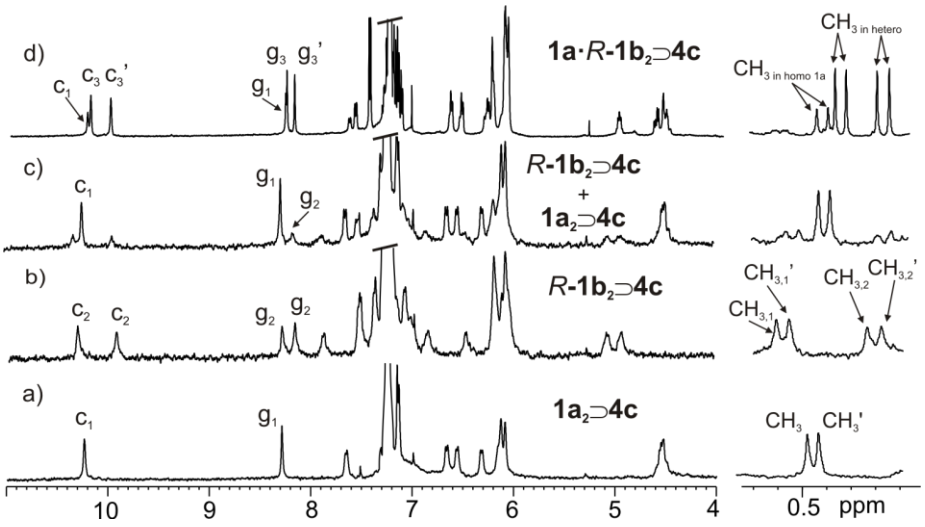

Figure 9: Selected upfield and downfield regions of the ^{1}H-NMR spectra in $CDCl_3$ of: a) homocapsule **1a•1a⊃4c**, b) homocapsule ***R*-1b •*R*-1b⊃4c**, c) heterocapsule **1a•*R*-1b⊃4c** starts to appear 30 min after mixing, and d) mixture of **1a•1a⊃4c + 1a•*R*-1b⊃4c**.

The mixture of two preformed homocapsule assemblies based on enantiomerically pure tetraureas and encapsulating the same guest, ***R*-1b•*R*-1b⊃4c** and ***S*-1b•*S*-1b⊃4c** (**Figure 10**) produced the heterocapsule as a minor component of the mixture several minutes after mixing. The heterocapsule was the exclusive assembly detected by ^{1}H NMR analysis of the mixture when the thermodynamic equilibrium was reached after t= 10 h.

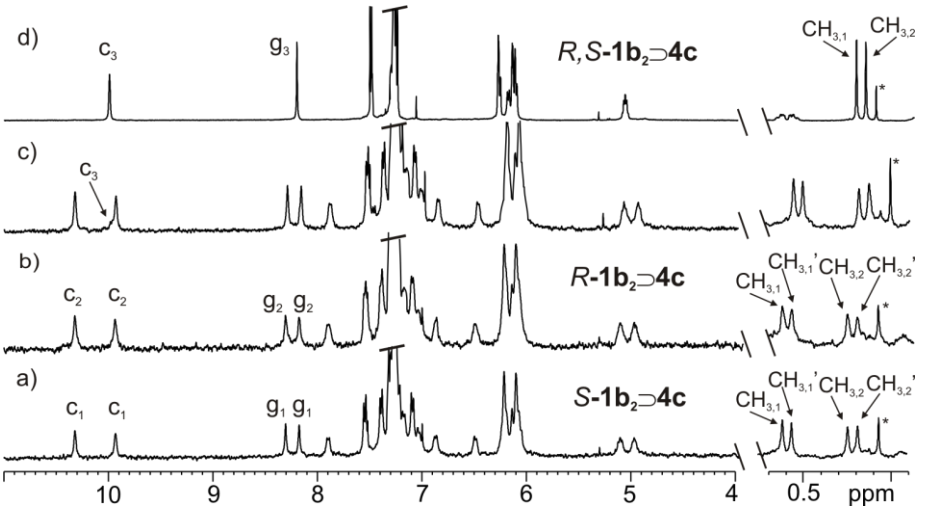

Figure 10: Selected upfield and downfield regions of the ^{1}H-NMR spectra in $CDCl_3$ of: a) homocapsule ***S*-1b •*S*-1b⊃4c**, b) homocapsule ***R*-1b•*R*-1b⊃4c**, c) mixture of homocapsules + heterocapsule ***R*-1b•*S*-1b⊃4c** which starts to appear immediately, and d) only heterocapsule present ***R*-1b•*S*-1b⊃4c**. * impurities.

The mixing of two enantiomeric homocapsules assembled from the enantiomerically pure tetraureas, ***S*-1b** and ***R*-1b**, but containing alkylic *N*-oxides of different length, ***S*-1b•*S*-1b⊃4b** and ***R*-1b•*R*-1b⊃4c**, afforded exclusively an equimolar mixture of the two heterocapsules in minutes demonstrating that the length of the included guests has a minimum impact in the kinetics of the self-sorting process (**Figure 11**).

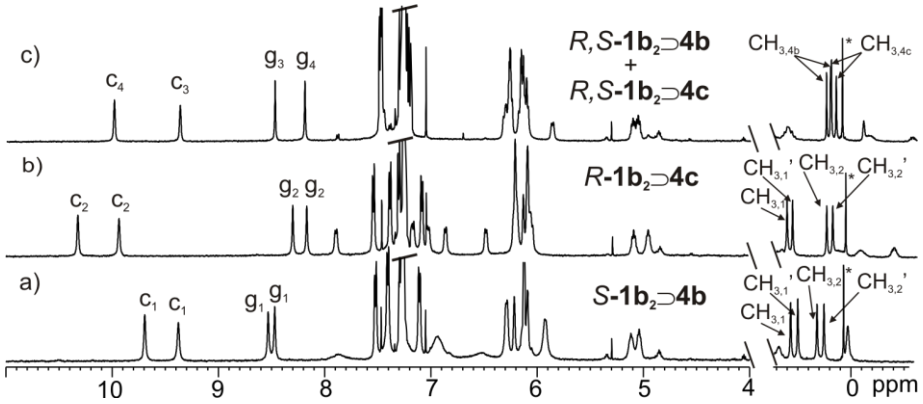

Figure 11: Selected upfield and downfield regions of the ^{1}H-NMR spectra in $CDCl_3$ of: a) homocapsule ***S*-1b•*S*-1b⊃4b** (assembly 1), b) homocapsule ***R*-1b•*R*-1b ⊃4c** (assembly 2), and c) heterocapsule ***S*-1b•*R*-1b⊃4b** (assembly 3) + heterocapsule ***S*-1b•*R*-1b⊃4c** (assembly 4) when the thermodynamic equililibrium was reached. * impurities.

Single crystals grew in the NMR tube from the chloroform solution obtained after mixing the two capsules ***S*-1b•*S*-1b⊃4b** and ***R*-1b•*R*-1b⊃4c**. Several of the obtained crystals were analyzed by X-ray diffraction. In all the attempts the crystals diffracted poorly, nevertheless the solid state structure of the crystal was partially solved and is depicted in **Figure 12**. The molecular structure of the encapsulated guest could not be fully solved due to severe disorder in the methyl groups of the *N*-oxide knob probably caused by the presence of two different guests in the encapsulation complexes forming the crystal packing. The structure of the encapsulation complex determined in the solid state coincides satisfactorily with the ones we proposed in solution. The urea belt of hydrogen bonds established between the urea groups that causes their unidirectional orientation is revealed. Interestingly, one molecule of acetonitrile is observed to be located in the external shallow cavity of the calix[4]pyrrole when the encapsulation complexes pack in the crystals. The formation of hydrogen bonds between the oxygen atom of the *N*-oxide knobs and the calix[4]pyrrole binding units is also detected in the solid-state.

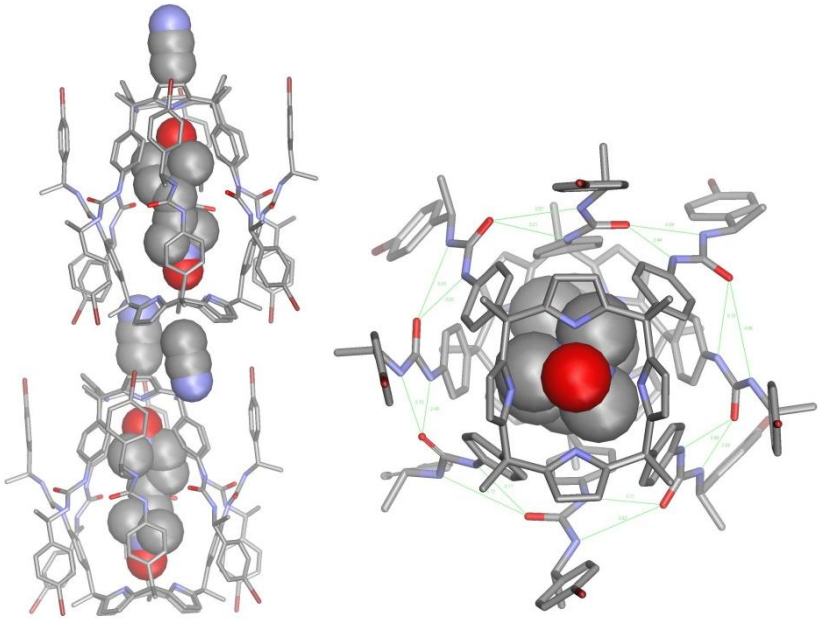

Figure 12: Solid-state (packing) structure from X-Ray diffraction of ***S*-1b•*R*-1b⊃4c** obtained after mixing chiral ***S*-1b•*S*-1b⊃4b** + ***R*-1b•*R*-1b⊃4c**. Crystals were obtained after a competitive experiment of mixing of two different capsules. Acetonitrile molecules are placed into the external pocket of the calix[4]pyrrole core. The crystal structure was not well resolved; there is a disorder in the guest. Encapsulated **4c** and solvent molecules are represented by CPK models. Hydrogen atoms are deleted for clarity.

3. Conclusion

We have shown that the assembly of dimeric capsule **1a•1a** can be templated by a series of bis(dimethyl-*N*-oxides) having alkyl chain spacers of different lengths. The capsule elongates and widens to accommodate the guest length. In turn, longer guests fold to adapt to the limiting dimensions of the capsule. The self-assembly adaptation process takes place as long as favorable binding interactions can compensate for the cost of a high-energy guest conformer to reside in the capsule's interior. The subtle balance of energies is not easy to deduce from simple molecular modeling studies. Furthermore, the methyl protons of the guests become diastereotopic when encapsulated. This asymmetry was proved to be transmitted by the unidirectionality of the rotation of the ureas of the host.

4. Experimental section

General information and instrumentation

Unless stated otherwise, all preparations were carried out under argon inert atmosphere and using standard techniques. All the reagents were obtained from commercial suppliers and used without further purification. Pyrrol was distilled under vacuum and freshly used. Anhydrous solvents were obtained from a solvent purification system SPS-800 from MBRAUN. HPLC grade quality solvents were obtained commercially and used without further purification. IR measurements were carried out on a Bruker Optics FTIR Alpha spectrometer equipped with a deuterated triglycine sulfate (DTGS) detector. Melting points were performed on a Mettler Toledo MP70 melting point system. Routine ^{1}H and ^{13}C NMR spectra were recorded with a Bruker Avance 400 (400 MHz) and Bruker Avance 500 (500 MHz) spectrometers with use of the solvent signals as internal reference. Flash chromatography was performed with Silica gel Scharlab60 and with Aluminium oxide 60, active basic, particle size 0.063-0.20 mm from Merck.

Synthesis

N,N,N',N'-tetramethylalkane bis-*N*-oxides 4 synthesis

The synthesis of bis-*N*-oxides **4a, 4b, 4d** was performed by oxidation of the corresponding commercial amines (1.24 g; 8.6 mmol) dissolved in methanol with hydrogen peroxide 30% aq. (1 g; 29.4 mmol) refluxing for 3 hours.[20,21] The product was purified by filtration in basic alumina.

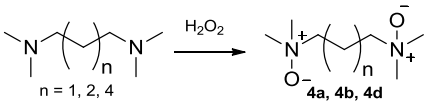

Scheme 1: Oxidation of the commercially available amines.

4a: hygroscopic white solid, 80%, ^{1}H-NMR (400 MHz, $CDCl_3$) δ (ppm): 3.44 (t, 4H), 3.41 (s, 12H), 2.58 (m, 2H).

4b: hygroscopic white solid, 75%, ^{1}H-NMR (400 MHz, $CDCl_3$) δ (ppm): 3.30 (m, 4H), 3.19 (s, 12H), 2.07 (m, 4H).

4d: hygroscopic white solid, 80%, ^{1}H-NMR (400 MHz, $CDCl_3$) δ (ppm): 3.22 (m, 4H), 3.17 (s, 12H), 1.93 (m, 4H), 1.44 (m, 4H).

The synthesis of guest **4c** was performed by dissolving sodium metal (1 g; 43.5 mmol) in methanol (10 mL) to obtain sodium methoxide (exothermic reaction). This solution was carefully added over dimethyl glutarate (30 mL, 200 mmol) under argon atmosphere. Then, a flux of dimethylamine gas was passed through the solution during 3 hours. The reaction mixture was stirred overnight. Methanol by-product and excess of dimethyl amine were slowly evaporated until a solid appeared. It was melted at 100ºC. Then, H_2SO_4 was added to neutralize the sodium methoxide present. The tetramethylglutaramide was obtained by distillation of the crude (130ºC, 2 mbar).[22] A solution of tetramethylglutaramide (3.2 g; 17.2 mmol) in diethyl ether (40 mL) was slowly added to a stirred suspension of lithium aluminium hydride (1.76 g; 46.4 mmol) in diethyl ether (80 mL) under argon atmosphere. The mixture was refluxed during 12 hours. Then, distilled H_2O (6mL) was slowly added to quench the reaction. The white salts obtained were filtered off and the solvent of the filtrate was evaporated. The crude product was purified by distillation using a Kugelrohr apparatus (90ºC, 15 mbar).[23] *N,N,N',N'*-tetramethylpentane-1,5-diamine (0.34 g; 2.16 mmol) was dissolved in methanol (0.5 mL) and added dropwise to a H_2O_2 30% solution (0.23 mL; 7.39 mmol). The reaction mixture was refluxed for 3

hours.[20,21] After evaporation of the solvent, the product was obtained by filtration in basic alumina of the crude product.

4c: hygroscopic white product, 35%, ^{1}H-NMR (400 MHz, $CDCl_3$) δ (ppm): 3.26 (m, 4H), 3.18 (s, 12H), 2.03 (m, 4H), 1.49 (m, 2H); ^{1}H-NMR (400 MHz, D_2O) δ (ppm): 3.26 (m, 4H), 3.10 (s, 12H), 1.79 (m, 4H), 1.35 (m, 2H); ^{13}C-NMR (100 MHz, D_2O) δ (ppm): 69.9 (CH_2), 57.3 (CH_3), 22.8 (CH_2), 22.6 (CH_2).

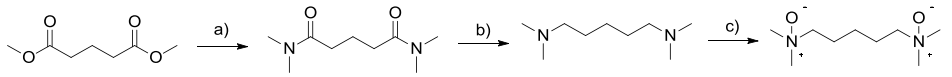

Scheme 2: Synthesis of *N,N,N',N'*-tetramethylpentane-1,5-diamine bis-*N*-oxide **4c**. a) $NaOCH_3$, $(CH_3)_2NH$, b) $Li[AlH_4]$, and c) H_2O_2.

Synthesis of guest **4e** was achieved by addition of 1,7-dibromoheptane (2.58 g; 10 mmol) to a stirred suspension of sodium carbonate (2.12 g; 20 mmol) in a mixture of EtOH/H_2O 4/1 (75 mL). Finally, the proper amount of dimethylamine (5.93 ml; 100 mmol) was added. The reaction mixture was refluxed for 24 hours. After that, the white solid was filtered off and the solvent of the filtrate was evaporated. The sticky yellowish residue was washed with diethyl ether (50 mL) to extract the product. The amine was obtained as a yellowish liquid.[16] Then, it was oxidized and purified as explained in the previous synthesis.

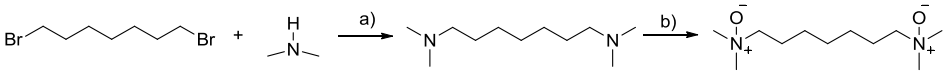

Scheme 3: Synthesis of *N,N,N',N'*-tetramethylheptane-1,7-diamine bis-*N*-oxide **4e**. a) Na_2CO_3, ethanol/water, and b) H_2O_2.

4e: white solid, 50%, ^{1}H-NMR (400 MHz, $CDCl_3$) δ (ppm): 3.20 (m, 4H), 3.15 (s, 12H), 1.88 (m, 4H), 1.38 (m, 6H); ^{13}C-NMR (100 MHz, D_2O) δ (ppm): 70.4 (CH_2), 57.0 (CH_3), 28.0 (CH_2), 25.5 (CH_2), 22.7 (CH_2).

Tetraurea bisloop calix[4]arene 1c

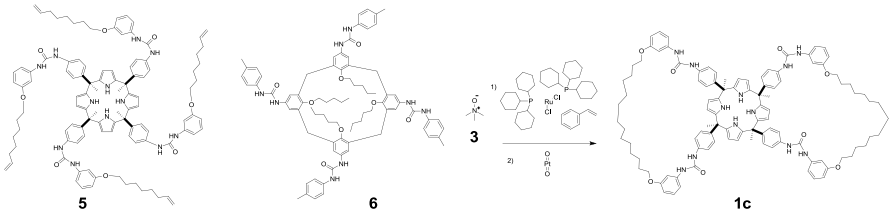

Tetraurea alkenyl calix[4]pyrrole **5**[24] (570 mg, 0.33 mmol), tetraurea calix[4]arene **6** (474 mg, 0.36 mmol) and trimethylamino *N*-oxide **3** (25 mg, 0.33 mmol) were dissolved in dry dichloromethane (300 mL, SPS quality), previously degassed by an argon flow. Then, a Grubbs I (111 mg, 0.3 mmol) catalyst solution in dichloromethane (100 mL) was added via cannula and the yellow-transparent solution turned brown immediately. It was left stirring under argon flow. The reaction was monitored by ^{1}H NMR spectroscopy. After 3h 30' the proton signals of calix[4]pyrrole **5** double bonds totally disappeared and a new proton signal (5.3 ppm) corresponding to a double bond appeared. Triethylamine (3-4 mL) was added over the reaction mixture and it was left stirring for 1 hour. After that, it was evaporated until dryness. The black residue was dissolved in THF (no stabilized) and methanol was added in order to precipitate the calix[4]arene **6**. The mixture was kept in the fridge to allow the total precipitation. 86 % of the initial calix[4]arene **6** was recovered using this precipitation method. The solid obtained from the mother liquors was purified by two silica column chromatography using as eluent a mixture THF/hexane 2/3, 1/0 in the first one and

methanol/dichloromethane 2/98 in the second one. The grey solid product obtained was dissolved in THF and hydrogenated using PtO_2 (75 mg, 0.33 mmol) under hydrogen atmosphere. The reaction was again monitored by ^{1}H NMR spectroscopy. The reaction mixture was filtered through celite and the crude product was purified by column chromatography (THF/hexane 2/3).

Grey solid, 300 mg, 50%, IR υ_{max} (cm^{-1}): 3330 (NH stretching), 1670 (C=O stretching); ^{1}H-NMR (400 MHz, DMSO) δ (ppm): 9.56 (br s, 4H), 8.57 (s, 4H), 8.48 (s, 4H), 7.32 (d, 8H), 7.09 (m, 8H), 6.86 (d, 8H), 6.80 (br s, 4H), 6.49 (m, 4H), 5.95 (br s, 8H), 3.88 (t, 8H), 1.78 (m, 16H), 1.63 (m, 10H), 1.37 (m, 12H), 1.22 (m, 32H). m. p.: T = 135-145ºC.

Individual binding experiments

Binding experiments

Individual encapsulation experiments were performed by adding 1 equivalent of the ditopic guests or 2 equivalents of the monotopic guests from a stock chloroform-*d* solution to an NMR tube containing a 1 mM suspension of the tetraurea calix[4]pyrrole **1** also in chloroform-*d*. Five to ten minutes after the addition, the resulting solution was analyzed using ^{1}H NMR spectroscopy.

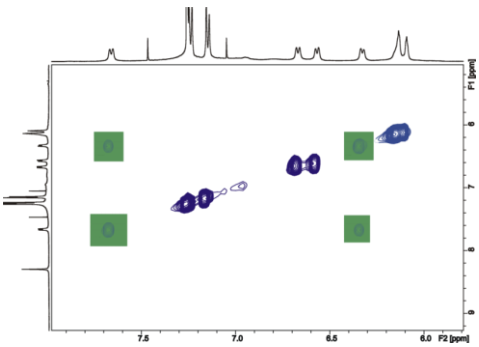

Figure 13: Selected aromatic region of an EXSY experiment for the assembly **1a•1a⊃4c**. The exchange cross-peaks marked in green are the ones used for barrier energy calculations.

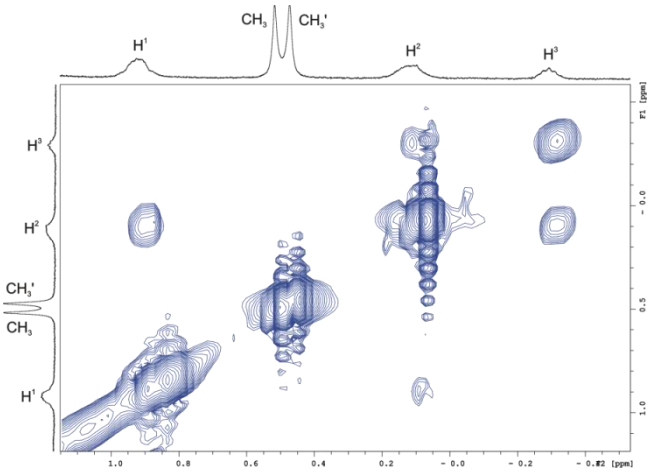

Figure 14: Upfield region of the COSY experiment corresponding to the assembly **1a•1a⊃4c**.

Calculation of the energy barrier of the rotation of the urea belt

The 2D EXSY experiments were run on 1 mM solutions of the corresponding capsular assemblies to calculate the energy barrier of the sense of rotation of the urea belt. The methodology for the calculation is explained using the assembly **1a•1a⊃4c** as an example. The mixing time was 0.3 s. The data size of the spectrum was 2048 x 256 points and 16 scans were taken. The rate constants were calculated using the D2DNMR software.[25] This program performs a kinetic matrix analysis of the cross peak intensities. The analysis provides the first-order rate constants for multisite exchange directly from the 2D EXSY spectrum peak volumes. Instead, the rate constants can be calculated applying the equation:[26]

$k = \frac{1}{\tau_m} ln \frac{r+1}{r-1}$ Where r is: $k = 4 \cdot \chi_A \cdot \chi_B \cdot \frac{I_{AA}+I_{BB}}{I_{AB}+I_{BA}} - (\chi_A - \chi_B)^2$

For example, the parameters obtained from the 2D EXSY of the assembly **1a•1a⊃4c** to calculate *k* were:

χ_A	0.5	I_{AA}	1	I_{AB}	0.95	τ_m	0.3 s
χ_B	0.5	I_{BB}	1	I_{BA}	0.95	**T**	298 K

Then, the free energy of activation was calculated by this equation which directly relates the free energy to the rate constant: $\Delta G^{\ddagger} = -RT ln \left(\frac{kh}{k_B T}\right)$; where h is the Planck constant ($1.58 \cdot 10^{-34}$ cal·s^{-1}) and k_B is the Boltzmann constant ($3.30 \cdot 10^{-24}$ cal·K^{-1}).

Competitive experiments between guests

Competitive experiments were carried out by adding 1 equivalent of the competing guest from a stock chloroform-*d* solution to an NMR tube containing a preformed capsular assembly of the guest to be displaced. The resulting solution was analyzed using ^{1}H NMR spectroscopy at different times.

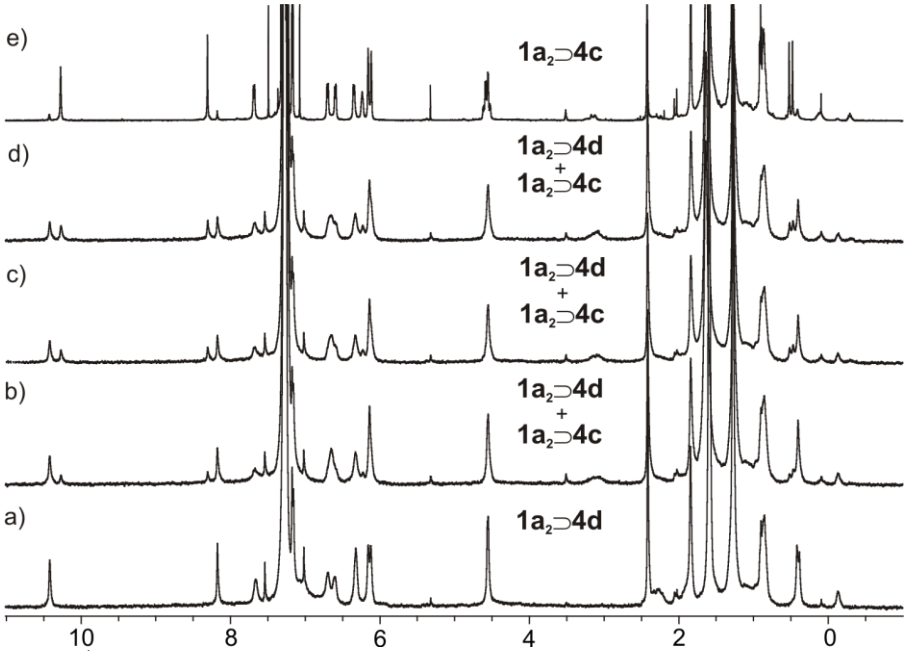

Figure 15: [1]H NMR spectra of the competition study of guest **4c** versus guest **4d**. a) **1a•1a⊃4d;** b) **1a•1a⊃4d** + 0.5 equivalents of **4c**, t = 0; c) **1a•1a⊃4d** + 0.5 equivalents of **4c**, t = 5 min; d) **1a•1a⊃4d** + 0.5 equivalents of **4c**, t = 10 min; e) **1a•1a⊃4d** + 0.5 equivalents of **4c**, thermodynamic equilibrium. Broad signal at 3 ppm corresponds to free guests. The competition of guest **4d** against guest **4c** was also studied but it is not showed here.

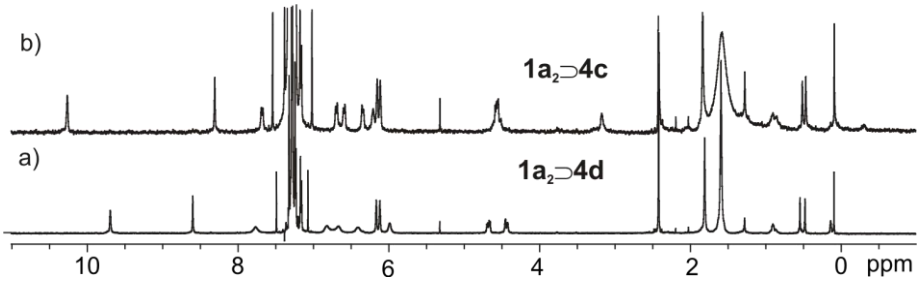

Figure 16: [1]H NMR spectra of the competition study of guest **4c** versus guest **4b**. a) **1a•1a⊃4b;** b) **1a•1a⊃4b** + 0.5 equivalents of **4c**, t = 0. The signals around 3 ppm correspond to free **4d**.

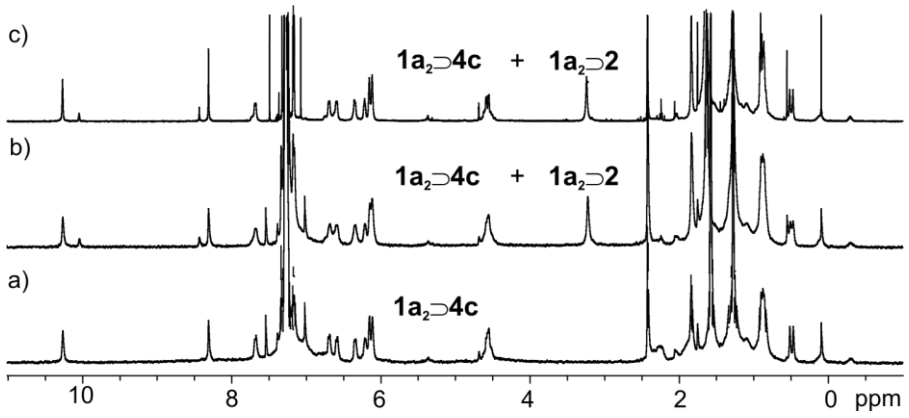

Figure 17: [1]H NMR spectra of the competition study of guest **2** versus guest **4c**. a) **1a•1a⊃4c;** b) **1a•1a⊃4c** + 1 equivalent of **2**, t = 0; c) **1a•1a⊃4c** + 1 equivalent of **2**, thermodynamic equilibrium. The competition of guest **4c** against guest **2** was also studied but it is not showed here.

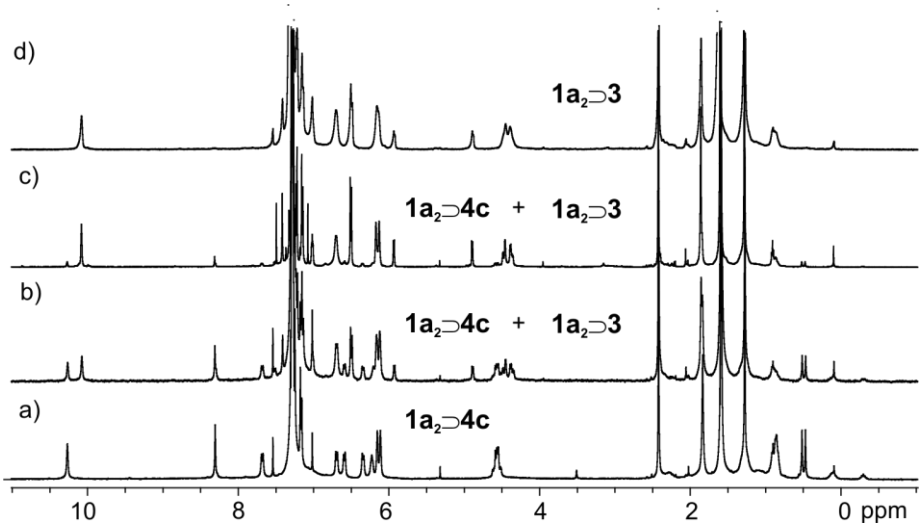

Figure 18: [1]H NMR spectra of the competition study of guest **3** versus guest **4c**. a) **1a•1a⊃4c;** b) **1a•1a⊃4c** + 0.5 equivalents of **3**, t = 0; c) **1a•1a⊃4c** + 0.5 equivalents of **3**, t = 6 min; d) **1a•1a⊃4c** + 0.5 equivalents of **3**, thermodynamic equilibrium. The competition of guest **4c** against guest **3** was also studied but it is not showed here.

Exploring the diasterotopicity of the guest signals

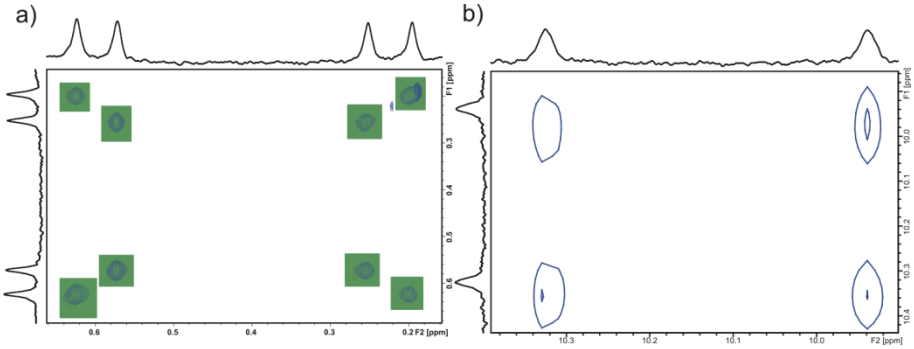

Figure 19: a) Upfield region of the EXSY experiment of the assembly **1b•1b⊃4c**. Cross-peaks between signals of the encapsulated guest placed in different hemispheres are visible. The exchange of these signals was calculated using the integration methodology, b) Downfield region of the ROESY experiment of the assembly **1b•1b⊃4c**. Cross-peaks between pyrrolic NHs.

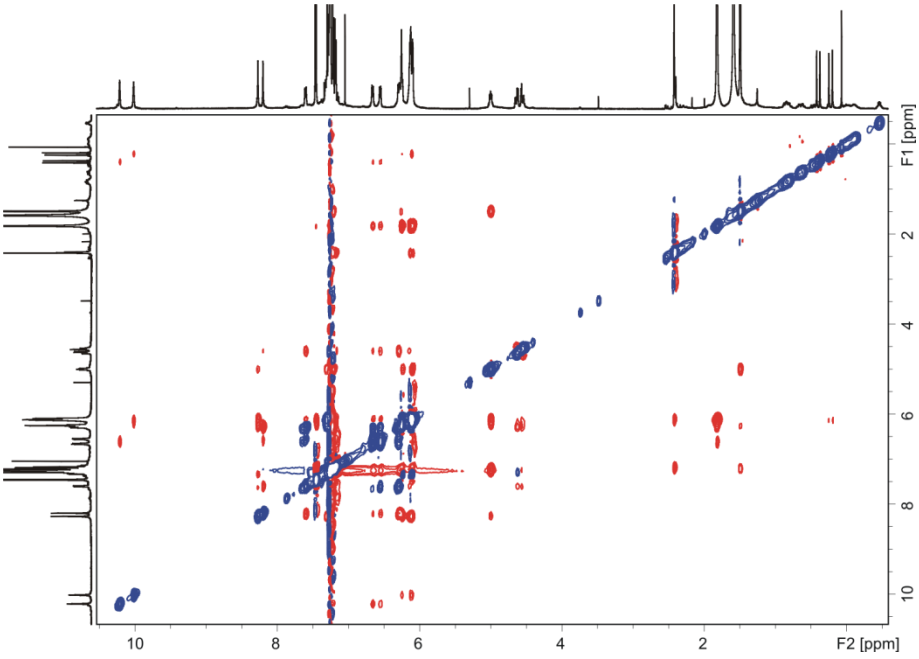

Figure 20: 2D ROESY experiment of the assembly **1a•*R*-1b⊃4c**. Intermolecular NOE contacts between the pyrrolic NH protons of the calix[4]pyrrole and the methyl protons of the encapsulated guest are visible.

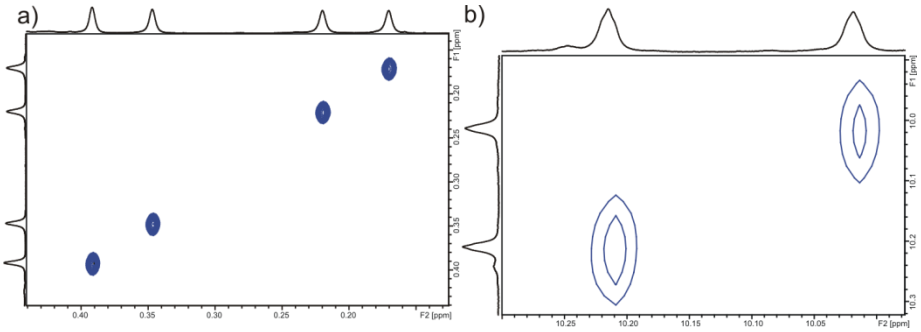

Figure 21: Bidimensional NMR experiments of the assembly **1a•*R*-1b⊃4c:** a) Upfield region of the 2D NOESY experiment. No cross-peaks between signals of the encapsulated guest are visible, b) Downfield region of the 2D ROESY experiment. No cross-peaks between the pyrrolic NH of different hemispheres.

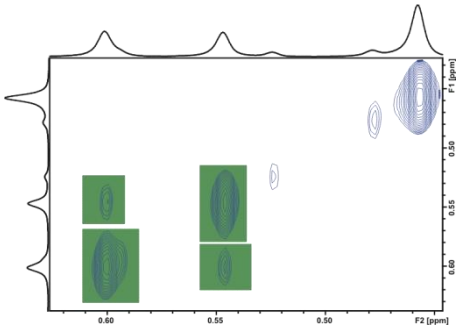

Figure 22: Upfield region of the 2D NOESY experiment of the pseudo-rotaxane assembly **1a•1c⊃4c**. Cross-peaks between signals of the encapsulated guest in one of the hemispheres are visible.

References and Notes

[1] Mecozzi, S.; Rebek, J. *Chem. Eur. J.* **1998**, *4*, 1016-1022.

[2] Swiss-Pdb Viewer 4.0.1 (cavity) http://spdbv.vital-it.ch and Mercury CSD (voids) http://www.ccdc.cam.ac.uk/mercury

[3] Korner, S. K.; Tucci, F. C.; Rudkevich, D. M.; Heinz, T.; Rebek, J. *Chem. Eur. J.* **2000**, *6*, 187-195.

[4] Gil-Ramirez, G.; Chas, M.; Ballester, P. *J. Am. Chem. Soc.* **2010**, *132*, 2520-2521.

[5] Ballester, P.; Gil-Ramirez, G. *Proc. Natl. Acad. Sci.* **2009**, *106*, 10455-10459.

[6] Chas, M.; Gil-Ramirez, G.; Escudero-Adan, E. C.; Benet-Buchholz, J.; Ballester, P. *Org. Lett.* **2010**, *12*, 1740-1743.

[7] Molokanova, O.; Bogdan, A.; Vysotsky, M. O.; Bolte, M.; Ikai, T.; Okamoto, Y.; Bohmer, V. *Chem. Eur. J.* **2007**, *13*, 6157-6170.

[8] Ajami, D.; Iwasawa, T.; Rebek, J. *Proc. Natl. Acad. Sci.* **2006**, *103*, 8934-8936.

[9] Mirtschin, S.; Slabon-Turski, A.; Scopelliti, R.; Velders, A. H.; Severin, K. *J. Am. Chem. Soc.* **2010**, *132*, 14004-14005.

[10] Gibb, C. L. D.; Gibb, B. C. *Chem. Commun.* **2007**, 1635-1637.

[11] The 3D nature of guests **4** makes the interconversion between aromatic meso-phenyl protons through rotation of the C_{meso}-C_{phenyl} bond to be sterically congested with a very high associated energy barrier.

[12] We assume here that an increase in the rotational energy barrier correlates with an energy stabilization in the hydrogen bonded state. Cozzi, F.; Ponzini, F.; Annunziata, R.; Cinquini, M.; Siegel, J. S. *Angew Chem Int Edit* **1995**, *34*, 1019-1020..

[13] The length and shape of the capsule is slightly modified in response to the size of the guest by sliding and flexing the urea arms, respectively. Both processes have a similar effect on the hydrogen bonding network of the urea belt.

[14] EXSY experiments revealed that the activation barrier for the interconversion between directional senses of the urea belt coincides with the interconversion barrier between diastereotopic methyl groups of encapsulated guests **4b** and **4c**, thus confirming the source of this latter asymmetry.

[15] Scarso, A.; Trembleau, L.; Rebek, J. *J. Am. Chem. Soc.* **2004**, *126*, 13512-13518.

[16] Liu, S.; Gibb, B. C. *Chem. Commun.* **2008**, 3709-3716.

[17] Jiang, W.; Ajami, D.; Rebek, J. *J. Am. Chem. Soc.* **2012**, *134*, 8070-8073.

[18] The coiling of the encapsulated guest probably has a reduced effect on its effective width due to the bulky N-oxide terminal knobs.

[19] Volumes and packing coefficients calculated after energy minimization of the structures.

[20] Bernier, D.; Wefelscheid, U. K.; Woodward, S. *Org. Prep. Proced. Int.* **2009**, *41*, 173-210.

[21] Steel, W. H.; Damkaci, F.; Nolan, R.; Walker, R. A. *J. Am. Chem. Soc.* **2002**, *124*, 4824-4831.

[22] Chas, M.; Gil-Ramirez, G.; Ballester, P. *Org. Lett.* **2011**, *13*, 3402-3405.

[23] Profit, A. A.; Lee, T. R.; Niu, J.; Lawrence, D. S. *J. Biol. Chem.* **2001**, *276*, 9446-9451.

[24] Chas, M.; Ballester, P. *Chem. Sci.* **2012**, *3*, 186-191.

[25] Abel, E. W.; Coston, T. P. J.; Orrell, K. G.; Sik, V.; Stephenson, D. *J. Magn. Reson.* **1986**, *70*, 34-53.

[26] Pons, M.; Millet, O. *Prog. Nucl. Magn. Reson. Spectrosc.* **2001**, *38*, 267-324.

CHAPTER 3

SYNTHESIS AND BINDING STUDIES OF SUPER-ARYLEXTENDED CALIX[4]PYRROLES

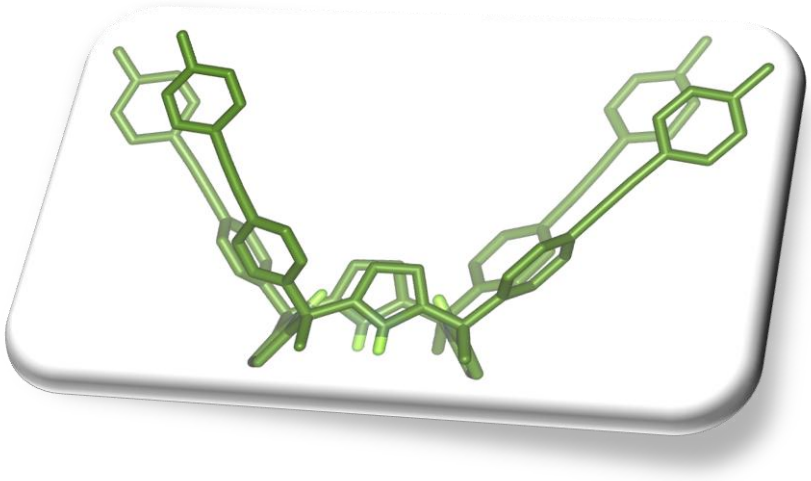

UNIVERSITAT ROVIRA I VIRGILI
REVERSIBLE MOLECULAR ENCAPSULATION IN SELF-ASSEMBLED AND MECHANICALLY LOCKED CONTAINERS WITH POLAR INTERIOR
Monica Espelt Ripoll
DL: T 1103-2014

1. Introduction

Previous work in our group has focused on the synthesis and encapsulation studies of *meso*-phenyl substituted tetraurea calix[4]pyrroles, known as aryl-extended calix[4]pyrroles. The dimerization of tetraurea derivatives of aryl-extended calix[4]pyrroles affords molecular capsules with an internal polar cavity and a volume of 312 Å^3, measured in the crystal structure of the capsular complex **2**⊂**1**·**1**.[1]

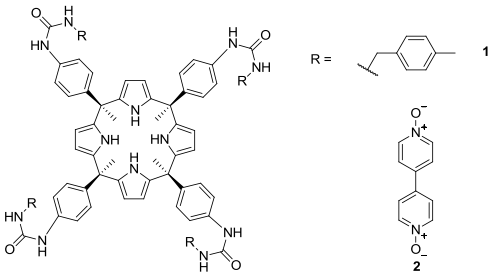

Figure 1: Molecular structures of aryl-extended tetraurea calix[4]pyrrole **1** and 4,4'-dipyridyl bis-*N*-oxide **2**.

The main objective of the work presented in this chapter is the elongation of the phenyl walls of a calix[4]pyrrole units in order to increase the volume of their aromatic cavity for the encapsulation of larger guests than the ones used so far.[2,3]

Several strategies for the expansion of a dimeric self-assembled capsule can be found in literature. For example, capsules derived from resorcinarene cavitands have been expanded by the use of glycoluril derivatives as spacer modules in the equator of a previously reported cylindrical capsule.[4] These spacers are complementary hydrogen bonding surfaces of the two main units of the capsular assembly. Extended and hyperextended cylindrical and curved[5] capsular assemblies were obtained by adding four,[6,7,8] eight [9,10] or twelve[9] spacer units. The extension of the capsules' length allowed for the encapsulation of longer guests. Another strategy to create capsules with larger internal cavities consists in increasing the number of phenyls or others aromatic panels present in the walls of the two monomers that shape the internal aromatic cavity. This

approach was employed to increase the aromatic cavity of calix[4]arene derived capsules using the Suzuki reaction.[11]

In order to increase the volume of the cavity provided by the α,α,α,α-isomer of an aryl-extended calix[4]pyrrole in the cone conformation, the lengthening of the phenyl walls seemed to us a sensible approach. The direct connection of two phenyl units (biphenyl) was discarded because the resulting biphenyl unit adopts a non flat conformation. That is, to avoid the steric interactions that exist between ortho and ortho prima protons, alpha to the single bond of the biphenyl unit in a flat conformation, an alternative conformation having a dihedral angle close to 20º is favoured. In this latter conformation, most of the enlarged space corresponding to the extra cavity is intruded by the aromatic panels defining it. To avoid this problem, already encountered when trying to enlarge the cavity of calix[4]arenes, the two phenyl groups (*meso* and extended) must be spaced through a triple bond rendering a complete co-planar unit.

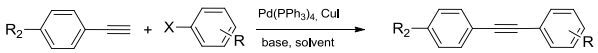

Scheme 1: Schematic representation of a general Sonogashira reaction.

The use of a Sonogashira reaction[12] (**Scheme 1**) would yield the desired phenyl-ethynyl-phenyl motif. The conjugation of the π-systems in this motif favours a co-planar conformation avoiding the intrusion of the cavity by the additional phenyl groups incorporated to the basic aryl-extended calix[4]pyrrole scaffold (**Figure 2**).

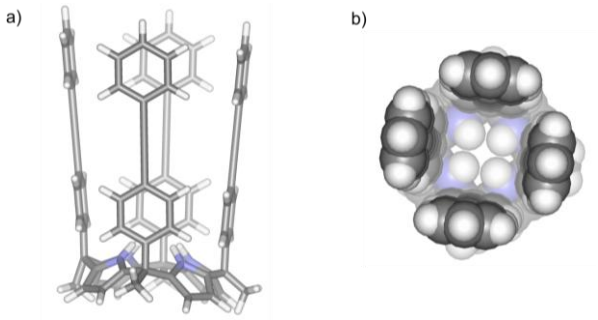

Figure 2: CAChe minimized structure of the super-extended aromatic calix[4]pyrrole that should be produced in the Sonogashira reaction: a) side view and b) top view of the CPK representation of the product.

An easy to obtain precursor for the elongation of the aromatic cavity of *meso*-phenyl substituted calix[4]pyrroles is the tetraiodo derivative **3** (**Scheme 2**). This compound possesses one iodo substituent in the *para*-position of its phenyl groups. Consequently, it can be easily elaborated into super-extended aromatic calix[4]pyrroles by using organometallic catalysis to promote C-C bond formation reaction with complementary aryl substituted compounds.

2. Results and Discussion

2.1. Synthesis

Super-extended calix[4]pyrroles **4** and **5** and tetraurea substituted super-extended calix[4]pyrroles **6** and **7** have been obtained following a general synthetic route based on the Sonogashira reaction. The starting material for this reaction was the α,α,α,α isomer of *p*-tetraiodophenyl calix[4]pyrrole (**Scheme 2**). The Sonogashira conditions consist on the reaction of our easily obtainable tetraiodo calix[4]pyrrole **3** and the appropriate 4-ethynyl-phenyl compound, with tetrakis(triphenylphospine) palladium (0) and cooper (I) iodide salt as catalysts in THF/Et_3N mixtures. This is a versatile synthetic method for obtaining calix[4]pyrroles with longer aromatic walls starting from the corresponding ethynyl compound.

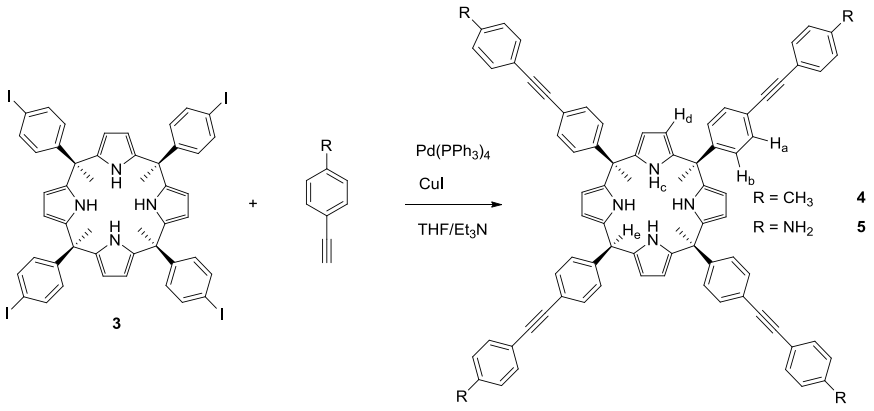

Scheme 2: Synthesis of super-extended calix[4]pyrrole **4** and tetraamine super extended calix[4]pyrrole **5.**

Single crystals of **4**, suitable for X-ray diffraction analysis were obtained from a dichloromethane/methanol solvent mixture.

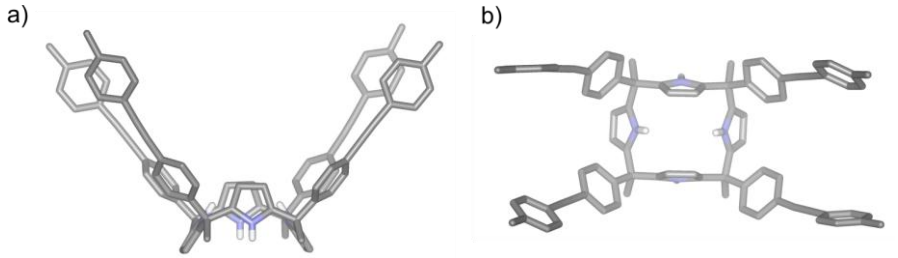

Figure 3: X-ray structure of super-extended calix[4]pyrrole **4** in a 1,3-alternate conformation, a) side view and b) top view.

The tetraurea calix[4]pyrroles **6** and **7**, were obtained by reaction of the tetraamine **5,** produced by Sonogashira reaction, with the corresponding isocyanate (**Scheme 3**).

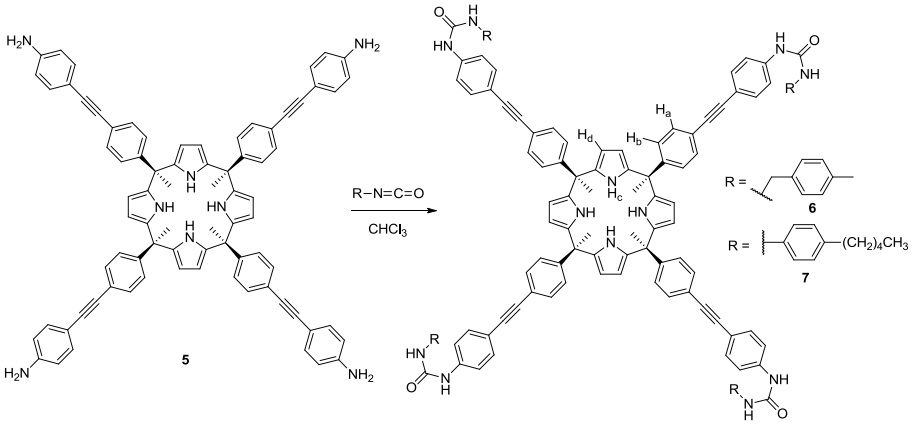

Scheme 3: Synthesis of super-arylextended tetraureas **6** and **7**.

The procedure used to synthesize the super extended tetraureas **6** and **7** is analogous to the one described in the literature to obtain aryl extended tetraurea calix[4]pyrrole derivatives.[2] All the isocyanates used were commercially available. The yields of the reactions producing the tetraurea calixpyrroles **6** and **7** are in the range of 40-50 %.

2.2. Binding studies

Super extended calix[4]pyrrole 4

Super-extended calix[4]pyrrole **4** was used to perform 1:1 complexation experiments in $CDCl_3$ (**4** was not soluble enough in acetonitrile to obtain a ^{1}H NMR spectrum) using dimethylamino pyridine *N*-oxide **8**, tetrametylphosphonium chloride **9** and tetrabutylamonium chloride **10** as guests (**Figure 4**). An stoichiometric amount of the corresponding guest was added to a 1 mM chloroform solution of the calix[4]pyrrole **4** and the ^{1}H-NMR spectrum of the solution was acquired. The results obtained in the complexation experiments were used to evaluate if the cone conformation was adopted by the bound receptor.

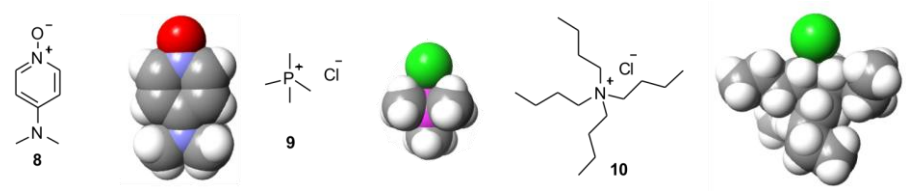

Figure 4: Molecules used in 1:1 complexation experiments with super-extended calix[4]pyrrole.

It is known from previous work with halide salts and aryl extended calix[4]pyrroles that, in general, the anion binds inside the aromatic deep cavity closed by the calix[4]pyrrole core and the cation is located in the external shallow cavity defined by the four pyrrole moieties in cone conformation (**Figure 5**).[13] The formation of four hydrogen bonds between the halide anion and the NH groups of the calix[4]pyrrole scaffold forces to position the anion above the planes of the π systems of the *meso* aryl substituents.[14] Other hydrogen-bonding acceptor substrates such as *N*-oxides have showed a similar tendency to be bound in the deep aromatic cavity of the calix[4]pyrrole moieties by means of hydrogen bonding, π-π and CH-π interactions.

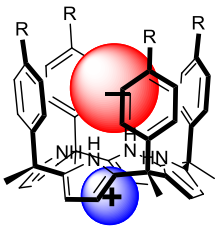

Figure 5: Schematic representation of an aryl extended calix[4]pyrrole receptor binding an ion-pair with a receptor-separated geometry. The anion is located in the deep aromatic cavity of the receptor and the cation is bound opposite to the anion in the shallow cavity defined by the pyrrole units in cone conformation.

We initially tested the complexation of *N*-oxide **8** with **4.** The addition of 0.5 equivalents of **8** to a chloroform solution of **4** induced the appearance of a new set of proton signals for the bound receptor. This result indicates that the binding process is slow on the ^{1}H NMR chemical shift timescale. When one equivalent of guest **8** was added to a calix[4]pyrrole **4** solution only the proton signals assigned to the bound host were observed in the ^{1}H-NMR spectrum of the mixture (**Figure 6c**). This observation suggest that the binding constant for the 1:1 complex **8⊂4** is larger than 10^4 M^{-1}. The signals of β-pyrrolic protons in the bound complex shifted downfield (6.13 ppm compared to 5.75 ppm for free **4**). The formation of the 1:1 complex was evidenced from the shift experienced by pyrrole NH protons resonating at 10.7 ppm in the bound receptor compared to 7.6 ppm in the free state. This significant change in the chemical shift of the NH protons indicates that the oxygen atom of the *N*-oxide **8** is hydrogen bonded to the NHs of the calix[4]pyrrole **4.** The addition of more than 1 equivalents of *N*-oxide **8** did not produce any change to the proton signals of the bound receptor. However, separate protons signals for the bound and free guest **8** were clearly detected. The signals of the aromatic protons for the bound guest **8** appeared upfield shifted ($\Delta\delta$ = 2.3 ppm) with respect to the free guest. In addition, the singlet corresponding to the methyl protons of the dimethylamino group in the bound *N*-oxide **8** also shifted downfield ($\Delta\delta$ = 2.18 ppm) from free guest due to the shielding that the aromatic rings from the host exert on the guest. Taken together, these observations indicate that the *N*-oxide **8** is included in the deep cavity of calix[4]pyrrole **4** and that the bound receptor **4** adopts the cone conformation. All the protons of the bound *N*-oxide **8** experience a

strong shielding, which is exerted by both the *meso* and the extended phenyl rings of the receptor **4**.

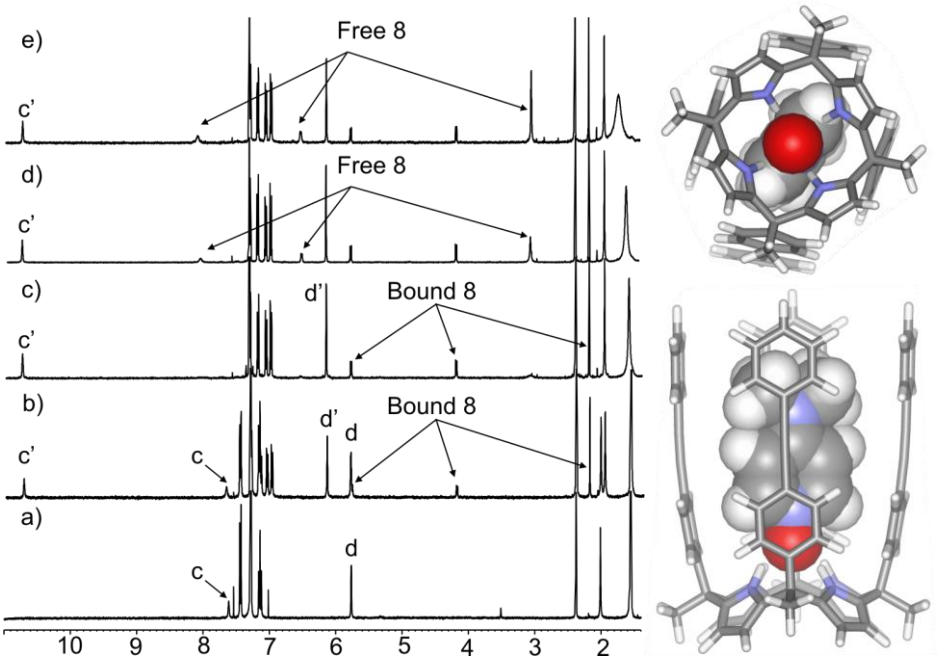

Figure 6: ^{1}H-NMR spectrum in $CDCl_3$ of a) **4**, b) **4** + 0.5 eq of **8**, c) **4** + 1 eq of **8**, d) **4** + 1.5 eq of **8**, e) **4** + 2 eq of **8**. Primed letters indicate bound host. See proton assignment in **Scheme 2**.

Next, we experimentally explored the inclusion of the two chloride salts in the cavities of **4**. The addition of less than 1 equivalent of tetramethylphosphonium chloride **9** to a chloroform solution containing host **4**, provoked the observation of separate proton signals for the free and bound receptor, indicating that the chemical exchange between them is slow on the ^{1}H NMR timescale (**Figure 7**). The signal of the methyl protons of tetramethylphosphonium cation of the ion-pair resonated at $\delta = 2.24$, d. This represents a significant upfield shift ($\Delta\delta = 1$ ppm) with respect to the signals for the methyl protons in the free ion-pair **9**. Most likely, the observed upfield shift for the methyl protons is due to the shielding caused by the pyrrole units of the calix[4]pyrrole core in conformation defining the shallow cavity where the cation is bound (receptor separated binding geometry). However, our results cannot rule the possibility that super extended calix[4]pyrrole **4** is able to bind the ion-pair **9** in close contact geometry. If this was the

case, the shielding experienced by the methyl protons of the phosphonium cation will result from the appended phenyl ring at the upper rim of **4**.

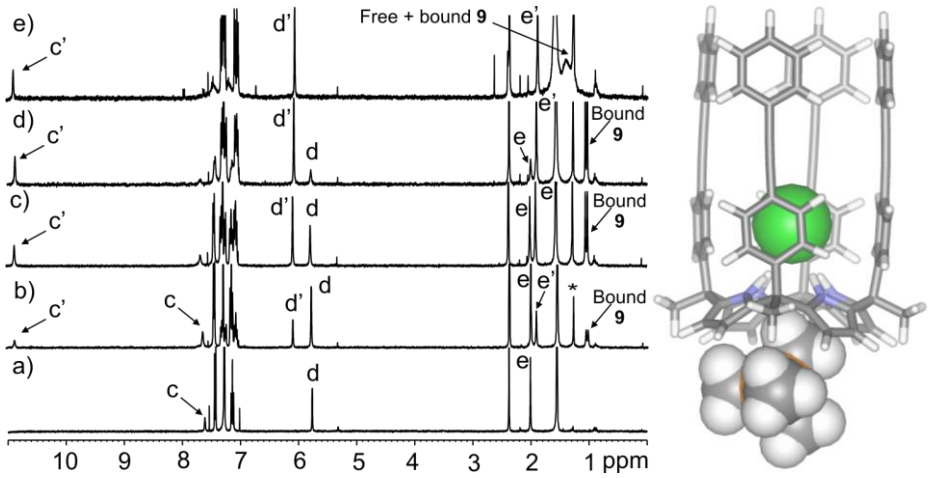

Figure 7: ^{1}H-NMR spectrum in $CDCl_3$ of a) **4**, b) **4** + 0.3 eq **9**, c) **4** + 0.6 eq **9**, d) **4** + 1 eq **9**, e) **4** + **9** excess. * impurity. Primed letters indicate bound host. See protons assignment in **Scheme 3**.

In close analogy to the binding studies performed with *N*-oxide **8**, the value of the binding constant for the **9⊂4** complex must be higher than 10^4 M^{-1} because in the presence of 1 equivalent of ion-pair **9** only the signals for the protons of the bound receptor are detected. When more than 1 equivalent of **9** was added, the chemical shifts of the proton signals of the bound **4** receptor were not affected. However, the proton signal of the methyl groups of the teramethylphosphonium (TMP) cation shifted downfield. This observation was indicative of the existence of a fast exchange on the ^{1}H NMR time scale between free and bound TMP cations. The inspection of different exchange dynamics between free and bound receptor and between free and bound cation pointed to the existence of two different exchange processes. Because of the inclusion of the anion in the deep aromatic cavity of **4**, the chemical exchange between free and bound host requires a conformational change of the calix[4]pyrrole core. Conversely, the chemical exchange between free and bound TMP cation seems to occur without this requirement. Thus, we conclude that TMP cation is located at the periphery of the anionic inclusion partially included in the shallow aromatic cavity distal to the bound

anion that is defined by the pyrrole rings of the calix[4]pyrrole core in cone conformation.

Finally, we investigated the complexation of tetrabutylammonium chloride **10** with receptor **4** (**Figure 8**). The ^{1}H-NMR spectrum of an equimolar mixture of **4** and **10** showed only signals for the protons of the free host and free guest. This result indicates that the binding process did not occur in any significant extent under these conditions. It is known that the tetrabutylammonium cation is a bad fit for the electron rich shallow cavity of the calix[4]pyrrole and that the effective complexation of ion pairs by calix[4]pyrrole receptors requires that both the anion and the cation have strong affinity for the binding sites of the receptor.[15,16]

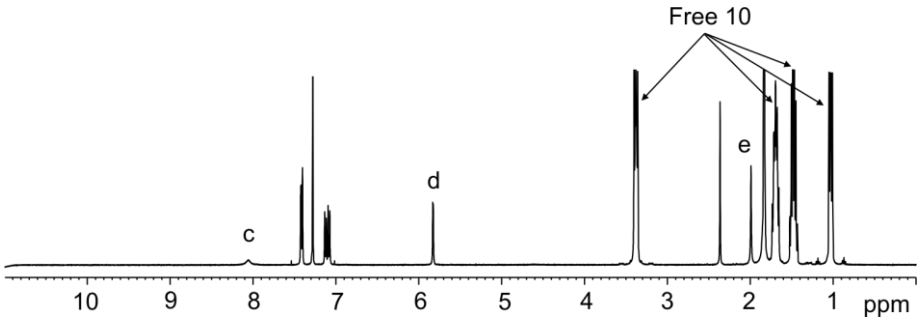

Figure 8: ^{1}H-NMR spectrum in $CDCl_3$ of **4** with large excess of **10**.

The obtained results in the previous complexation experiments provided some hints on the binding behaviour of the super-extended calix[4]pyrrole **4**. We demonstrated that receptor **4** binds ion-pairs and *N*-oxides in a similar manner than the parent aryl extended calix[4]pyrroles. For this reason, we decided to synthesize the corresponding tetraurea calix[4]pyrroles derived from the super-extended scaffolds and investigate their dimerization properties in order to produced capsular assemblies.

Tetraurea super-extended calix[4]pyrroles

Two tetraureas derived from the super-extended calix[4]pyrrole tetraamino scaffold were synthetized as described above. The potential dimerization of these tetraureas would provide dimeric capsules with polar interior and having an internal volume of

approximately 450 Å^3 (**Figure 9**). This represents an increase of 100 Å^3 with respect to the capsules assembled using tetraureas derived from the aryl extended calix[4]pyrrole.[1]

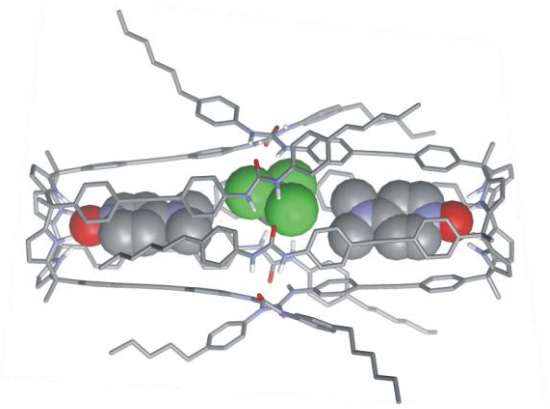

Figure 9: Energy minimized structure of a possible capsule **7⊃8•CHCl$_3$•8**

The super extended tetraurea calix[4]pyrrole **7** was synthesized as described above**.** Tetraurea **7** was significantly soluble in chlorinated solvent due to the alkyl substituents installed in the external phenyl groups. We investigated the potential self-assembly of **7** in dimeric capsules using several *N*-oxides and ion-pair as template molecules (**Figure 10**). All three experiments were carried out at 1 mM concentration of the tetraurea **7** in $CDCl_3$ solution.

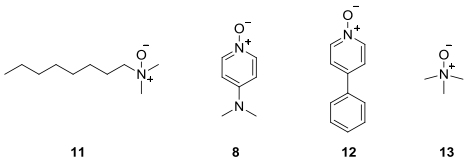

Figure 10: Molecular structures of the templates used in dimerization experiments of tetraurea calix[4]pyrrole **7**.

It is known that tetraurea aryl-extended calix[4]pyrroles need a suitable template to self-assemble into dimeric capsules. In our dimerization experiments we used exclusively mono *N*-oxides (**8**, **11**, **12** and **13**). We expected that the mono-*N*-oxides would act as monotopic guests. One molecule of *N*-oxide will be encapsulated in each one of the two endohedral binding sites of the putative dimeric capsule $\mathbf{7_2}$ and one or several molecules

of solvent will be located between the bound guests to complete the ideal packing coefficient of the cavity. In all cases, the ^{1}H-NMR spectra of equimolar mixtures of **7** and the *N*-oxides showed broad signals. We decide to focus on the chemical shift value of the pyrrole NHs. The observation of a downfield signal (>10 ppm) for the NHs protons indicates the existence of hydrogen bonding interactions between the tetraurea and the *N*-oxides.

In particular, the individual mixtures of tetraurea **7** with *N*-oxides **12** and **13** provided suspensions. In trying to induce the solubility of the suspension, we added few drops of deuterated THF. However, the suspension remained and we decided to filter it. For the experiment of the tetraurea **7** and trimethylamino *N*-oxide **13**, the analysis of the solution obtained after filtration using ^{1}H-NMR spectroscopy did not allowed the observation of proton signals. Conversely, the ^{1}H-NMR spectra of the solutions containing **7**+**11** and **7**+**12**, revealed the presence of a downfield shifted signals resonating at 10.3-10.4 ppm. Although these signals appeared at the chemical shift values expected for the pyrrole NHs protons, we consider that they are too weak to be unambiguously assigned (**Figure 11**). In general, the ^{1}H-NMR spectra of these mixtures are so broad that no useful information could be extracted from them.

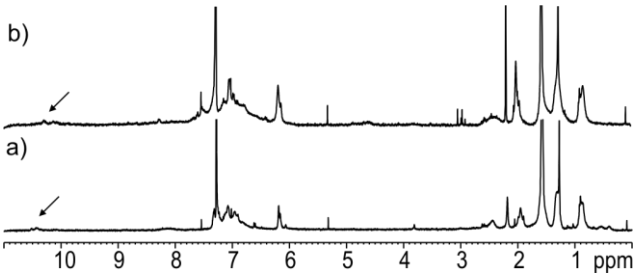

Figure 11: ^{1}H-NMR in $CDCl_3$ of: a) **7 + 11**; b) **7 + 12**.

Interestingly, the ^{1}H-NMR spectrum (**Figure 12**) of the solution obtained after the addition of an equimolar amount of dimethylamino pyridine *N*-oxide **8** to a suspension of tetraurea **7** shows one strong signal that could be assigned to bound pyrrole NH protons. In addition, two broad doublets resonating at δ = 5.77 and δ = 4.09 ppm and a singlet at δ = 1.98 ppm were visible. These doublets showed an intense cross peak in the

COSY spectrum of the above mixture (**Figure 13** in *Experimental Section*) and we assigned them to the aromatic protons of the bound *N*-oxide **8**. The high upfield shift experienced by the signals of the protons in the bound *N*-oxide ($\Delta\delta$ = 2.25 and $\Delta\delta$ = 2.40 ppm, for the aromatics, respectively; $\Delta\delta$ = 1.11 ppm, for the methyls), suggest that it is located in the deep aromatic cavity of the tetraurea calix[4]pyrrole **7** experiencing the magnetic shielding exerted by the aromatic walls.

The signals of the included guest **8** in the tetraurea calix[4]pyrrole **7** present a very close chemical shift to the protons of the guest **8** bound to the calix[4]pyrrole **4**. This means that the guest **8** is surrounded by the same chemical environment when included in both hosts (**4** and **7**) and, most probably, that the tetraurea calix[4]pyrrole **7** undergoes a conformational change to adopt the cone conformation upon guest inclusion.

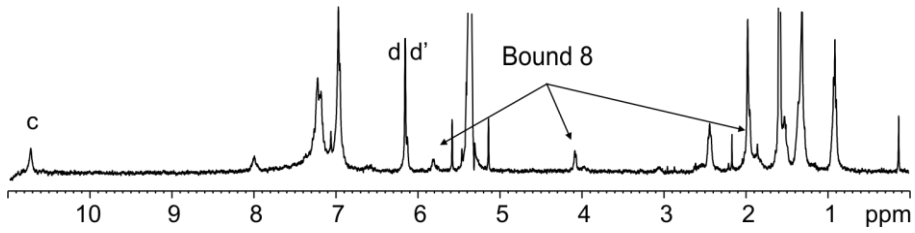

Figure 12: ^{1}H-NMR spectrum in CD_2Cl_2 of 1:1 mixture of **7** and **8**.

The chemical shift changes described above clearly support the existence of an interaction between tetraurea **7** and *N*-oxide **8**. Unfortunately, from this data it is not possible to conclude that the molecular capsule $\mathbf{7_2}$ has been assembled in solution. The formation of simple 1:1 complexes **8@7** represents a sensible alternative. In the search for additional information to verify or to rule out the formation of the capsule we analyzed the solution containing equimolar amounts of tetraurea **7** and *N*-oxide **8** using mass spectrometry. The MALDI$^+$ MS spectrum did not show any ion peak that could be assigned to the capsular assembly encapsulating two molecules of *N*-oxide **8** (MW: 3927), instead three ion peaks corresponding to monocharged species and with m/z ratios of 1894, 2032, and 3788 were obtained. The first peak can be assigned to the protonated ion of the tetraurea **7** (M+H), the second correspond to the protonated 1:1 complex **8@7** and the one appearing at the highest m/z ratio corresponds to a protonated

tetraurea dimer $\mathbf{7_2}$.[i] Taken in concert, the results obtained do not provide strong support to the assembly of the capsular architecture $\mathbf{8_2 \subset 7_2}$.

The reduced solubility demonstrated by the tetraurea super-extended species in chlorinated solvent was the main problem encountered in the study of their self-assembly into dimeric capsules.

3. Conclusion

The enhancement of the volume of the aromatic cavity of calix[4]pyrroles was achieved by increasing the length of the phenyl walls yielding the so-called super-arylextended calix[4]pyrroles and super-arylextended tetraurea calix[4]pyrroles. Binding of *N*-oxides was demonstrated for both super-arylextended calix[4]pyrroles and super-arylextended tetraureas calix[4]pyrroles showing similar binding behavior than their precursors, the aryl extended calix[4]pyrroles. Moreover, the super-arylextended calix[4]pyrroles were proved to bind also ion pairs.

It is worth noting that the self-assembly studies of super-arylextended tetraureas calix[4]pyrroles with *N*-oxides by NMR spectroscopy was particularly difficult due to solubility problems of the host. We could not found evidences of capsule formation with the molecules used as potential guest. Only 1:1 complexes could be characterized by mass spectrometry. Remarkably, these results are in contrast with the molecular modeling predictions.

Most probably, the success of tetraureas self-assembly lies in finding a guest(s) able to pre-organize both super-extended tetraureas around it (them) and fix them at the precise distance to build the urea belt hydrogen bond network. Additionally, the self-assembly should compensate for the cost of desolvation of the monomers to allow the interdigitation of the walls and construct the hydrogen-bonding network between the urea functions. More efforts should be directed towards the finding of a new guest that better fits the capsule's cavity.

[i] Probably this peak corresponds to an aggregate of two molecules of tetraurea **7**.

4. Experimental section

4.1. General information and instrumentation

Unless stated otherwise, all preparations were carried out under argon inert atmosphere and using standard techniques. All the reagents were obtained from commercial suppliers and used without further purification. Pyrrol was distilled under vacuum and freshly used. Anhydrous solvents were obtained from a solvent purification system SPS-800 from MBRAUN. HPLC grade quality solvents were obtained commercially and used without further purification. Routine ^{1}H and ^{13}C NMR spectra were recorded with a Bruker Avance 400 (400 MHz) and Bruker Avance 500 (500 MHz) spectrometers with use of the solvent signals as internal reference. Mass Spectrometry data were obtained from a Bruker Autoflex MALDI-TOF Mass Spectrometer. Flash chromatography was performed with Silica gel Scharlab60 and with Aluminium oxide 60, active basic, particle size 0.063-0.20 mm from Merck.

4.2. Synthesis

Synthesis super-extended calix[4]pyrroles 4, 5

4-iodoacetophenone (6 g, 24.39 mmol) was dissolved in CH_2Cl_2 (200 mL), flushed with argon and protected from light. Then HCl 37% (0.75 mL, 24.39 mmol) was added dropwise while stirring. Freshly distilled pyrrole was also added dropwise (1.7 mL, 24.39 mmol). The resulting mixture was left stirring at room temperature under argon protected from light during 68 hours. Dark solid precipitate was filtered off and methanol (250 mL) was added. CH_2Cl_2 was removed under vacuum and the resulting methanol solution was slowly evaporated to induce the precipitation of the tetraiodo calix[4]pyrrole. The precipitation process ended in the fridge overnight. The solid was filtered and washed with cold methanol first and then with cold acetonitrile. White crystals were isolated after crystallizing several times by diffusion in CH_2Cl_2/methanol. Tetraiodo calix[4]pyrrole **3** was obtained in 5% yield. Tetraiodo calix[4]pyrrole **3** (0.085 mmol), CuI (0.034 mmol) and $[Pd(PPh_3)_4]$ (0.034 mmol) were suspended in freshly distilled triethylamine (6 mL) while the system was under argon atmosphere. Then, the appropriate terminal alkyne (4-ethynyl toluene or 4-ethynylaniline) (0.678 mmol) was added and dry THF (4 mL) was added the last. After stirring at r. t. for 24 hours, the crude product was purified by column chromatography (CH_2Cl_2: hexane 1:1) to give the corresponding super-extended calix[4]pyrrole (**4** or **5**) in 40% yield. White crystals of **4** were obtained by diffusion of a CH_2Cl_2 solution through methanol.

4: 33 mg, white crystalls, 40%, ^{1}H-NMR (400 MHz, $CDCl_3$) δ (ppm): 7.61 (br s, 4H) 7.44 (d, 16H), 7.15 (d, 8H), 7.13 (d, 8H), 5.82 (d, 8H), 2.42 (s, 3H), 2.00 (s, 3H).

5: 55 mg, 45%, ^{1}H-NMR (400 MHz, $CDCl_3$) δ (ppm): 7.60 (br s, 4H), 7.40 (d, 8H), 7.35 (d, 8H), 7.10 (d, 8H), 5.76 (br s, 8H), 3.82 (br s, 8H), 2.00 (s,12H).

Synthesis of super-extended tetraureas 6, 7

Tetraiodo calix[4]pyrrol (100 mg, 0.085 mmol), CuI (8 mg, 0.042 mmol), $[Pd(PPh_3)_4]$ (30 mg, 0.042 mmol) and 4-ethynylaniline (40 mg, 0.339 mmol) were placed in a Schlenk tube. Then, freshly distilled triethylamine (6 mL) and THF (4 mL) were added while the tube was under argon atmosphere. The mixture was stirred at room temperature under argon atmosphere during 48 hours. Crude product was purified by column chromatography using CH_2Cl_2: methanol mixture (24:1) to yield 55 mg. Tetraamine (47 mg, 0.041 mmol) was suspended in $CHCl_3$ (5 mL) and 4-pentylphenyl isocyanate or methylbenzyl isocyanate (5 eq) was added dropwise. The resulting solution was stirred at room temperature under argon and light protected during 24 hours. The reaction mixture was evaporated until dryness. The brown solid was washed with methanol and filtered and dried under vacuum.

6: 36 mg, brownish solid, 40 %, ^{1}H-NMR (400 MHz, DMSO-d_6) δ (ppm): 9.60 (br s, 4H), 8.74 (s, 4H), 7.53 (d, 8H), 7.41 (d, 8H), 7.37 (d, 8H), 7.18 (d, 8H), 7.12 (d, 8H), 6.98 (d, 8H), 6.63 (t, 4H), 5.94 (br, 8H), 4.24 (d, 8H), 2.27 (s, 12H), 1.84 (br s, 12H).

7: 30 mg, brown solid, 40%, ^{1}H-NMR (400 MHz, DMSO-d_6) δ (ppm): 9.58 (s, broad, 4H), 8.80 (s, broad, 4H), 8.59 (s, broad, 4H), 7.56 (d, 8H), 7.44 (m, 16H), 7.32 (d, 8H), 7.06 (d, 8H), 6.99 (d, 8H), 5.97 (s, broad, 8H), 1.85 (m, 8H), 1.52 (m, 8H), 1.27 (m, 16H), 0.86 (t, 12H).

4.3. Binding studies

Individual inclusion experiments were performed by adding 1 equivalent of the corresponding guest from a stock CD_2Cl_2 solution to an NMR tube containing a 1 mM solution of the super-extended calix[4]pyrrole **4** or a suspension/solution of the tetraurea calix[4]pyrrole **7** in CD_2Cl_2. Five to ten minutes after the addition, the resulting solution was analyzed using ^{1}H NMR spectroscopy.

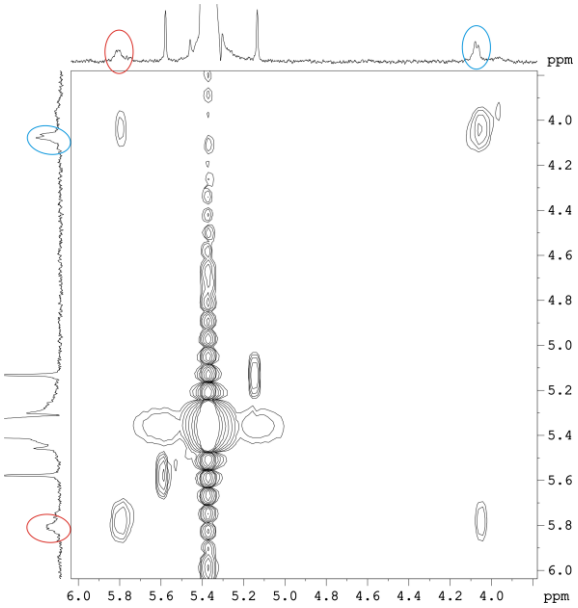

Figure 13: COSY experiment showing the correlation between the signals of the guest **8@7**.

References and notes

[1] Chas, M.; Gil-Ramirez, G.; Escudero-Adan, E. C.; Benet-Buchholz, J.; Ballester, P. *Org. Lett.* **2010**, *12*, 1740-1743.

[2] Ballester, P.; Gil-Ramirez, G. *Proc. Natl. Acad. Sci.* **2009**, *106*, 10455-10459.

[3] Gil-Ramirez, G.; Chas, M.; Ballester, P. *J. Am. Chem. Soc.* **2010**, *132*, 2520.

[4] Heinz, T.; Rudkevich, D. M.; Rebek, J. *Nature* **1998**, *394*, 764-766.

[5] Tiefenbacher, K.; Ajami, D.; Rebek, J. *Angew. Chem., Int. Ed.* **2011**, *50*, 12003-12007.

[6] Ajami, D.; Rebek, J. *J. Am. Chem. Soc.* **2006**, *128*, 5314-5315.

[7] Ajami, D.; Rebek, J. *Proc. Natl. Acad. Sci.* **2007**, *104*, 16000-16003.

[8] Ajami, D.; Rebek, J. *J. Org. Chem.* **2009**, *74*, 6584-6591.

[9] Ajami, D.; Rebek, J. *Angew. Chem., Int. Ed.* **2007**, *46*, 9283-9286.

[10] Taira, T.; Ajami, D.; Rebek, J. *J. Am. Chem. Soc.* **2012**, *134*, 11971-11973.

[11] Cho, Y. L.; Rudkevich, D. M.; Rebek, J. *J. Am. Chem. Soc.* **2000**, *122*, 9868-9869.

[12] Chinchilla, R.; Najera, C. *Chem. Soc. Rev.* **2011**, *40*, 5084-5121.

[13] Custelcean, R.; Delmau, L. H.; Moyer, B. A.; Sessler, J. L.; Cho, W. S.; Gross, D.; Bates, G. W.; Brooks, S. J.; Light, M. E.; Gale, P. A. *Angew. Chem., Int. Ed.* **2005**, *44*, 2537-2542.

[14] Gil-Ramirez, G.; Escudero-Adan, E. C.; Benet-Buchholz, J.; Ballester, P. *Angew. Chem., Int. Ed.* **2008**, *47*, 4114-4118.

[15] Valderrey, V.; Escudero-Adan, E. C.; Ballester, P. *Angew. Chem., Int. Ed.* **2013**, *52*, 6898-6902.

[16] Gross, D. E.; Schmidtchen, F. P.; Antonius, W.; Gale, P. A.; Lynch, V. M.; Sessler, J. L. *Chem. Eur. J.* **2008**, *14*, 7822-7827.

CHAPTER 4

SYNTHESIS AND BINDING STUDIES OF A BIS[2]CATENANE CALIX[4]ARENE – CALIX[4]PYRROLE MOLECULAR CAPSULE

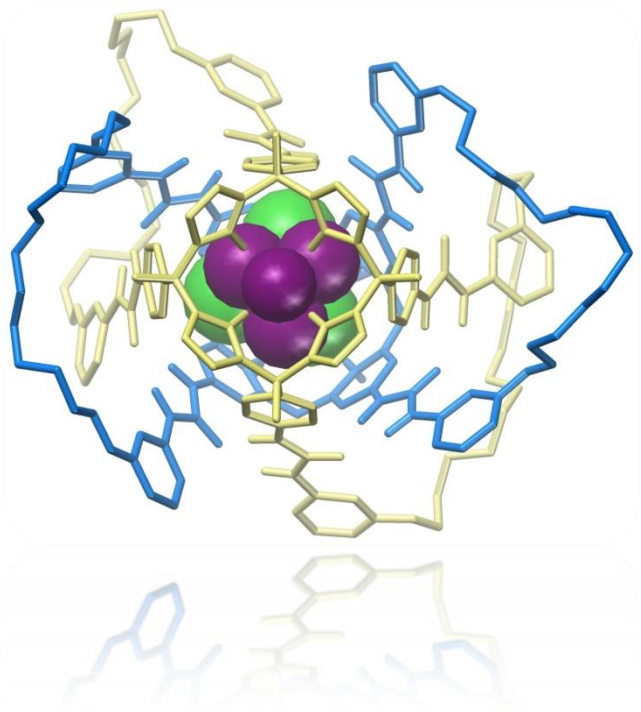

UNIVERSITAT ROVIRA I VIRGILI
REVERSIBLE MOLECULAR ENCAPSULATION IN SELF-ASSEMBLED AND MECHANICALLY LOCKED CONTAINERS WITH POLAR INTERIOR
Monica Espelt Ripoll
DL: T 1103-2014

1. Introduction

The capsules formed by two different hemispheres are of special interest as they present lower symmetry than the homocapsules analogues, making a completely anisotropic cavity. Previous works on self-sorting of tetraurea calix[4]arenes heterodimeric capsules reported by Rebek and Böhmer were based on the different functionalization of the two calix[4]arene components of the assembly.[1] Lately, an unprecedented exclusive self-sorting[2] of a hybrid molecular capsule was recently published in our group. The new system involved two different tetraurea components which are structurally similar scaffolds: a tolyl calix[4]arene **1a** and a benzyl calix[4]pyrrole **2** (**Figure 1**). Although both components were different, they presented good complementarity in the disposition of the urea groups to form the hydrogen bonding urea belt that holds together the two hemispheres of the heterodimeric capsule. Moreover, this molecular dimeric capsule had one polar hemisphere (the calix[4]pyrrole core) and displayed a bigger volume (280 $Å^3$) compared to the analogous heterocapsules based on tetraurea calix[4]arenes.

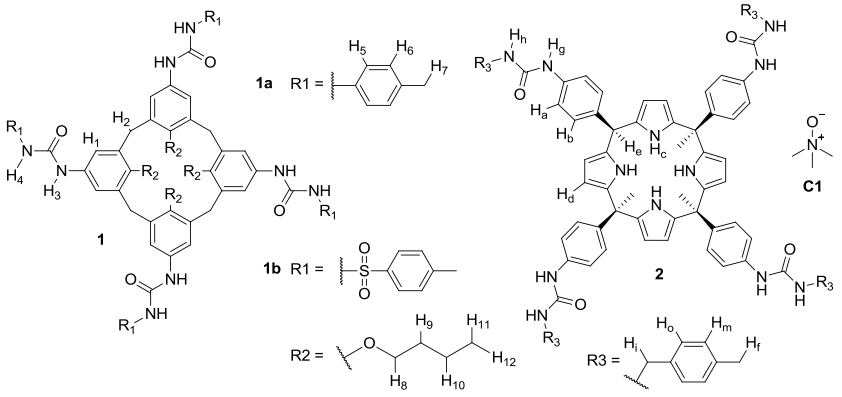

Figure 1: Calix[4]arenes **1a** and **1b** and calix[4]pyrrole **2**.

The self-sorting of this system was studied in two different solvents (chloroform-*d* and dichloromethane-d_2) and *N*-oxide **C1** was used as guest (**Figure 1**). This guest was ideal for the calix[4]pyrrole hemisphere, selectively oriented within the calix[4]pyrrole cavity through the formation of four hydrogen bonds with the pyrrole NHs.

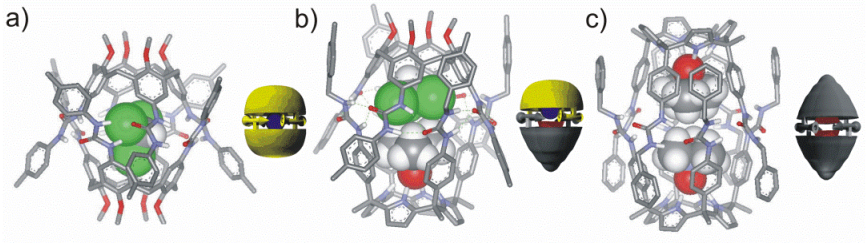

Figure 2: a) Homocapsule of calix[4]arene **1a·1a**; b) heterocapsule calix[4]arene-calix[4]pyrrole **1a·2⊃ C1**; c) homocapsule of calix[4]pyrrole **2·2⊃C1$_2$**.

The formation of three different assemblies was achieved when using chloroform-*d* as solvent (**Figure 2**): the known homocapsules of calix[4]pyrrole and calix[4]arene (solvent as guest) and a new hybrid capsule. It is worthy to note that in the mixture the calix[4]arene homocapsule **1a·1a** was the major assembly observed. On the other hand, the studies in dichloromethane-d_2 (**Figure 3**) revealed the exclusive formation of the hybrid capsule. In this case, the **1a·1a** capsule is not favored, as the Rebek's 55% occupancy rule[3] is not satisfied (dichloromethane-d_2 is a small solvent). It was observed that the solvent plays an important role in the self-sorting of the system not only by assisting the adequately filling of the cavity but by the maximization of the number of available intermolecular interactions due to the disruption of one of the possible homocapsules (**1a·1a**).

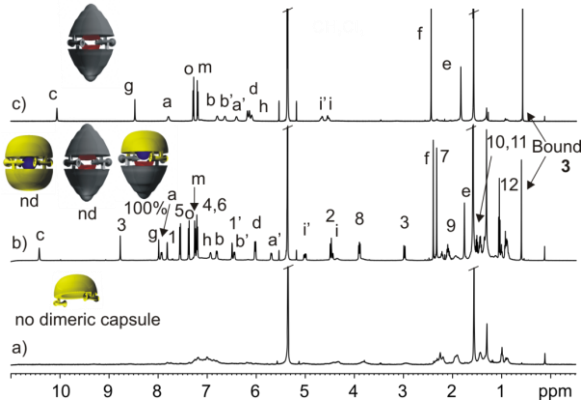

Figure 3: ^{1}H NMR spectra in CD_2Cl_2 of: a) calix[4]arene **1a**; b) capsule **1a·2**; c) homocapsule **2·2⊃C1$_2$**. nd: not detected.

In order to avoid the solvent influence and to create a thermodynamically more robust heterodimeric capsular system, a mechanically locked molecular capsule (**6**, **Scheme 1**) was designed and synthesized.[4] The knowledge of the formation of the exclusive heterodimeric capsule shown above in combination with other known assembly phenomena in calixarenes, i.e., the exclusive heterodimerization of capsules involving tetratolyl **1a** and tetratosyl ureas **1b**[1a-c] (**Figure 1**) to obtain bisloop tetraurea calix[4]arenes (like **3**),[5] were used in the synthetic strategy. The bisloop **3** cannot dimerize and can be efficiently employed in the synthesis of interlocked structures such as catenanes[6] and rotaxanes.[7]

The self-sorting behavior cannot exist in the mechanically locked bis[2]catenane **6**. Because both hemispheres are covalently linked, the hybrid capsule is the unique possible assembly regardless of the guest or solvent used.

The preliminary encapsulation experiments using bis[2]catenane **6** showed reversible molecular co-encapsulation of one neutral molecule (an *N*-oxide), two different neutral molecules (an *N*-oxide and a solvent molecule) or two oppositely charged ions (ion pairs).[4] With these results at hand, we were curious to evaluate the interior cavity by encapsulation of a series of *N,N'*-dimethylalkyl *N*-oxides with an increasing number of methylene units in its aliphatic chain. Likewise, the encapsulation behavior of the series of *N*-oxides was also evaluated in the supramolecular analogue capsule **1a·2** taking into account the influence of the solvent in the self-sorting (*vide supra*).[2]

In typical molecular capsules formed from other different cavitands (mainly based on calix[4]arenes), guests are devoid of organization when bound due to the lack of polar groups and only contribute with C-H-π interactions with the host to the thermodynamic stabilization of the encapsulation complex.[8] Conversely, in the work reported herein the *N*-oxide guest is anchored to the endohedral hydrogen bond donor sites of the calix[4]pyrrole moiety by hydrogen bonds. In this way, it can be compared to a co-factor of an enzyme or protein active site.

The bis[2]catenane **6** contains an anisotropic, polarized internal cavity. The calix[4]arene hemisphere consists of an electron rich surface able to include quaternary

ammonium species.[9] The calix[4]pyrrole deep aromatic cavity ended with four pyrrole NHs pointing inside is suitable for the inclusion of anions[10] and electron rich guests[11] anchoring the guests by hydrogen bonding interactions. Taking into account these properties, the ability of the bis[2]catenane **6** as receptor of ion pairs, biologically relevant zwitterions or electrochemically active-molecules receptor was also evaluated and the obtained results are described in this chapter.

2. Results and Discussion

2.1. Synthesis of the calix[4]arene-calix[4]pyrrole bis[2]catenane

The synthesis of the calix[4]arene-calix[4]pyrrole bis[2]catenane **6** was originally achieved in our group by Dr. Marcos Chas and reported in 2011.[4] After this initial account, the synthesis has been repeated to improve several steps and some purification procedures. The synthetic path to obtain compound **6** is far from being simple and consists of 14 synthetic steps and laborious chromatographic purifications.

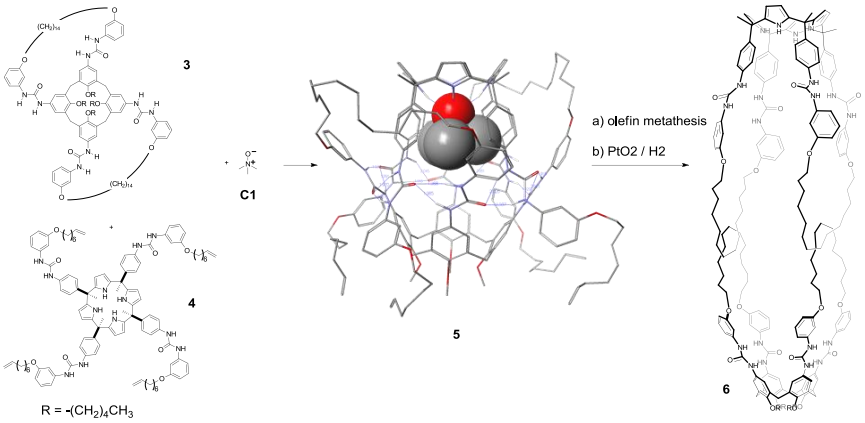

Scheme 1: Synthesis of the bis[2]catenane **6**.

Bis[2]catenane **6**, based on a calix[4]arene and a calix[4]pyrrole scaffolds, was obtained by metathesis reaction between bisloop calix[4]arene **3** and tetraurea alkenyl calix[4]pyrrole **4** using reaction conditions similar to those developed by Böhmer.[12] The assembly of the corresponding bis-pseudo-rotaxane capsule **5**, between the two partners

3 and **4,** was induced by the encapsulation of an adequate guest **C1** prior to the metathesis reaction. The use of the guest is a necessary condition to induce the cone conformation of the calix[4]pyrrole counterpart which is needed for the interpenetration of its urea arms through the loops of the calix[4]arene component. In turn, the tetraurea alkenyl calix[4]pyrrole **4** was prepared by acylation of the corresponding tetraamine[13] with the activated urethane.[14] The heterodimerization of **3** and **4** and the metathesis reaction were monitored by ^{1}H NMR spectroscopy. After metathesis and subsequent catalytic hydrogenation with PtO_2/H_2, the bis[2]catenane **6** was obtained as a white solid in 65 % yield after column chromatography purification.

2.2. Inclusion experiments

The binding studies carried out with the bis[2]catenane **6** are discussed in this section. The compounds used as guests were *N*-oxides, ion pairs, zwitterions and metallocenes.

2.2.1. Inclusion experiments involving *N*-oxides

Binding studies with single N-oxides.

The ^{1}H NMR spectrum of the "free" bis[2]catenane **6** (**Figure 5**a) in $CDCl_3$[i] solution shows both broad and sharp proton signals. Several proton signals were assigned based on the previous knowledge of the group in these types of assemblies. The sharp signals between δ = 9 – 9.5 ppm correspond to urea NHs (H_g, H_3) (see **Figure 4** for proton assignment). The pyrrolic NH protons, H_c, appear at 8.6 ppm. The signals for the aromatic protons are spread between 8 and 5.5 ppm. The β-pyrrolic protons, H_d, resonate at 6 ppm. Methylene bridges of the calix[4]arene, H_2, appear as diastereotopic protons in three different multiplets at 4.2 ppm (4H), 3.0 ppm (2H) and 2.9 ppm (2H). The O-CH_2 unit of the *meta*-substituted ring of both calixarene and calixpyrrole loops H_9, H_n gave a broad multiplet at 3.9 ppm and the O-CH_2, H_{10}, of the aliphatic chains of the calixarene core appear also as a broad multiplet signal at 3.7 ppm.

[i] Experiments were also performed in CD_2Cl_2 but they are not described here.

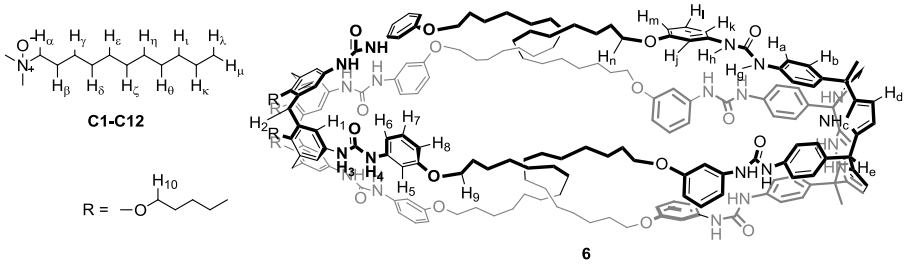

Figure 4: Bis[2]catenane **6** and *N,N'*-dimethylalkyl *N*-oxides **C1-C12** series used as guests in the encapsulation experiments.

The binding studies were performed by adding one equivalent of the corresponding *N*-oxide to a 1 mM solution of bis[2]catenane **6** in $CDCl_3$ and the encapsulation was studied by ^{1}H NMR spectroscopy.

The main diagnostic signals that indicate the inclusion of the *N,N*-dimethyl-*N*-alkyl *N*-oxide, inside a molecular assembly containing a calixpyrrole moiety are the chemical shift changes experienced by the pyrrolic NH protons and the signals of the included guest. The pyrrolic NH protons are downfield shifted to values higher than 10 ppm as a result of the hydrogen bond interaction established between the hydrogens of the pyrrolic NHs and the oxygen of the *N*-oxide guest. The proton signals of the guest appear upfield shifted as a consequence of the magnetic shielding provoked by the aromatic rings of the cavity. The chemical shift changes in the rest of the signals of the assembly will be discussed later on the chapter.

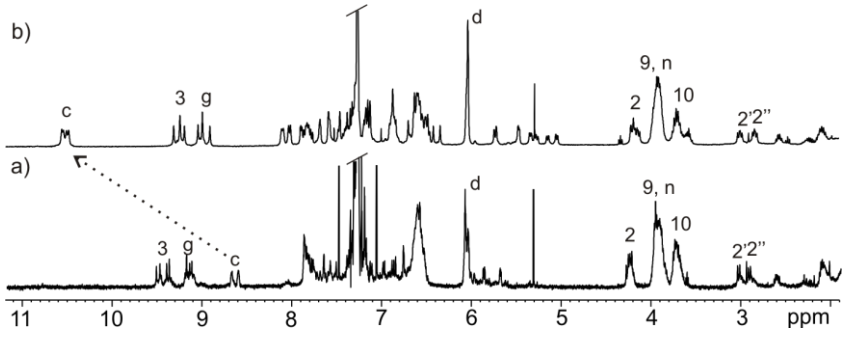

Figure 5: ^{1}H NMR spectra in $CDCl_3$ solution of: a) bis[2]catenane **6**; b) **6⊃3C**. Encapsulation of guest **C3** is selected as example to illustrate the change observed in the ^{1}H NMR spectrum of **6** upon guest encapsulation.

Upon guest encapsulation (**Figure 5b**), the pyrrole NH protons, H_c, shift downfield from *ca*. 8.6 ppm to *ca.* 10.5 ppm (the chemical shift change depends on how depth the included guest is placed into the calixpyrrole core). The observed downfield shift points out the existence of hydrogen bonding interaction between the NH pyrrolic protons of **6** and the oxygen of the encapsulated *N*-oxide guest. Additional proton signals of the bis[2]catenane **6** were assigned using 2D-NMR experiments (COSY, NOESY and ROESY). The proton signals corresponding to the *meta*-substituted rings could not be unequivocally assigned to a specific hemisphere due to lack of evidence.

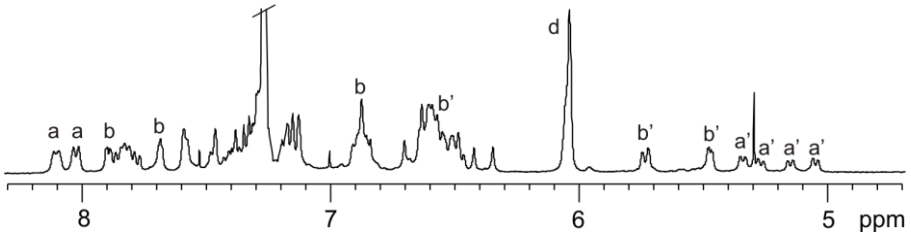

Figure 6: Selected region of the ^{1}H NMR spectrum of **6⊃C3.** The signals were assigned based on the 2D NMR experiments. Not all the proton signals could be identified.

The NH protons of the urea groups alpha to the calix[4]arene and the calix[4]pyrrole units resonate as eight different signals (4 + 4) due to the dissymmetric properties of the bis-catenane. The bis[2]catenane has C_2 symmetry with the C_2 axis coinciding with the molecular axis passing through the centroids defined by the four *meso* carbons and the four methylene bridges (**Figure 7**) (based on this symmetry we expect 2 signals for the urea NHs in each hemisphere: intraloop and extraloop). However, the unidirectional sense of direction of the urea groups that is present in the hydrogen bonding belt of **6** together with the slow interconversion between clockwise and anticlockwise directions on the ^{1}H NMR timescale adds an additional element of asymmetry to the bis-catenane.[4] (the 2 signals expected for the urea NHs in each hemisphere become diasteretopic and split into 4 different signals, a total of eight for the whole capsule because is composed of two different hemispheres). In short, the bis-catenane **6** and their complexes exist in solution as a mixture of two diastereomers.

The number of signals observed for the pyrrolic NH protons (4 signals in almost all inclusion experiments) is explained by the presence of two diastereomeric complexes as described above.

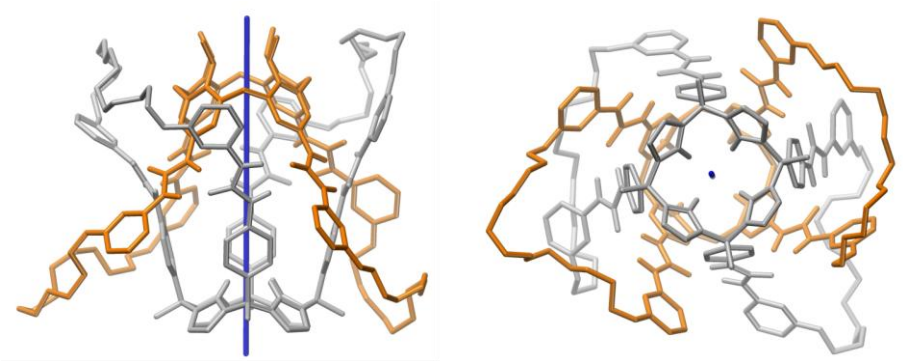

Figure 7: C_2 symmetry axis of the bis[2]catenane **6**. Side and top view.

The packing coefficients (PC) of the inclusion complexes were calculated and they are summarized in **Table 1**.[15] Taking into account these PC values one would expect that the inclusion would occur until the length of the alkyl chain in the *N*-*N*-dimethyl-*N*-alkyl *N*-oxide reaches a maximum of 6 carbon atoms (PC = 61%).

guest	guest volume (Å^3)	PC[ǂ]	guest	guest volume (Å^3)	PC[ǂ]
C1	90	32	C5	156	55
C1 + solv	167	59	C6	173	61
C2	106	37	C7	193	68
C2 + solv	178	63	C8	210	74
C3	124	44	C9	227	80
C3 + solv	193	68	C10	273	86
C4	140	49	C11	264	93
C4 + solv	218	77	C12	281	99

[ǂ] The cavity volume used to calculate the PC values was 284 Å^3, which was taken from *Chem. Sci.*, **2012**, *3*, 186-191.

Table 1: Guest's volume and packing coefficients calculated using Swiss-Pdb Viewer. From **C1**-**C6** (except for **C4**) the guest volume corresponds to an extended conformation; from **C7** to **C12** and **C4** the guest volume corresponds to a coiled structure to fit into the bis[2]catenane cavity. The solvent used in the packing coefficient calculations is chloroform-*d*.

We performed inclusion experiments, in order to compare the encapsulation behavior of the mechanically locked capsule **6** with that of the supramolecular analogue **1a•2** (similar internal volume) and to investigate the maximum length of the alkyl chain of the *N*-oxides that can be hosted in the cavities of the respective containers. The inclusion of the guest was confirmed by the downfield shift of the signal corresponding to pyrrolic NH and the upfield shift of guest signals (between 0.5 and -2.5 ppm) (see **Figure 8a**). From the obtained results with the supramolecular capsule **1a•**2 we conclude that *N*-oxide **C5** is the larger guest that can be accommodate in its internal aromatic cavity.

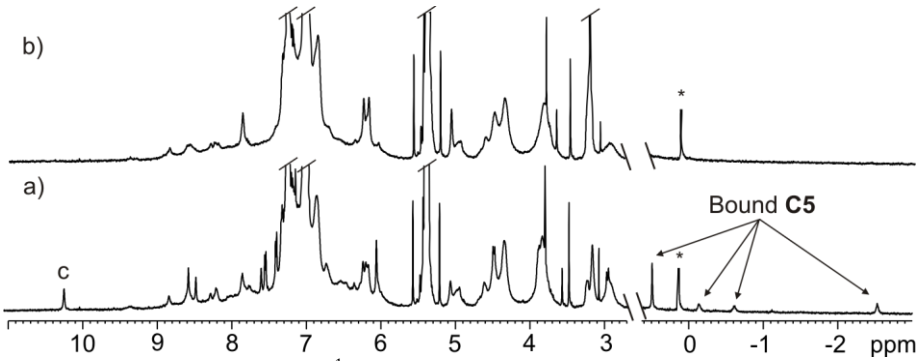

Figure 8: Selected regions of the ^{1}H NMR spectra in CD_2Cl_2 of: a) **1a·2⊃C5**; b) 1 equivalent of **C6** + 1 equivalent of **1a** + 1 equivalent of **2**. Guest **C6** does not get included into the supramolecular capsule. * impurities.

Conversely, we have observed encapsulation of *N*-oxides bearing up to 11 carbons alkyl chains in the interlocked bis-catenane capsular container **6**. The encapsulation of guests larger than **C5** has no precedent in the supramolecular assembly **1a·2**, analog to the bis[2]catenane **6**. Exploring in more depth the energy minimized molecular models of the complexes, we realized that the inner cavity of the bis[2]catenane **6** displayed significant different volumes depending on the included guest. Thus, these results demonstrated the ability of the catenane **6** to adapt its cavity volume to the guests' dimensions. In other words, a cavity modulation is exerted through inclusion of the guest. New packing coefficients were calculated from the energy minimized inclusion complexes (**Table 2**).

guest	guest volume (Å^3)	cavity volume (Å^3)	PC	guest	guest volume (Å^3)	cavity volume (Å^3)	PC
C1	90	271	33	**C5**	156	276	57
C1 + sol	167	279	60	**C6**	173	283	61
C2	106	270	39	**C7**	193	301	64
C2 + sol	178	282	63	**C8**	210	309	68
C3	124	273	45	**C9**	227	313	73
C3 + sol	193	284	68	**C10**	273	327	74
C4	140	268	52	**C11**	264	348	76
C4 + sol	218	314	69	**C12**	281	387	73

Table 2: Guest's volume, cavities' volume and packing coefficients calculated using Swiss-Pdb Viewer. The cavity volumes were calculated after guest deletion in the energy minimized structure. Even if guest **C12** and **C9** have the same packing coefficient it does not mean that **C12** should be included, as the calculated cavity volume also increased due to the higher volume of the guest. The solvent used in the packing coefficient calculations is chloroform-*d*.

The longest guest included into the bis[2]catenane **6** was **C11** (**Figure 27** displays the spectra of all the assemblies, *Experimental Section*), with a calculated PC = 76% which is a very high value and quite close to the packing density of proteins. These PC values (**Table 2**) of the inclusion experiments gave us an idea about the increased thermodynamic stability that the loops confer to the interlocked capsular assemblies compared to the supramolecular analogue.

The inclusions of large *N*-oxides are only possible when both hemispheres of the capsule are connected by mechanically bonds, so the capsular assembly cannot dissociate in its two halves. The loops of the bis[2]catenane **6** increase the thermodynamic stability of the urea belt and avoids the rupture of the hydrogen bonding array even when large guest are encapsulated. These large guests must experience strong folding to adapt its structure to the dimensions of the cavity. In doing so, energetically disfavored gauche interactions appear in the guest conformation that can be compensate only by the increase in thermodynamic stability of the hydrogen bonding belt provided by the bis-catenane topology of the container. On the contrary, the enthalpy gained during the assembly of the supramolecular container **1a·2** is not sufficient to overcome the enthalpy penalty provoked by the gauche interactions.

Upfield region. Co-encapsulation of solvent.

Analyzing more in depth the upfield region of the ^{1}H NMR spectra (see extension in **Figure 9**), we observe signals for the protons of the alkyl chain of the encapsulated guest spread out between 0.76 and -2.72 ppm. The number of signals in this region depends on the length of the alkyl chain of the encapsulated guest. The signals that are higher upfield shifted correspond to the protons more deeply included in the calix[4]arene cavity, due to the shielding of the aromatic rings. One could think that the protons more deeply included into the calix[4]arene hemisphere are those of the terminal methyl group of the alkylic chain, as we know that the guest *N,N*-dimethyl *N*-oxide knob is anchored within the calixpyrrole cavity. This statement is only true in the case of guests included in fully extended conformation and without a co-encapsulated molecule of solvent.

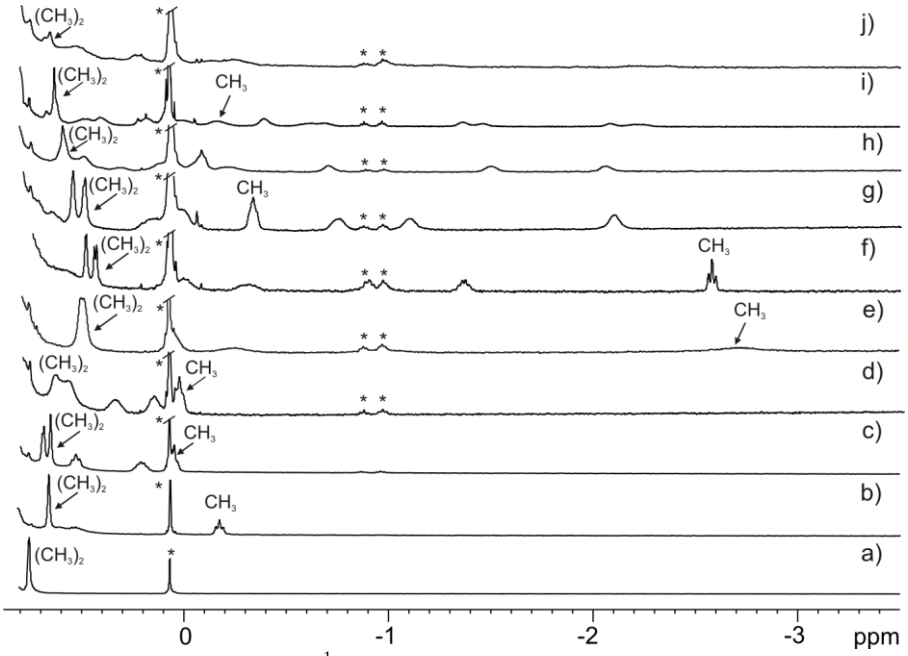

Figure 9: Upfield region of the ^{1}H NMR spectra in $CDCl_3$ of: a) **6⊃C1**, b) **6⊃C2**, c) **6⊃C3**, d) **6⊃C4**, e) **6⊃C5**, f) **6⊃C6**, g) **6⊃C8**, h) **6⊃C9**, i) **6⊃C10**, j) **6⊃C11**. * indicates impurities.

Molecular modeling studies indicated that *N*-oxide **C5** is the only guest that can be included in a fully extended conformation (7.56 Å, calculated from the oxygen to the furthest hydrogen), slightly helical, but it also fits with one gauche interaction. PC

calculations indicated that the supramolecular assembly **C5⊂6** features an optimal value of 57 % (**Table 2**). Guest **C6** folds in order to adapt to the limited dimensions of the capsule's interior. Based on molecular modeling studies, however, the included guest shows an almost fully extended conformation with a single gauche interaction. The most upfield shifted signal in the ^{1}H NMR spectrum for both guests, **C5** and **C6**, corresponds to the proton of the terminal methyl group of the alkyl chain. The methyl group must be deeply located inside the aromatic cavity of the calix[4]arene hemisphere. Interestingly, the terminal methyl group of the alkyl substituent in *N,N'*-dimethylpentyl *N*-oxide **C5** undergoes the most significant chemical shift change (3H, δ = -2.72 ppm, **Table 3**) for the complete *N*-oxides series.

capsule	cavity volume (Å^3)	Guests' terminal Me (ppm)	packing motif	chloroform co-encapsulation
7⊃C1	279	0,76	-	Yes
7⊃C2	282	-0,17	Extended	Yes
7⊃C3	284	0,047	Extended	Yes
7⊃C4	314	0,019	Folded	Yes
7⊃C5	276	-2,72	Extended	No
7⊃C6	283	-2,57	Extended-gauche	No
7⊃C8	309	-0,33	Folded	No
7⊃C10	327	-0,16	Folded	No

Table 3: Proton chemical shift values for the terminal methyl groups of the included *N*-oxides. The volumes of the cavity for each encapsulation complex and the conformation of the guest induced by the encapsulation are also indicated.

The broad proton signals observed for the included **C5** guest could indicate that the several conformation of the bound guest are in intermediate chemical exchange.

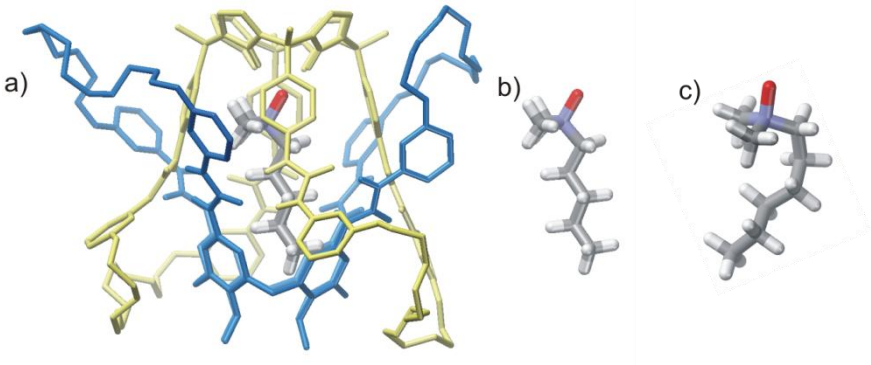

Figure 10: Energy minimized structures of: a) **6⊃C5**; b) **C5** exhibits an extended conformation (guest structure obtained after host deletion), c) **C6** gets included in a folded conformation (after host deletion).

The length of the capsule's cavity varies form from 10.53 Å when **C5** is encapsulated to 10.92 Å when **C9** is bound. The cavity length is measured as the distance between one nitrogen atom of the calixpyrrole core (NH) and the centroid of the calixarene core defined by the four methylene bridges. If the typical distance for a hydrogen bond (3 Å) is subtracted to the calculated cavity length (10.5-10.9 Å), we deduce that the molecules longer than 7.5 Å must fold to fit within the limits of the capsule. For example, **C8** in extended conformation is greater than the cavity size (11.38 Å vs 10.68 Å). Helical folding has been proposed as one of the most effective conformation to pack linear alkanes encapsulated in molecular capsules. We propose that large *N*-oxides also adopt helical conformations upon folding in the interior of **6**. The most upfield shifted signal in the encapsulation complexes **6⊃C8, 6⊃C9** and **6⊃C10** corresponds to a methylene group of the *N*-oxide alkyl. For example, methylene protons H_{κ} (**Figure 4**) in guest **C8** (**Figure 11**) are the most upfield shifted. The terminal methyl group of the alkyl chain in encapsulated **C8** exhibits a NOE cross-peak with one of the CH_3-N groups (*N*-oxide knob) supporting the folding of the bound guest.

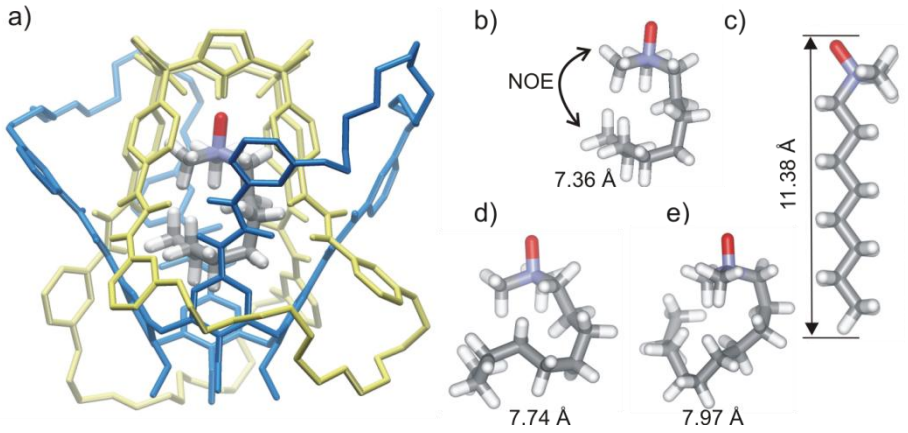

Figure 11: Energy minimized structures of: a) **6⊃C8**; b) **C8** shows a folded conformation upon encapsulation (after host deletion), c) **C8** in extended conformation measures 11.38 Å, d) **C9** in folded conformation, e) **C10** in folded conformation. Distances measured in Workspace.

Based on the previous observations, is no wonder that a nonlinear relationship exists between the chemical shift value for the protons in the terminal methyl group of the alkyl chain of the encapsulated *N*-oxides and the cavity volume.

The volumes of *N*-oxides **C1** to **C3** (90, 106 and 124 $Å^3$, respectively, **Table 2**) are too small to fulfill the 55% packing coefficient rule if they are the only encapsulated species (33%, 39% and 45%, respectively). Co-encapsulation with one molecule of solvent is necessary to reach adequate packing coefficient values. GOESY experiments in non-deuterated chloroform were performed to demonstrate the co-encapsulation of one molecule of solvent with these *N*-oxides. To this end, we selectively irradiated the signal of the proton for free chloroform (7.26 ppm) and hoped to detect in the GOESY spectrum a small signal in chemical exchange with the former. If this is the case, the small signal can be assigned to the proton of the co-encapsulated molecule of chloroform. This type of experiment could not be performed when working in dichloromethane as this solvent is smaller compared to chloroform and exchanges at a very fast rate on the ^{1}H NMR timescale with the bulk solvent. After irradiating the signal of free chloroform, we observed a new signal of low intensity in the GOESY spectra of the assemblies **6⊃C2** and **6⊃C4** (**Figure 12b,c**). The same behavior was observed for the assembly **6⊃C3** but it is not shown here. These results pointed out that

the encapsulated chloroform is indeed involved in slow chemical exchange on the NMR timescale with free chloroform molecules in the bulk solution. The different chemical shifts observed for the proton of the encapsulated chloroform (3.34 ppm for **C2** and 4.15 ppm for **C4**) indicate that the bound solvent experience a slightly different chemical environment in each of the two encapsulation complexes. In addition, the difference in the broadening of the signals can be related to a more restricted motion (rotation and tumbling) for the encapsulated solvent molecule in the assembly **6⊃C4**. In striking contrast, the assembly **6⊃C5** did not show signs of chemical exchange between free and bound solvent. Taken together, these results indicate that **C4** is the larger guest that is co-encapsulated with one molecule of chloroform. This is a remarkable result because the encapsulation of *N*-oxide **C4** provides a PC value of 52 %, very close to the ideal 55% packing coefficient rule.

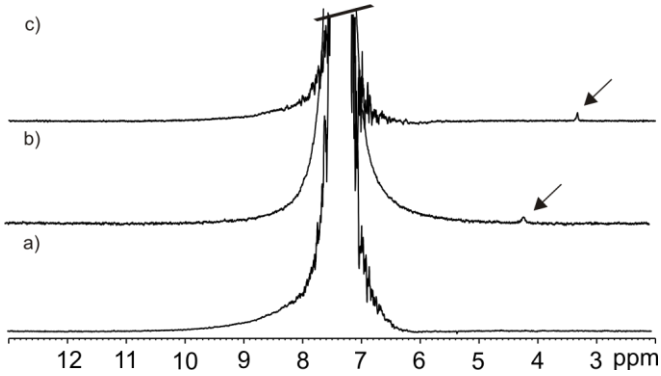

Figure 12: ^{1}H GOESY NMR spectra in non deuterated chloroform with selective excitation of the solvent signal: a) assembly **6⊃C5**, the lack of observation of a signal in chemical exchange with free chloroform indicates that the only guest is encapsulated; b) assembly **6⊃C4**, signal at 4.15 ppm indicates co-encapsulation with solvent; and c) assembly **6⊃C2**, signal at 3.34 ppm indicates co-encapsulation with a molecule of solvent.

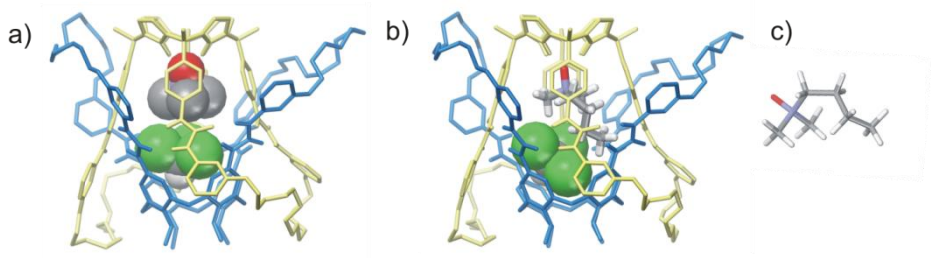

Figure 13: Energy minimized structures of: a) **6⊃C1·CDCl$_3$**, b) **6⊃C4·CDCl$_3$** and c) **C4** displays a folded structure upon encapsulation (after host and co-encapsulated solvent molecule deletion).

In general, the use of chloroform-*d* or dichloromethane-d_2 provided very similar ^{1}H NMR spectra, except for the assemblies **6⊃C4** and **6⊃C5**. The main differences observed in the ^{1}H NMR spectra for the assembly **6⊃C5** in both solvents are in the chemical shift values of the signals of the included guest protons. As we already know (*vide supra*), guest **C5** experiences single encapsulation in chloroform-*d*. Most likely, the **6⊃C5** assembly formed in dichloromethane-d_2 contains a co-encapsulated solvent molecules. The protons of the guest in dichloromethane shows signals that are significantly less upfield shifted (**Figure 14**) supporting a folded structure due to the co-encapsulation with the solvent.

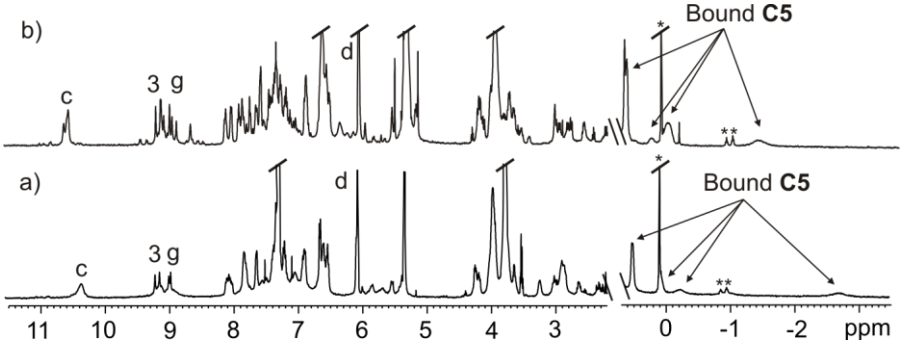

Figure 14: Selected regions of the ^{1}H NMR spectra in of: a) **6⊃C5** in $CDCl_3$, and b) **6⊃C5** in CD_2Cl_2. * impurities.

Remarkably, the encapsulation process of **C4** in the bis-catenane **6** solution provided sharper signals for the protons of the host in dichloromethane-d_2 solution than in

chloroform-*d* (**Figure 15**). We have demonstrated the co-encapsulation of a chloroform molecule with guest **C4** and we surmise that this is also the case in dichloromethane solution. The observation of broader signals in chloroform solution for the protons of encapsulated **C4** and the container **6** is assigned to a higher packing coefficient for the pairwise encapsulation in this solvent than in dichloromethane. The tighter fit provided by the pairwise encapsulation of one solvent molecule and the *N*-oxide, when the solvent is chloroform, difficult a fast interconversion between different conformations of the encapsulated guests. In turn, the combination of encapsulated *N*-oxide **C4** and chloroform exerts more pressure to the ends and sides of the internal cavity of **6** than **C4** + CD_2Cl_2 and forces the two hemispheres and the attached urea groups to slip partially in order to increase the dimension of the capsule. Most likely, this cavity enlargement reduces the thermodynamic stability of the urea belt and induces a faster interconversion on the ^{1}H NMR timescale between the two unidirectional senses of rotation of the urea groups of the hydrogen bonded belt in the capsular assembly **6⊃C4**+$CDCl_3$ than in **6⊃C4**·CD_2Cl_2. The observation of significantly broadened signals for the protons of the container in the assembly **6⊃C4**·$CDCl_3$ supports this hypothesis.

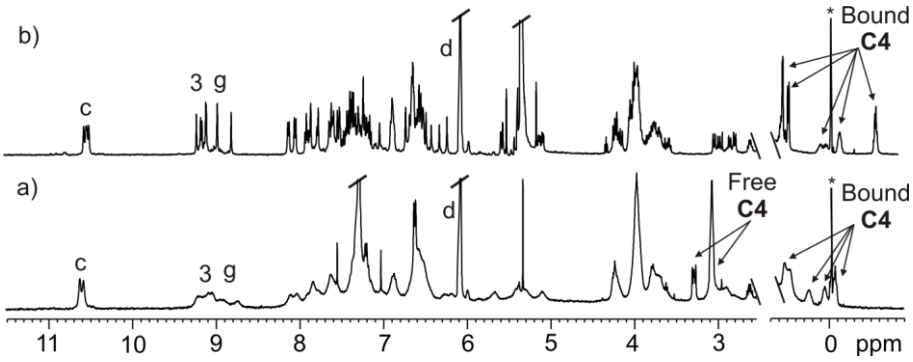

Figure 15: Selected regions of the ^{1}H NMR spectra of: a) **6⊃C4** in $CDCl_3$ solution, and b) **6⊃C4** in CD_2Cl_2 solution. The addition of more than 1equiv of the *N*-oxide in the $CDCl_3$ solution results in the observation of separated proton signals for the free and bound species. * impurities.

Downfield region: pyrrole NH signals.

As stated in *Chapter 2*, the larger the guest's alkyl chain, the deeper the *N*-oxide knob is positioned into the calix[4]pyrrole aromatic cavity yielding shorter hydrogen bonds with the pyrrole NHs. Consequently, one could expect a gradual increase in the downfield shift value of the pyrrole NHs as the number of methylene units in the guest chain increases. However, the initial monotonic trend of downfield shifts observed for the pyrrole NHs protons in response to guest's lengths for **C1** to **C4** stops when guest **C5** is encapsulated (**Figure 16**). Interestingly, a second monotonic trend of downfield shifts for the pyrrole NHs is detected in the encapsulation processes of the *N*-oxide series ranging from **C5** to **C10**.

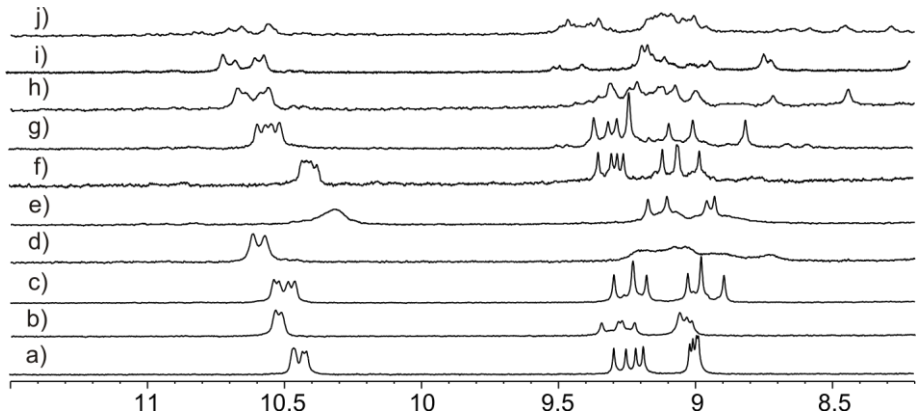

Figure 16: Selected downfield region of the ^{1}H NMR spectra in $CDCl_3$ of: a) **6⊃C1**, b) **6⊃C2**, c) **6⊃C3**, d) **6⊃C4**, e) **6⊃C5**, f) **6⊃C6**, g) **6⊃C8**, h) **6⊃C9**, i) **6⊃C10**, j) **6⊃C11**.

The observed chemical shift behavior for the pyrrole NHs in response to the encapsulation of the *N*-oxide series can be explained assuming the pairwise encapsulation of the shorter guests, **C1** to **C4**, with one molecule of solvent.

The encapsulation assemblies **6⊃C4•**$CDCl_3$ and **6⊃C8** display the same chemical shift value for the pyrrole NH protons suggesting that the *N*-oxide knob is equally deep included in the calix[4]pyrrole aromatic cavity . The fact that the calculated volumes for **C8** (V_{C8} = 68 Å^3, V_{cavity} = 309 Å^3) and **C4** plus one molecule of chloroform ($V_{C4+CDCl3}$ = 69 Å^3, V_{cavity} = 314 Å^3) are almost identical serves to rationalize the previous observation and gives additional support to solvent co-encapsulation in the case of **C4**.

The plot of the pyrrole NH chemical shift values of the different assemblies resulting from the encapsulation of *N*-oxides **C5** to **C11** in front of the volume's cavity shows a linear relationship (**Figure 17**). Conversely, a similar plot for the guest series from C1 to C4 shows no evidence of a straight line. We hypothesize that the different trends observed for the two series of guests is a consequence of single encapsulation (linear) or co-encapsulation of a solvent molecule with the guest (no trend).

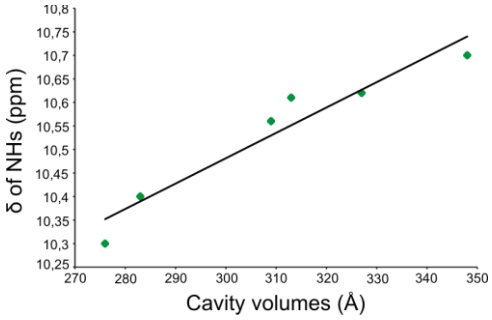

Figure 17: NH chemical shift of versus cavity volume of the assemblies **6⊃C5** to **6⊃C11** displays a linear trend.

The ^{1}H NMR spectrum of the **6⊃C10** assembly shows broad signals for the protons of the host. As discussed previously for the **6⊃C4•**$CDCl_3$ assembly, the inclusion of guest(s) that are tightly packed in the cavity of the container exerts pressure in the sides and ends of it. This forces the two hemispheres to partially slip and weakens the thermodynamic stability of the hydrogen bonded belt of ureas. This effect translates in a lower energy barrier required for the interconversion between the two senses of the unidirectional orientation of the eight urea groups. In agreement with this rationale, molecular modeling studies revealed the existence of a significant elongation in the hydrogen bonds of the urea belt of those assemblies featuring ^{1}H NMR spectra broad signals for the protons of container **6**.

Pairwise competitive encapsulation experiments

Similarly to the experiments described in *Chapter* 2, we performed competitive encapsulation experiments in order to gain some knowledge on the relative binding affinities of bis-catenane **6** for the *N*-oxide series. The results of the competitive experiment between guest **C1**, the smallest guest of the series, and **C5**, the first guest of

the series which undergoes single encapsulation, is explained in this section. One equivalent of guest **C1** was added to the solution containing the preformed assembly **6⊃C5** (**Figure 18a**). The addition of **C1** provokes the appearance of a new set of signals in the ^{1}H NMR spectrum of the mixture that were assigned to the protons of the bound host in a new encapsulation complex. Separate signals for the free and bound protons of **C1** were also apparent. Taken together, these results suggested the instantaneous formation of the **6⊃C1** complex in significant extent (**Figure 18b**). After three days, the ^{1}H NMR analysis of the mixture evidenced that **C1** had completely displaced **C5** from the capsule's interior. The signals corresponding to the protons of free **C5** were visible in the ^{1}H NMR spectrum (**Figure 18c**) and the signals assigned to the capsule's protons in the assembly **6⊃C1** were exclusively detected. In short, the pairwise encapsulation of the smallest guest **C1** and one molecule of $CDCl_3$ produce a multiparticle assembly that is thermodynamically more stable than the 6⊃**C5** complex. To us, this was a surprising result because the PC values for **6⊃C1**•$CDCl_3$ and **6⊃C5** are not very different, 60 and 57%, respectively.

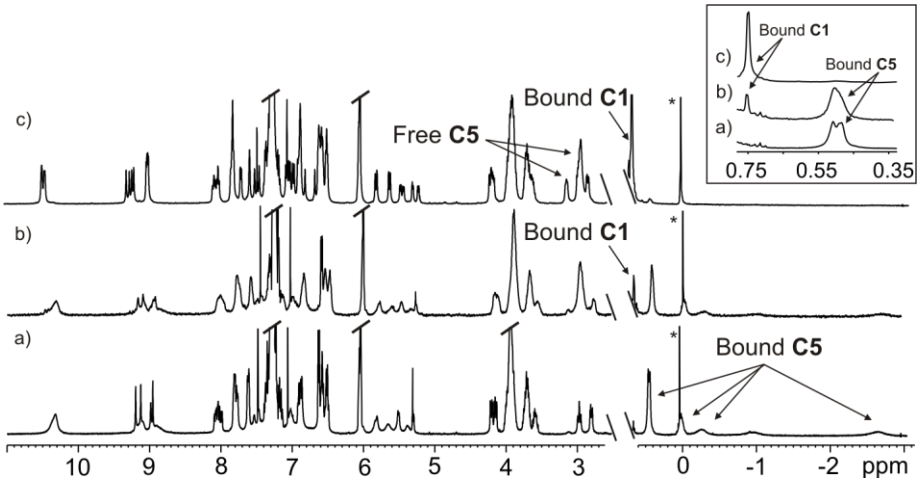

Figure 18: Selected regions of the ^{1}H NMR spectra in $CDCl_3$ solution of the pairwise competitive experiment of **C1** *vs* **C5**: a) **6** + 1 eq of **C5**: **6⊃C5**, b) **6** + 1 eq of **C5 +** 1 eq of **C1**: **6⊃C5** + **6⊃C1**, and c) **6** + 1 eq of **C5 +** 1 eq of **C1**, 3 days after addition: **6⊃C1**. * impurities.

Due to the different stoichiometry of the assemblies **6⊃C1**•$CDCl_3$ and **6⊃C5** it is difficult to establish a relative stability of their stability constants. However, the

obtained results suggest that the combination of **C1**•$CDCl_3$ represents a better fit for the cavity of **6** than a single molecule of **C5**. The reasons for this preference are not clear to us and could result from the sum of subtle energy differences in various intra and intermolecular interactions, i.e., differences in the strength of the hydrogen bonded belt, presence of gauche interactions in encapsulated **C5**, enhanced van der Waals interactions for the **C1**•$CDCl_3$ combination etc.

2.2.2. Ion pairs inclusion and extraction from aqueous solution

As we mentioned in the Introduction, the bis[2]catenane **6** contains a polarized interior. The calix[4]arene hemisphere consists of an electron rich surface able to include quaternary ammonium species.[9] On the other hand, the calix[4]pyrrole unit has a deep aromatic cavity closed at one end with four pyrrole NHs that are inwardly oriented and, for this reason, it is suitable for the inclusion of anions[10] and other electron rich guests.[11] For the reasons stated above, the bis[2]catenane **6** is a potential receptor for the encapsulation ion pairs in a close-contact binding geometry. Examples of ion-pair receptors built from calixarene-calixpyrrole scaffolds are scarce in literature.[16,17] Three different binding modes of the ion pairs to the calix[4]pyrrole unit are reported: close-contact, ion-separated and solvent-bridged.[17,18] It was recently demonstrated in our group that **6** is a perfect host for the encapsulation of ion pairs like tetramethyl phosphonium chloride **7a**$^+$**Cl**$^-$, tetramethyl ammonium chloride **8a**$^+$**Cl**$^-$ and tetraethyl ammonium chloride **8b**$^+$**Cl**$^-$[4] (**Figure 19**).

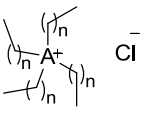

A = P or N
n = 0, 1, 3

7a$^+$; A = P, n = 0
7b$^+$; A = P, n = 1
7c$^+$; A = P, n = 3
8a$^+$; A = N, n = 0
8b$^+$; A = N, n = 1
8c$^+$; A = N, n = 3

Figure 19: Ion pairs used as guests in this and previous binding studies with **6**.

Here we describe the obtained results in the inclusion studies of tetraethylphosphonium chloride **7b**$^+$**Cl**$^-$, tetrabutylphosphonium chloride **7c**$^+$**Cl**$^-$, and tetrabutylammonium

chloride **8c$^+$Cl$^-$** salts within the bis[2]catenane **6** in chloroform-*d*. We wanted to investigate the differences in binding affinity, if any, that existed between tetralkyl-ammonium and phosphonium salts. The inclusion experiments consisted in the addition of 1 equivalent of the corresponding salt previously dissolved in methanol-d_3 to a 1 mM $CDCl_3$ solution of the bis[2]catenane **6** . The encapsulation experiments were monitored using ^{1}H NMR spectroscopy, as well as ^{31}P NMR spectroscopy, in the cases of phosphonium chloride salts. The earmarks of ion-pair encapsulation consists in the observation of a dramatic downfield shift for the pyrrolic NH protons (H_c), due to the hydrogen bond formation with the anion[19], and the upfield shift of the signals for the protons of the encapsulated cation, which are shielded by the electron rich aromatic rings of the calix[4]arene that surround most of its surface. First, we studied the encapsulation of the phosphonium salts. When using the tetramethyl and tetraethyl phosphonium chlorides (**7a$^+$Cl$^-$** and **7b$^+$Cl$^-$**, respectively), the ion pairs with the smallest cations, the diagnostic signals of inclusion are present in the ^{1}H NMR spectra of the corresponding equimolar mixtures (**Figure 20a,b**). The methyl signal of the tetramethylammonium chloride **7a$^+$Cl$^-$** shifted upfield to -0.40 ppm ($\Delta\delta$ = 2.64 ppm) and the signal of the pyrrolic NH protons (H_c) shifted downfield to 10.69 ppm. Similarly, the methylene protons *alpha* to the phosphorus atom for the tetraethylammonium chloride **7b$^+$Cl** encapsulated in the catenane **6** resonate at 0.31 ppm ($\Delta\delta$ = -2.00 ppm) and the methyl protons appear at -0.72 ppm ($\Delta\delta$ = -2.23 ppm). The pyrrolic NH protons, H_c, shifted downfield at 10.98 ppm. Both systems **6⊃7a$^+$Cl$^-$** and **6⊃7b$^+$Cl$^-$** present a binding constant higher to 10^4 M^{-1} since only the signals of the **6⊃7$^+$Cl$^-$** complexes appear in the ^{1}H NMR spectrum of the equimolar mixture and no signals are detected for **6** or **7$^+$Cl$^-$** free in solution. The encapsulation experiment of tetrabutylphosphonium chloride **7c$^+$Cl$^-$** (**Figure 20c**) did not produce any evidence of the formation of the complex. Only signals corresponding to the protons of the cation free in solution and the free catenane **6** were observed. In particular, the protons *alpha* to the phosphorus at 2.32 ppm slightly upfield shifted ($\Delta\delta$ = 0.13 ppm). The ^{31}P NMR spectra shows one signal for the encapsulated phosphorous atom in the assemblies **6⊃7a$^+$Cl$^-$** and **6⊃7b$^+$Cl$^-$** that are slightly upfield shifted ($\Delta\delta$ = -1.67 ppm) compared to

those of the free phosphonium cations; and one signal for the phosphorous atom in the mixture of **6 + 7c$^+$Cl$^-$**, which coincides with the phosphorus signal of the free guest.

These results can be explained based on the dielectric properties of the used solvent and the volume of the phosphonium cations. When working in a solvent with a low dielectric constant, like chloroform, the attractive intermolecular electrostatic interaction between the cation and the anion of the ion pair is maximized. In other words, the ion pair is strongly associated.[20] In terms of complexation, this means that both the anion and the cation get included together as close-contact ion pair in the capsule's interior. The interior of the bis[2]catenane **6** in acts as a heteroditopic ion-pair receptor binding the ion pair in close-contact mode. If the volume of the phosphonium ion pair is too large to fit in the capsule's cavity, the inclusion of the ion pair is not observed, as in the case of the **7c$^+$Cl$^-$** salt.

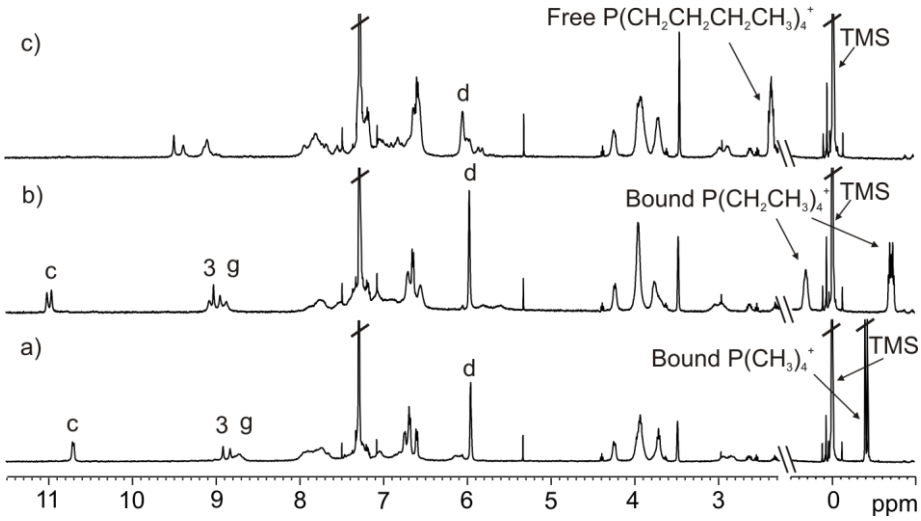

Figure 20: ^{1}H NMR spectra in $CDCl_3$ solution of: a) **6⊃7a$^+$Cl$^-$**, b) **6⊃7b$^+$Cl$^-$** and c) 1 eq of **7c$^+$Cl$^-$** + 1 eq of **6**. Signal at 0 ppm is tetramethyl silane which was used as reference.

The encapsulation experiments performed with the series of tetraalkylammonium chloride salts **8$^+$Cl$^-$** provided a different result than the one described above for the phosphonium analogs. The tetramethyl and the tetraethyl ammonium chloride, **8a$^+$Cl$^-$** and **8b$^+$Cl$^-$** (**Figure 21a**), get included within **6** as the phosphonium analogues **7a$^+$Cl$^-$** and **7b$^+$Cl$^-$** did. Remarkably, the addition of 1 equivalent of tetrabutylammonium

chloride **8c$^+$Cl$^-$** to a $CDCl_3$ solution of bis[2]catenane **6** (**Figure 21b**) induced the downfield shift of the pyrrole NH protons (H_c = 10.98 ppm) indicating that they become hydrogen bonded to the chloride anion. Nevertheless, no upfield shifted signals were observed that could be assigned to the protons of the included cation. Only the signal for the protons of the tetrabutylammonium cation *alpha* to the nitrogen atom was observed. The signals of the rest of the protons of **8c$^+$** are buried under intense signals of protons of the catenane. The protons *alpha* to the nitrogen atom of **8c$^+$**, H_α, resonate at 3.41 ppm. This is slightly upfield shifted ($\Delta\delta$ = 0.16 ppm) with respect to free guest. Most likely, this is due to the interaction of the alkylammonium cation **8c$^+$** with the shallow and electron rich aromatic cavity provided by the pyrrole rings of calix[4]pyrrole core in cone conformation. This cavity is located in the external surface of the catenane.

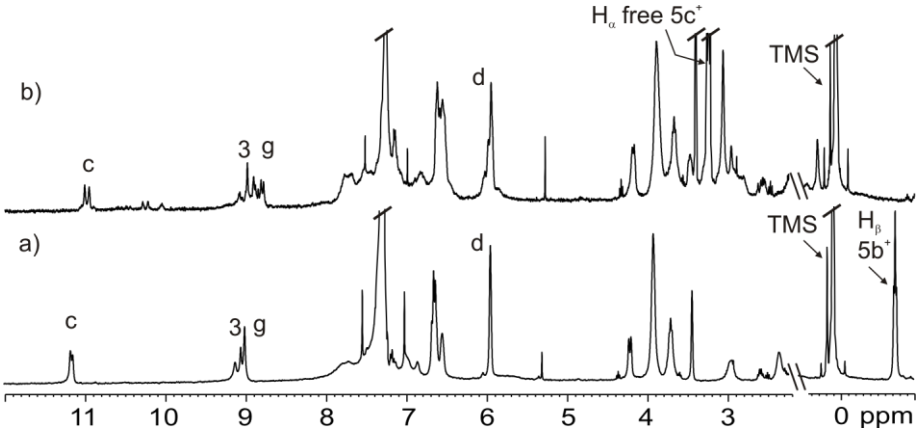

Figure 21: ^{1}H NMR spectra in $CDCl_3$ solution of: a) **6⊃8b$^+$Cl$^-$**, b) **6⊃Cl$^-$** + **8c$^+$**. Signal at 0 ppm is tetramethyl silane which was used as reference.

It is known that upon interaction with a strongly-bound anion, as chloride, the calix[4]pyrrole scaffold locks into the so-called cone conformation.[21] The bowl-shaped and electron-rich aromatic pocket created by this structural locking can complex the tetrabutylammonium cation, which exhibits suitable size and shape (**Figure 22**) for complexation. The magnitude of the cation complexation is strongly dependent on the complementarity between the cavity and the cation size.

Molecular modeling studies suggest that the tetrabutylammonium cation is too large to fit inside the calix[4]arene hemisphere and that it is preferentially located in the electron rich cup of the calix[4]pyrrole, opposite to the encapsulated chloride anion. The bound ion pair **8c$^+$Cl$^-$** results in a receptor-separated binding geometry, the cation and the anion are separated by the calix[4]pyrrole scaffold (see the energy minimized structure in **Figure 22**). It is worthy to note that the chloride anion alone does not fulfill the packing requirements of the cavity. Most likely a molecule of solvent or methanol is co-encapsulated to satisfy an optimum packing coefficient of the cavity (PC = 51%).

In order to explain the binding of the catenane **6** with the different salts, two different processes must be considered: the dissociation of the ion pair and the binding of each dissociated ion to the receptor. It is plausible that the dissociation of the ion pair for the tetrabutylammonium chloride **8c$^+$Cl$^-$** salt is higher than for the phosphonium analog **7c$^+$Cl$^-$** and/or the ammonium cation binds with higher affinity to the electron-rich cup provided by the pyrrole ring than the phosphonium counterpart.

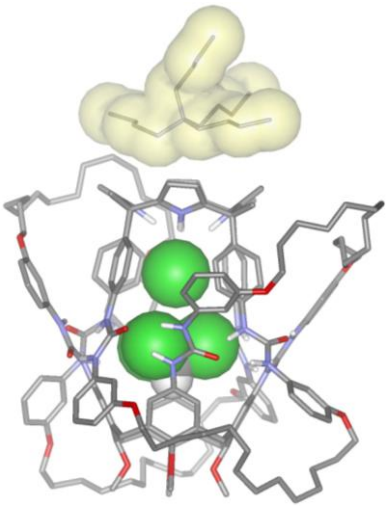

Figure 22: Energy minimized structure of the possible assembly when using **8c$^+$Cl$^-$**: **8c$^+$·6⊃Cl$^-$·CDCl$_3$**. The packing coefficient calculated for the encapsulation is 51%.

In conclusion, we have found that the bis[2]catenane **6** is a good receptor for ion pairs. The encapsulation of the intimate contact ion-pair depends on the size of the cation. The

single inclusion of the anion relies on the nature of the tetraalkyl salt ammonium or phospnonium.

Extraction of the ion pairs from an aqueous solution

Previous work reported the liquid-liquid extraction of ion pairs.[22] One of the simplest calix[4]pyrroles involved in the extraction of cesium halide salts is octamethylcalix[4]pyrrole. To the best of our knowledge, there are no reports of receptors containing calixarene-calixpyrrole scaffolds able to extract ion pairs in liquid-liquid extraction experiments. The ability of a host molecule to extract certain salt form a water solution could be useful to reduce the concentration of this particular salt.

We described in the preceding section that bis[2]catenane **6** acts as an effective ion-pair receptor for several ammonium and phosphonium chloride salts in chlorinated solvents. We decided to investigate the possibility to use the bis[2]catenane **6** for the encapsulation of ion pairs in liquid-liquid extraction experiments. Two phosphonium salts, which were included as ion pairs in the catenane in chloroform solution, were selected for the liquid-liquid extraction experiments, tetramethyl and tetraethyl phosphonium chlorides **7a**$^{+}$**Cl**$^{-}$ and **7b**$^{+}$**Cl**$^{-}$.

After sonication for 15 minutes a two-phase mixture containing a 1 mM solution of **6** in chloroform-*d* and a 10 mM distilled water solution of the ion pair (**7a**$^{+}$**Cl**$^{-}$, **7b**$^{+}$**Cl**$^{-}$), the ^{1}H NMR analysis of the organic phase showed the diagnostic signals for ion-pair encapsulation (see above, **Figure 20**). Even though, the extraction was not quantitative: we observed a 30% formation of capsule (roughly calculated by integration of the free and bound signals of the pyrrolic NH_c).

2.2.3. Inclusion of electrochemically active compounds

The inclusion of electroactive metallocenes in cyclodextrins,[23] cucurbit[7]urils,[24] tetraurea calix[4]arene capsules[25] and cavitands based on resorcin[4]arenes[26] has been precisely reported in the literature. We wanted to evaluate the inclusion of negatively charged organometallic sandwich complexes, which are electrochemically active compounds, and the modification of its electrochemical behavior upon inclusion in the

bis[2]catenane **6**. We expected to detect a different electrochemical behavior of the guest when included than free in solution. Ferrocene carboxylic acid **9** possesses an appropriate size (PC = 63%) and functionalization (carboxylated group for hydrogen bonding the pyrrolic NH protons) to be included in the cavity of **6**. For these reasons, it seemed to us as a good candidate for our purposes (**Figure 23**) and we studied the encapsulation of this substrate in the catenane **6**.

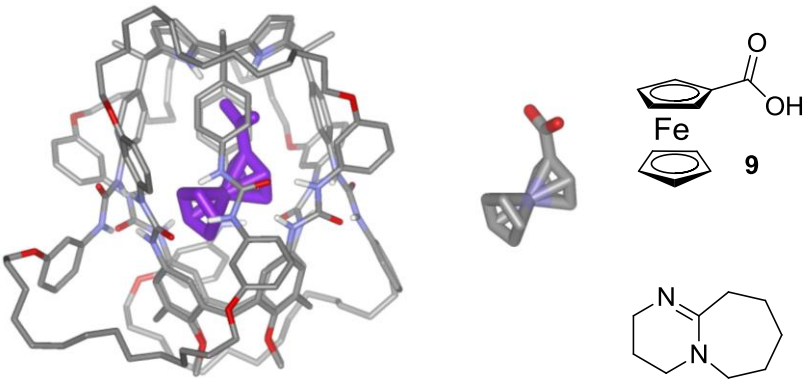

Figure 23: Energy minimized structure of the ferrocene carboxylate included in the bis[2]catenane, **6⊃9**$^-$ (left), ferrocene carboxylate **9**$^-$ (center). ChemDraw structures of ferrocene carboxylic acid **9** (right top) and 1,8-Diazabicyclo[5.4.0]undec-7-ene, DBU (right bottom).

First of all, we investigated the voltammetry of ferrocene carboxylate **9**$^-$ [ii] in dichloromethane. By means of cyclic voltammetry experiments[iii] the half-wave potential ($E_{1/2}$) of **9**$^-$ was determined. The oxidized and reduced states of the compound were characterized by UV-visible spectroscopy. It was observed that after a bulk oxidation of a solution of **(Fe^{2+})-9**$^-$ the characteristic band at 311 nm slightly shifted to 306 nm indicating the formation of the ferricenium carboxylate **(Fe^{3+})-9**$^-$.

The addition of the metallocene **9** to a $CDCl_3$ solution of bis[2]catenane **6** resulted in no changes for the proton signals of the host and in the appearance of three new signals corresponding to the protons of free **9** (4.81 ppm, 2H; 4.47 ppm, 2H; 4.25 ppm, 5H).

[ii] 1,8-Diazabicyclo[5.4.0]undec-7-ene (DBU) was used as a base to deprotonate the ferrocene carboxylic acid **9**.

[iii] See conditions and plots in the Experimental Section.

Upon addition of DBU to induce the deprotonation of the carboxylic acid, some changes in the ^{1}H NMR spectrum of the mixture were observed (**Figure 24c**). New protons signals appeared in the downfield region of the spectrum: one broad signal resonating at 10.91 ppm and four singlets centered at 12 ppm (12.46, 12.10, 12.03 and 11.69 ppm). The more downfield shifted signals were assigned to the pyrrolic NH protons (H_c) belonging to two diastereomeric encapsulation assemblies. The higher downfield shift ($\Delta\delta_{average}$ = 3.6 ppm) is in agreement with the hydrogen bonding of the carboxylate and the broad signal ($\Delta\delta$ = 2.4 ppm) corresponds to the inclusion of the $DBUH^+$. At this point, we found out that the DBU is competing with the ferrocene carboxylate for the calix[4]pyrrole binding site. The proton signals of free **9** disappeared as a consequence of the deprotonation of the carboxylic acid and new signals more upfield shifted appeared at 4.73, 4.20 and 4.10 ppm, which could be assigned to the encapsulated $\mathbf{9}^-$. Even though these new signals are upfield shifted with respect to free **9**, they are a little bit downfield shifted when compared to the proton resonances of free $\mathbf{9}^-$.

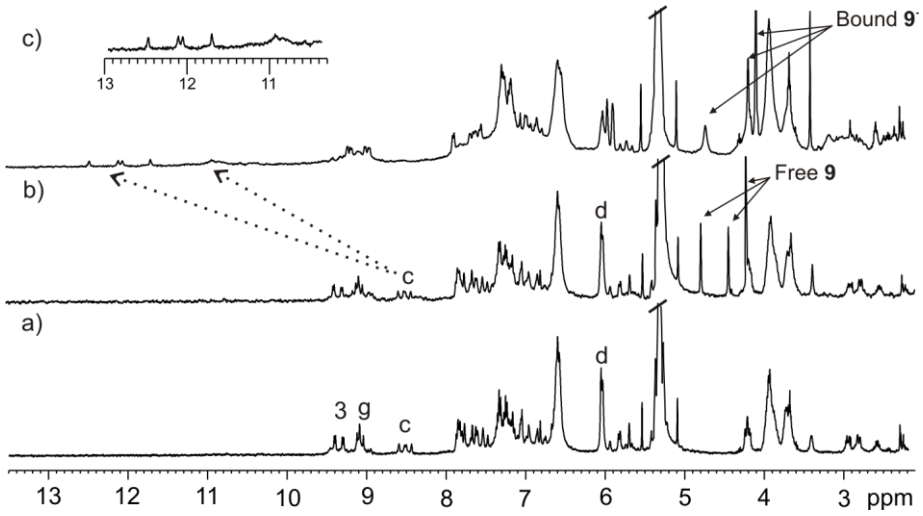

Figure 24: Selected region of the downfield region of the ^{1}H NMR spectra in $CDCl_3$ of: a) **6**, b) **6** + 1 eq ferrocene carboxylic acid, and c) **6** + 1 eq ferrocene carboxylic acid + 1 eq DBU.

These inclusion experiments were repeated at several concentrations and it was observed that when the concentration of bis[2]catenane was between 0.60-0.77 mM

both assemblies were present, whereas at higher concentrations only the assembly containing the DBU was detected by ^{1}H NMR spectroscopy.

The deprotonation of **9** was also evaluated using tetrahexylammonium hydroxide. A ^{1}H NMR titration of the bis[2]catenane **6** with the tetrahexylammonium ferrocene carboxylate was run and it was observed that the proton signals corresponding to the ferrocene carboxylic acid appeared again, indicating that the carboxylate was protonated and it could not be included.

Spectroelectrochemical studies of the inclusion of guest $\mathbf{9}^-$ have not been performed yet due to the impossibility of obtaining a quantitative encapsulation of the metallocene.

2.2.4. Inclusion of biologically relevant compounds

The studies of encapsulation or complexation of biologically relevant compounds in synthetic hosts is important for understanding the recognition of biological receptors. The preliminary studies of inclusion of several biologically relevant zwitterions (**Figure 25**) in the bis[2]catenane **6** was studied. The zwitterions used in these experiments were taurine and L-carnitine. Taurine plays an important role in the transmission of neuronal information and L-carnitine is involved in the generation of methabolic energy. They both are available as nutritional supplements.

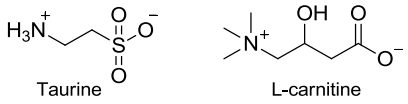

Figure 25: Zwitterions used in the inclusion experiments.

The addition of L-carnitine, dissolved in methanol-d_3, showed the earmarks for capsule formation (**Figure 26**). The pyrrolic NH protons (H_c) experience a dramatic shift to 11 ppm, a typical downfield shift for anion binding. Moreover, broad signals at high-field (-0.5 ppm) could probably be assigned to the encapsulated guest. The rest of the signals of the included L-carnitine are hidden by the loops of the host and this region of the

spectrum is omitted in the figure. On the other hand, taurine was added as a solid due to its limited solubility and it did not get included.

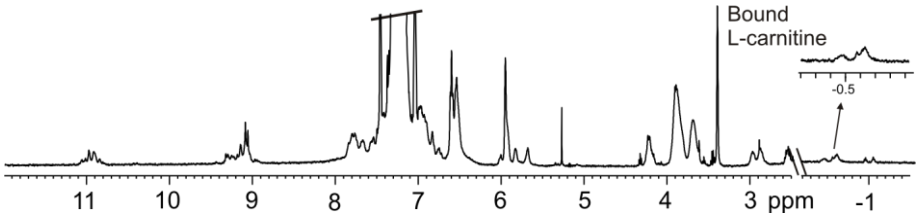

Figure 26: Selected upfield and downfield regions of the ^{1}H NMR spectra in $CDCl_3$ of **6**⊃L-carnitine.

3. Conclusion

We have observed that a mechanically interlocked capsule is able to host much longer alkyl dimethylamino *N*-oxide guests than the supramolecular capsule analog. The capsular assembly tetraurea-calix[4]arene – tetraurea-calix[4]pyrrole gains an additional stability when covalently linked. Even when the hydrogen bonds of urea belt are stretching a lot due to the pressure that a big guest exerts in the cavity interior (high packing coefficients), the capsule still retains the guest inside. We have seen a variety of stable complexes with a wide range of PC values from 57 to 74. It was also found that when the guest is small to fulfill the adequate packing coefficient, a molecule of solvent is co-encapsulated with the guest. The mechanically locked capsules present an enhanced binding ability with respect to the supramolecular capsule analogue. The bis[2]catenane **6** was also found to be an ion-pair receptor of tetraalkyl ammonium and phosphonium chloride salts, in a close-contact and separated binding modes, depending on the size of the counteraction and possibly on the affinity of the cation for the external cup of the calix[4]pyrrole. Moreover, the bis[2]catenane has been proven to be a neutral extractant of those ion pairs from aqueous solutions. The inclusion of electrochemically active metallocenes in the bis[2]catenane **6** was evaluated. Nevertheless, the encapsulation was not successful enough to develop the studies of voltammetry and this system is still under study. Finally, the bis[2]catenane **6** ability to include biologically relevant zwitterions was evaluated but only successful for one substrate. This field is currently under investigation in our research group.

4. Experimental section

4.1. General information and instrumentation

Unless stated otherwise, all preparations were carried out under argon inert atmosphere and using standard techniques. All the reagents were obtained from commercial suppliers and used without further purification. Pyrrol was distilled under vacuum and freshly used. Anhydrous solvents were obtained from a solvent purification system SPS-800 from MBRAUN. HPLC grade quality solvents were obtained commercially and used without further purification. Routine ^{1}H and ^{13}C NMR spectra were recorded with a Bruker Avance 400 (400 MHz) and Bruker Avance 500 (500 MHz) spectrometers with use of the solvent signals as internal reference. Mass Spectrometry data were obtained from a Bruker Autoflex MALDI-TOF Mass Spectrometer.
Flash chromatography was performed with Silica gel Scharlab60 and with Aluminium oxide 60, active basic, particle size 0.063-0.20 mm from Merck. High performance liquid chromatography analyses were performed on an Agilent 1100 series equipped with a UV-Vis detector.

4.2. Synthesis

Calix[4]arenes **1a**, **1b**[1a] and calix[4]pyrrole **2**[27] were synthetized using described procedures.

4.2.1. Synthetic procedure for the bis[2]catenane 6

Synthesis of calix[4]arene bisloop 3 (the reported procedure[4] was modified in the purification steps): Commercial 4-tert-butyl-calix[4]arene (9 g, 13.87 mmol) was suspended on dry DMF (250 mL). Sodium hydride (suspended on mineral oil, 17.3g, 721 mmol) was added to the suspension. 1-bromopentane (25.1 g, 166 mmol) was added the last. The reaction mixture was left stirring under argon at room temperature for one week. Distilled water (20 mL) was carefully added and the resulting slurry was diluted with chloroform (250 mL) and a solution of 15% HCl (300 mL) was added. The layers were separated and the organic layer was washed with brine (2x300 mL), dried over $MgSO_4$ and evaporated to dryness. The crude product was chromatographed using first hexane as eluent and later a mixture hexane/dichloromethane (10/3) to give 9.2 g (71%) of alkylated product. It (6.2 g, 6.67 mmol) was dissolved in dichloromethane (250 mL). Glacial acetic acid (61 mL) and nitric acid (100%, 23.3 mL, 547 mmol) were added. The mixture was stirred until the solution turned orange. Then, the reaction mixture was poured on water (400 mL) for 20 min. The layers were separated and the organic layer was neutralized with Na_2CO_3. The organic layer was additionally washed with brine and the solvent evaporated to yield 5.11 g (86%) of an orange solid, tetranitro calix[4]arene. The tetranitro calix[4]arene (5.11 g, 5.77 mmol) was dissolved in warm toluene (60ºC). Ni Raney catalyst was added and the reaction was left stirring under hydrogen atmosphere for some hours. Then, it was filtered over celite and the solvent evaporated to yield 3.9 g (88%). The tetraamino calix[4]arene (2.53 g, 3.31 mmol) was dissolved in dry DMF (10 mL) and dry triethylamine (2.3 mL, 16.54 mmol) was added. Then, the 4-nitrophenyl-*N*-[3-(oct-7- enyloxy)phenyl]carbamate (6.36 g, 16.54 mmol) was added. The reaction mixture was left stirring under argon for 2 days. The reaction mixture was diluted with 250 mL of dichloromethane and 200 mL of a 1M aq. solution of K_2CO_3 was added and then the mixture was left stirring for 1 hour. Then, the organic layer was washed with of 0.3M aq K_2CO_3 (3 x 300mL), dried with $MgS0_4$ anhydrous. The crude product was purified by silica chromatographic column using a solvent mixture of AcOEt/hexane 1/4 (75%).
A mixture of tetraalkenyl calix[4]arene (1.81 g, 1.04 mmol) and tolyl calix[4]arene **1b** (1.85 g, 1.19 mmol) were refluxed in benzene (500 mL) until full solubilization. The mixture was left to cool to room temperature. Then, it was degassed with argon for 30 minutes and a solution of Grubbs first generation catalyst (0.85 g, 1.03 mmol) was added via cannula in benzene. The reaction mixture was left stirring for 2 days. Note: using a continuous argon flow the reaction finishes in 2-3 hours and the amount of catalyst is significantly decreased (0.2-0.4 eq). The metathesis reaction was followed by ^{1}H NMR spectroscopy. Triethylamine (3 mL) was added and the mixture was stirred for one hour. The bisloop was purified by column chromatography (silica) using THF(distilled)/hexane 1/2 (35%) The hydrogenation of the bisloop was carried out in dry THF (20 mL) and in the presence of PtO_2 (0.23 g, 1.03 mmol) at atmospheric pressure. Several cycles vacuum/hydrogen were done and the reaction was left stirring overnight under hydrogen atmosphere. The reaction was followed by ^{1}H NMR spectroscopy. It was purified by (several) column chromatography (silica) using a THF(distilled)/hexane, from 1/3 to 2/3 (50%).

Yield: 20%; ^{1}H NMR (400 MHz, THF-d_8, 25ºC) δ (ppm) 7.53 (s, 4H), 7.47 (s, 4H), 7.12 (t, 4H, *J* = 2.1 Hz), 7.32 (t, 4H, *J* = 8.2 Hz), 6.89 (d, 4H, *J* = 2.5 Hz), 6.82 (dd, 4H, *J* = 8.1 Hz, *J* = 1.3 Hz), 6.77 (d, 4H, *J* = 2.5 Hz), 6.43 (dd, 4H, *J* = 8.2 Hz, *J* = 2.0 Hz), 4.45 (dd, 4H, *J* = 12.8 Hz, *J* = 1.8 Hz), 3.89 (t, 8H, *J* = 6.7 Hz), 3.62 (t, 8H, *J* = 6.5 Hz), 3.10 (dd, 4H, *J* = 12.6 Hz, *J* = 5.3 Hz), 2.00 – 1.91 (m, 8H), 1.51– 1.41 (br m, 26H), 1.38 – 1.26 (br m, 36H), 0.98 (t, 12H, *J* = 6.8 Hz).

Calix[4]arene: MALDI-TOF: *m/z* (%): 1769.4 (100) $[M+Na]^+$

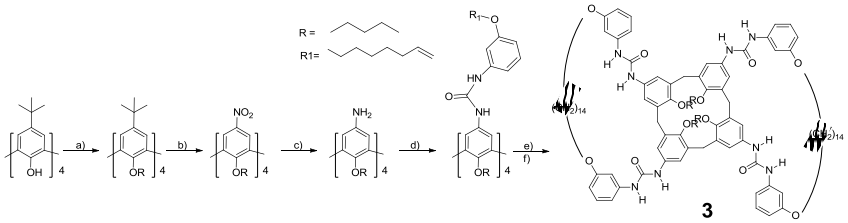

Scheme 2: Tetraurea calix[4]arene synthesis. a) NaH, DMF, b) HNO_3, acetic acid/CH_2Cl_2 1/0.245, c) Ni Raney, toluene, d) Et_3N, DMF, 4-nitrophenyl-*N*-[3-(oct-7- enyloxy)phenyl]carbamate, e) benzene, Grubbs I, and f) PtO_2/H_2, tetrahydrofuran.

Synthesis of tetraurea calix[4]pyrrole 4 (the reported procedures[27,4] were sligthly modified)**:** 4-nitroacetophenone (8.1 g, 49 mmol) was dissolved in CH_2Cl_2 (250 mL of HPLC quality). Then, HCl aq (0.75 mL, 24.5 mmol) was added dropwise while stirring under argon atmosphere. Finally, freshly distilled pyrrol (3.4 mL, 49 mmol) was also added dropwise. The resulting solution was left stirring under argon atmosphere protected from light. One week later, the reaction mixture was filtered and the black solid rejected. After evaporation of the solvent, the crude product was purified by column chromatography using a mixture of CH_2Cl_2/hexane as eluent (3/2, 3/1.3, 3/1) to yield 1.48 g of an orange/yellow solid. The tetranitro calix[4]pyrrole obtained (500 mg, 0.584 mmol) was dissolved in ethyl acetate (150 mL of HPLC quality) and hydrogenated under hydrogen pressure (4 bar) using Pd/C (360 mg) as catalyst during 15 hours. The reaction mixture was filtered through celite and then evaporated until dryness to give 351 mg (81%) of white solid. The tetraamine obtained (329 mg, 0.446 mmol) was dissolved in dry DMF (25 mL) and dry triethylamine (0.3 mL, 2.232 mmol) was added. The 4-nitrophenyl-*N*-[3-(oct-7- enyloxy)phenyl]carbamate (858 mg, 2.232 mmol) was added the last. It was left stirring at room temperature under argon atmosphere. After two days, the reaction mixture was diluted with CH_2Cl_2 (200 mL) and 1M K_2CO_3 aq. (150 mL). The mixture was stirred for one hour. Then, the layers were separated and the organic layer was washed with 0.3 M K_2CO_3 aq. (4x150 mL) until the yellow color of the organic layer disappears. The organic layer was dried ($MgSO_4$). It was purified by column chromatography (silica) using CH_2Cl_2/MeOH 98/2 as eluent.

Yield: 88%, MALDI-TOF: *m/z* (%): 1718.3 (100) $[M]^+$.^{1}H NMR (400 MHz, DMSO-d_6, 25ºC) δ (ppm) 9.61 (br s, 4H), 8.56 (s, 4H), 8.52 (s, 4H), 7.32 (d, 8H, *J* = 8.6 Hz), 7.10 – 7.06 (m, 8H), 6.84 – 6.90 (m, 12 H), 6.50 (dd, 4H, *J* = 8.4, *J* = 1.9 Hz), 5.94 (br s, 8H), 5.82 – 5.74 (m, 4H), 5.00 – 4.90 (m, 8H), 3.88 (t, *J* = 6.6, 8H), 2.00 – 1.98 (m, 8H), 1.79 (s, 12H), 1.69 – 1.62 (m, 8H), 1.41 – 1.27 (m, 24H); ^{13}C NMR (100 MHz, DMSO-d_6,) δ (ppm) 159.8 (C), 152.9 (C), 144.0 (C), 141.5 (C), 139.5 (CH), 138.7 (C), 137.7 (C), 130.0 (CH), 127.8 (CH), 118.5 (CH), 115.1 (CH_2), 110.9 (CH), 107.9 (CH), 105.2 (CH), 105.0 (CH), 67.7 (CH_2), 44.1 (C), 33.6 (CH_2), 31.6 (CH_3), 29.1 (CH_2), 28.7 (CH_2), 25.8 (CH_2).

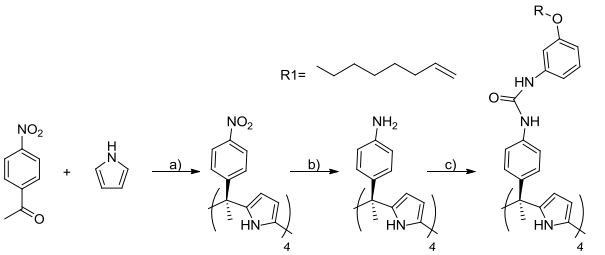

Scheme 3: Synthesis of tetraurea calix[4]pyrrole **4**. a) CH_2Cl_2, HCl 37%, b) ethyl acetate, Pd/C, H_2, and c) Et_3N, DMF, 4-nitrophenyl-*N*-[3-(oct-7- enyloxy)phenyl]carbamate.

Synthesis of bis[2]catenane 6

Bisloop calix[4]arene **3** (194 mg, 0.12 mmol), tetraurea calix[4]pyrrole **4** (198 mg, 0.12 mmol), and trimethylamine *N*-oxide **C1** (8.6 mg, 0.12 mmol) were dissolved in dry CH_2Cl_2 (100 mL). The resulting yellowish solution was degassed with argon during 30 minutes and then a solution of the Grubbs catalyst (45 mg, 0.055 mmol) in CH_2Cl_2 was added via cannula. The resulting purple reaction mixture was left stirring at room temperature for 2-3 hours under an argon flow. The metathesis reaction was followed by ^{1}H NMR spectroscopy. Then, triethylamine (0.5 mL) was added and the solvents evaporated. The dark solid residue was purified by column chromatography (CH_2Cl_2/CH_3CN 95/5 and THF/hexane 1/3, 1/2). The resulting white solid was hydrogenated in dry THF (25 mL) with platinum dioxide (108 mg, 0.48 mmol) under hydrogen at atmospheric pressure. The reduction was followed by ^{1}H NMR. The reaction mixture was filtered through celite and evaporated to yield a white solid.

Yield 65%. The ^{1}H NMR of this compound without the presence of an adequate guest affords not well defined proton signals. MS (MALDI$^+$/[M]$^+$): 3359.7. The separation of the two enantiomers of the catenane was performed on a chiral Chiralpack IB 250 x 4.6 mm, 5µm analytical column using as eluent a mixture MeOH/CH_2Cl_2/EtOH with 1% diethylamine 45/10/45.

(+)-**3•5**: $[\alpha]_{435}^{25}$ +5.5° (*c* 0.145 CH_2Cl_2). (-)-**3•5**: $[\alpha]_{435}^{25}$ -4.3° (*c* 0.145 CH_2Cl_2).

4.2.2. Synthetic procedure for the *N,N'*-dimethylalkyl *N*-oxides

Guests **C1** and **C12** were commercially available. Guest **C7** could not be obtained by the standard procedures used in other guests' synthesis. After 3 trials, no more synthetic effort was invested because it was not completely necessary to use this guest.

Synthetic procedure for guests C2, C3, C4, C6, C8 and C11

The corresponding commercially available *N,N*-dimethylalkylamine (1 mmol) was placed into a sealed tube and dissolved in 2-3 mL of methanol. While stirring and with the tube open to air, H_2O_2 (2 mmol) was added dropwise (exothermic reaction). The reaction was heated at 90ºC for 3 hours. The closed tube acted as a reflux. After that, the reaction mixture was evaporated until dryness at 60ºC. A white hygroscopic solid was obtained. It was necessary to dry it better under vacuum using an oil bath at 55ºC during approximately 6 hours. The *N*-oxides obtained were filtered through a basic alumina column (eluent: CH_2Cl_2, MeOH/CH_2Cl_2 5/95).

C2: white hygroscopic solid, 80%, ^{1}H-NMR (D_2O, 400 MHz, 25ºC) δ (ppm) 3.3 (q, 2H, CH_2N), 3.0 (s, 6H, (CH_3)$_2$N), 1.2 (t, 3H); ^{13}C-NMR (D_2O, 400 MHz, 25ºC) δ (ppm) 65 (*C*H_2N), 57 (*C*H_3N), 8 (*C*H_3).

C3: white hygroscopic solid, 75%, ^{1}H-NMR (D_2O, 400 MHz, 25ºC) δ (ppm) 3.2 (m, 2H, CH_2N), 3.1 (s, 6H, (CH_3)$_2$N), 1.7 (m, 2H), 0.9 (t, 3H).

C4: white hygroscopic solid, 70%, ^{1}H-NMR (D_2O, 400 MHz, 25ºC) δ (ppm) 3.2 (m, 2H, CH_2N), 3.0 (s, 6H, (CH_3)$_2$N), 1.7 (m, 2H), 1.3 (m, 2H), 0.9 (t, 3H).

C6*:* slightly green hygroscopic solid, 81%, ^{1}H-NMR (D_2O, 400 MHz, 25ºC) δ (ppm) 3.2 (m, 2H, CH_2N), 3.0 (s, 6H, (CH_3)$_2$N), 1.7 (m, 2H), 1.3 (m, 6H), 0.8 (t, 3H).

C8: white hygroscopic solid, 90%, ^{1}H-NMR ($CDCl_3$, 400 MHz, 25ºC) δ (ppm) 3.3 (m, 2H, CH_2N), 3.2 (s, 6H, (CH_3)$_2$N), 1.8 (br m, 2H), 1.3 (br m, 4H), 1.2 (br m, 6H), 0.9 (t, 3H).

C11: white solid, %, ^{1}H-NMR ($CDCl_3$, 400 MHz, 25ºC) δ (ppm) 3.3 (m, 2H, CH_2N), 3.2 (s, 6H, (CH_3)$_2$N), 2.0 (br s, 4H), 1.9 (br m, 2H), 1.4 (br s, 4H), 1.3 (br s, 14H), 0.9 (t, 3H).

Synthesis of guest C5, C9 and C10

Sodium carbonate (1.7 g, 16.1 mmol) was suspended on 12.5 mL of a mixture ethanol/water 4/1. Then, a solution formed by the corresponding 1-bromoalkane (2 mL, 16.1 mmol) and dimethylamine 33% ethanolic solution (6.7 mL, 113 mmol) was added. The resulting suspension was refluxed at 100ºC. After 24 hours, the reaction mixture was left to cool to room temperature. The white solid obtained was filtered off and washed with ethanol. Then, the filtrate was acidified with a 1M HCl solution (14 mL) and it was evaporated until dryness to yield the amino-chlorhydrate as a yellowish and hygroscopic solid. The solid was dissolved in water (10 mL) and 1M NaOH solution (5-6 mL) was added to deprotonate the chlorhydrate, so then it was extracted with diethyl ether (3x10 mL). The organic extracts, after drying with $MgSO_4$, were carefully evaporated to yield a slightly yellow liquid (23%) which smells like amines. The amine (420 mg, 3.65 mmol) was transferred to a sealed tube and it was dissolved in methanol (2-4 mL). Then, H_2O_2 (0.282 mL, 9.11 mmol) was added carefully. When the reaction stopped bubbling, the tube was closed and it was refluxed to 100ºC during 4 hours. After that, the reaction mixture was left to cool to room temperature. Then, the solvents were evaporated to obtain a slightly yellow hygroscopic solid. It was purified using basic alumina column (CH_2Cl_2, MeOH/CH_2Cl_2 5/95).
C5: slightly yellow solid, 64%, ^{1}H-NMR (D_2O, 400 MHz, 25ºC) δ (ppm) 3.2 (m, 2H, CH_2N), 3.1 (s, 6H, (CH_3)$_2$N), 1.8 (m, 2H), 1.3 (m, 4H), 0.9 (t, 3H); ^{13}C-NMR (D_2O): 70 ppm (*C*H_2N), 57 ppm ((*C*H_3)$_2$N), 28 ppm (CH_2), 23 ppm (CH_2), 22 ppm (CH_2), 13 ppm (CH_3).
C9: yellowish solid, 43%, ^{1}H-NMR ($CDCl_3$, 400 MHz, 25ºC) δ (ppm) 3.2 (m, 2H, CH_2N), 3.1 (s, 6H, (CH_3)$_2$N), 1.9 (m, 2H), 1.4 (m, 4H), 1.3 (m, 8H), 0.9 (t, 3H).
C10: white solid, 44%, ^{1}H-NMR (CD_2Cl_2, 400 MHz, 25ºC) δ (ppm) 3.2 (m, 2H, CH_2N), 3.1 (s, 6H, (CH_3)$_2$N), 1.8 (m, 2H), 1.4 – 1.2 (m, 14H), 0.9 (t, 3H).

4.3. Binding studies

4.3.1. Individual encapsulation studies

The individual encapsulation experiments were performed by adding 1 eq of the guest from a stock solution in chloroform-*d* to an NMR tube containing a 1 mM solution of the bis[2]catenane **6** in chloroform-*d*. Then, the mixtures were analyzed by ^{1}H NMR and 2D NMR spectroscopy.

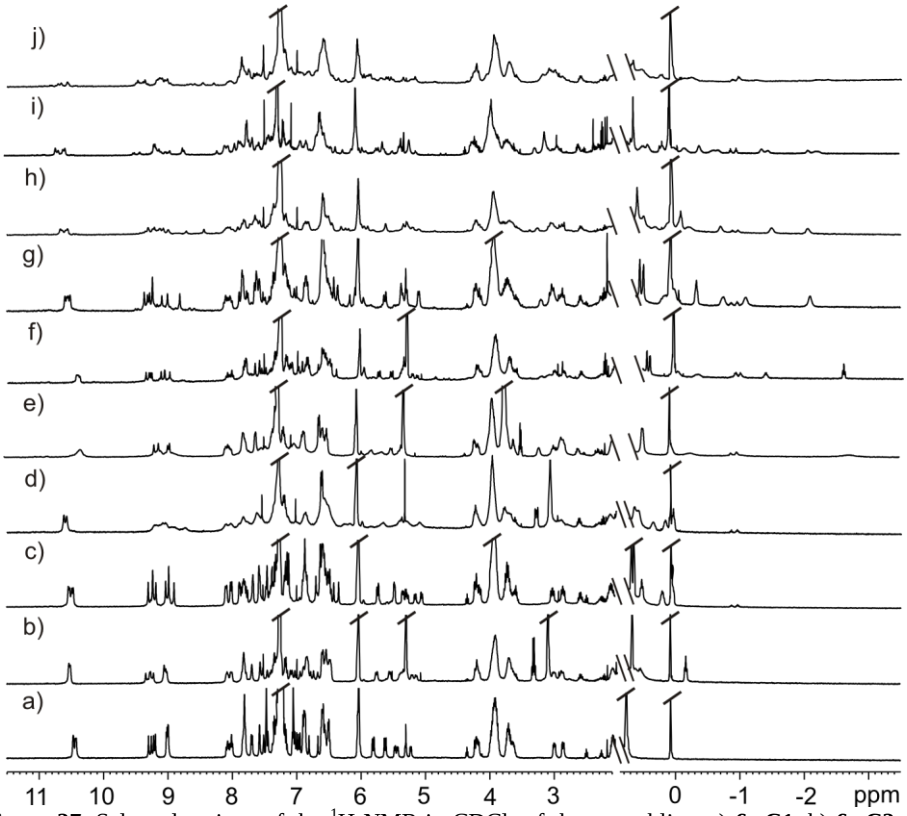

Figure 27: Selected regions of the ^{1}H NMR in $CDCl_3$ of the assemblies: a) **6⊃C1**, b) **6⊃C2**, c) **6⊃C3**, d) **6⊃C4**, e) **6⊃C5**, f) **6⊃C6**, g) **6⊃C8**, h) **6⊃C9**, i) **6⊃C10**, j) **6⊃C11**. Guest **C12** does not get included into the catenane.

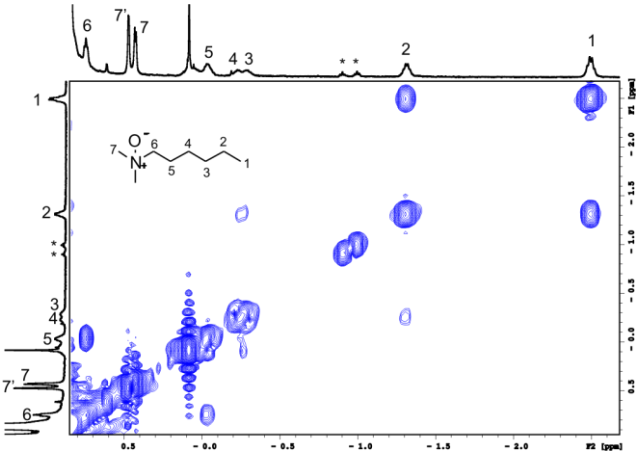

Figure 28: COSY experiment of **6⊃C6.**

4.3.2. Competitive experiments between guests

The competitive experiments were carried out by adding 1 eq of a guest from a stock solution to an NMR tube containing a preformed assembly of the guest to compete with. The mixtures were analyzed by ^{1}H NMR spectroscopy.

4.3.3. Inclusion of ion pairs and extraction from aqueous solution

Experiments of ion pairs (**7**$^{+}$**Cl**$^{-}$**, 8**$^{+}$**Cl**$^{-}$) inclusion were performed by adding 1 eq of the ion pair, from a guest stock solution in methanol-d_3 because they were not soluble enough in chloroform-*d*, to an NMR tube containing a 1 mM solution of the bis[2]catenane **7**. Then, the solutions were analyzed by ^{1}H NMR and ^{31}P NMR (in the case of phosphonium salts) spectroscopy.
The extraction of the phosphonium chloride salts (**7**$^{+}$**Cl**$^{-}$) was performed by mixing a 1 mM solution (0.5 mL) of bis[2]catenane **6** in $CDCl_3$ and a 10 mM solution (1 mL) of the corresponding ion pair in distilled water. The mixture was sonicated for 15 minutes. After that, the organic phase was taken with a syringe and analyzed by ^{1}H NMR spectroscopy.

4.3.4. Inclusion of electrochemically active compounds

The conditions for the cyclic voltammetry were the ones that follow: 1) Reference electrode: Ag/AgCl in saturated solution of KCl, 2) Auxiliary electrode: Pt wire, 3) Working electrode: Pt disk and 4) Electrolyte: 0.1 M tetrabutylammonium hexafluorophosphate in dichloromethane. 1mM solution of the ferrocene or ferrocene carboxylate.

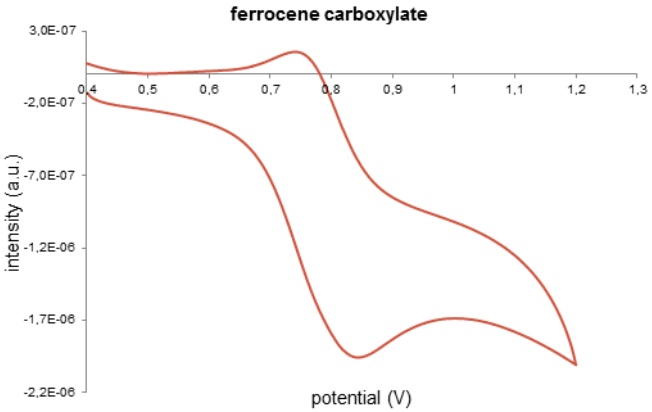

Figure 29: Cyclic voltammetry of ferrocene carboxylate (DBU used to deprotonate).

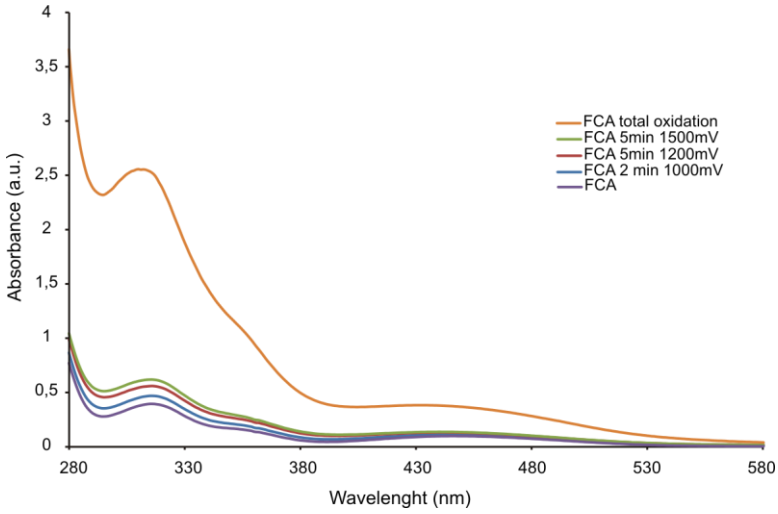

Figure 30: UV-vis spectra obtained after bulk oxidation of ferrocene carboxylate at different voltage and during different periods of time (see the legend). The band at 311 nm shifted to 306 nm after the total oxidation.

References and notes

[1] a) Rudzevich, Y.; Vysotsky, M. O.; Bohmer, V.; Brody, M. S.; Rebek, J.; Broda, F.; Thondorf, I. *Org. Biomol. Chem.* **2004**, *2*, 3080-3084.; b) Castellano, R. K.; Kim, B. H.; Rebek, J. *J. Am. Chem. Soc.* **1997**, *119*, 12671-12672.; c) Thondorf, I.; Rudzevich, Y.; Rudzevich, V.; Bohmer, V. *Org. Biomol. Chem.* **2007**, *5*, 2775-2782.; d) Castellano, R. K.; Nuckolls, C.; Rebek, J. *J. Am. Chem. Soc.* **1999**, *121*, 11156-11163.; e) Rudzevich, Y.; Rudzevich, V.; Klautzsch, F.; Schalley, C. A.; Bohmer, V. *Angew. Chem.-Int. Edit.* **2009**, *48*, 3867-3871.; f) Rudzevich, Y.; Rudzevich, V.; Bohmer, V. *Chem.-Eur. J.* **2010**, *16*, 4541-4549.

[2] Chas, M.; Gil-Ramirez, G.; Ballester, P. *Org. Lett.* **2011**, *13*, 3402-3405.

[3] Mecozzi, S.; Rebek, J. *Chem.-Eur. J.* **1998**, *4*, 1016-1022.

[4] Chas, M.; Ballester, P. *Chem. Sci.* **2012**, *3*, 186-191.

[5] Vysotsky, M. O.; Bogdan, A.; Wang, L. Y.; Bohmer, V. *Chem. Commun.* **2004**, 1268-1269.

[6] Wang, L. Y.; Vysotsky, M. O.; Bogdan, A.; Bolte, M.; Bohmer, V. *Science* **2004**, *304*, 1312-1314.

[7] Bogdan, A.; Rudzevich, Y.; Vysotsky, M. O.; Bohmer, V. *Chem. Commun.* **2006**, 2941-2952.

[8] Gibb, C. L. D.; Gibb, B. C. *Chem. Commun.* **2007**, 1635-1637.

[9] Harrowfield, J. M.; Richmond, W. R.; Sobolev, A. N. *J. Inclusion Phenom. Mol. Recognit. Chem.* **1994**, *19*, 257-276.

[10] Gale, P. A.; Sessler, J. L.; Kral, V.; Lynch, V. *J. Am. Chem. Soc.* **1996**, *118*, 5140-5141.

[11] Allen, W. E.; Gale, P. A.; Brown, C. T.; Lynch, V. M.; Sessler, J. L. *J. Am. Chem. Soc.* **1996**, *118*, 12471-12472.

[12] Molokanova, O.; Bogdan, A.; Vysotsky, M. O.; Bolte, M.; Ikai, T.; Okamoto, Y.; Bohmer, V. *Chem.-Eur. J.* **2007**, *13*, 6157-6170.

[13] Ballester, P.; Gil-Ramirez, G. *Proc. Natl. Acad. Sci. U. S. A.* **2009**, *106*, 10455-10459.

[14] Bogdan, A.; Vysotsky, M. O.; Ikai, T.; Okamoto, Y.; Bohmer, V. *Chem.-Eur. J.* **2004**, *10*, 3324-3330.

[15] Guests' volumes and cavities' volumes were calculated using the free software Swiss PDB Viewer.

[16] Sessler, J. L.; Kim, S. K.; Gross, D. E.; Lee, C. H.; Kim, J. S.; Lynch, V. M. *J. Am. Chem. Soc.* **2008**, *130*, 13162-13166.

[17] Kim, S. K.; Sessler, J. L.; Gross, D. E.; Lee, C. H.; Kim, J. S.; Lynch, V. M.; Delmau, L. H.; Hay, B. P. *J. Am. Chem. Soc.* **2010**, *132*, 5827-5836.

[18] Ciardi, M.; Tancini, F.; Gil-Ramirez, G.; Escudero-Adan, E. C.; Massera, C.; Dalcanale, E.; Ballester, P. *J. Am. Chem. Soc.* **2012**, *134*, 13121-13132.

[19] Analogous behavior was observed in the inclusion of chloride to aryl extended calix[4]pyrroles: Gil-Ramirez, G.; Escudero-Adan, E. C.; Benet-Buchholz, J.; Ballester, P. *Angew. Chem.-Int. Edit.* **2008**, *47*, 4114-4118.

[20] de Namor, A. F. D.; Khalife, R. *Phys. Chem. Chem. Phys.* **2010**, *12*, 753-760.

[21] Gale, P. A.; Sessler, J. L.; Kral, V. *Chem. Commun.* **1998**, 1-8.

[22] Wintergerst, M. P.; Levitskaia, T. G.; Moyer, B. A.; Sessler, J. L.; Delmau, L. H. *J. Am. Chem. Soc.* **2008**, *130*, 4129-4139.

[23] Kaifer, A. E. *Accounts Chem. Res.* **1999**, *32*, 62-71.

[24] Ong, W.; Kaifer, A. E. *Organomet.* **2003**, *22*, 4181-4183.

[25] Frish, L.; Vysotsky, M. O.; Bohmer, V.; Cohen, Y. *Org. Biomol. Chem.* **2003**, *1*, 2011-2014.

[26] Sarmentero, M. A.; Ballester, P. *Org. Biomol. Chem.* **2007**, *5*, 3046-3054.

[27] Ballester, P.; Gil-Ramirez, G. *Proc. Natl. Acad. Sci. U. S. A.* **2009**, *106*, 10455-10459.

UNIVERSITAT ROVIRA I VIRGILI
REVERSIBLE MOLECULAR ENCAPSULATION IN SELF-ASSEMBLED AND MECHANICALLY LOCKED CONTAINERS WITH POLAR INTERIOR
Monica Espelt Ripoll
DL: T 1103-2014

CHAPTER 5

SYNTHESIS AND BINDING STUDIES OF A BIS[2]CATENANE CALIX[4]PYRROLE – CALIX[4]PYRROLE MOLECULAR CAPSULE

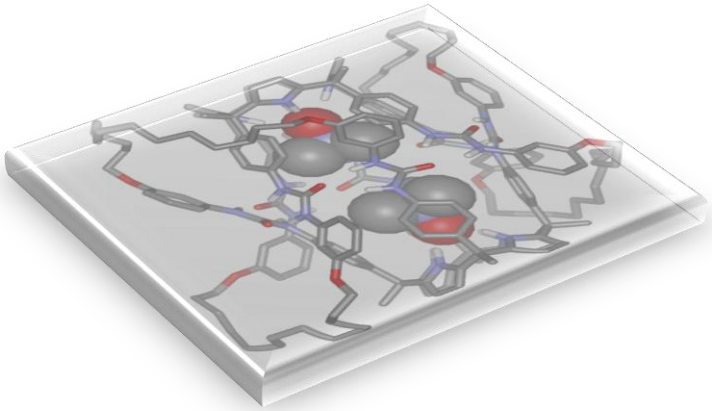

UNIVERSITAT ROVIRA I VIRGILI
REVERSIBLE MOLECULAR ENCAPSULATION IN SELF-ASSEMBLED AND MECHANICALLY LOCKED CONTAINERS WITH POLAR INTERIOR
Monica Espelt Ripoll
DL: T 1103-2014

1. Introduction

One of the goals of our research group is the extension of the dimensions of the internal cavity provided by bimolecular capsular structures based on calix[4]pyrrole scaffolds. The aim of this research is, ultimately, the use of these structures as reaction molecular vessels in the near future. To this end, capsules featuring polar interiors are highly recommended in order to control the relative orientation of the substrates able to be included in the cavity and to allow the reactive groups to converge.

We designed the synthesis of a mechanically locked dimeric capsule based on the linkage of two molecules of calix[4]pyrrole. There are two different approaches for the synthesis of a catenane: the statistical approach and "directed synthesis" approaches. The statistical approach was applied for the first synthesis of a bis[2]catenane.[1] The second methodology is related to self-assembly strategies, for example, templation by transition metals,[2] templation by anions,[3,4] templation by π-π stacking interactions,[5] the self-assembly of catenanes from two preformed molecular rings,[6] etc. The design of our synthesis is based on the host-guest directed synthesis using an *N*-oxide to induce the cone conformation of the calix[4]pyrrole core by hydrogen-bonding interactions and the subsequent self-assembly of the two components of the catenane: the tetraurea alkenyl calix[4]pyrrole **1** and the tetraurea bisloop calix[4]pyrrole **2**.

This new bis[2]catenane will display an increased volume of approximately 60 $Å^3$ with respect to the previous calix[4]arene-calix[4]pyrrole bis[2]catenane.[7] Moreover, this structure possesses two convergent binding sites in its internal cavity and allows for the orientation of the guests in the two hemispheres, in contrast with the previous bis[2]catenane which only could organize the guest in a certain position in one hemiphere. We consider that the synthetic effort involved in the synthesis of this capsular structure is worthed. The availability of this molecular container will represent a significant progress towards the encapsulation of larger and highly functionalized molecules. Taking into consideration the results obtained with the analogous calixpyrrole-calixarene bis[2]catenane discussed in Chapter 4, we suspect that this mechanically locked capsule will be more versatile than its supramolecular counterpart

for the encapsulation of a wider variety of molecules. Likewise, we expect that the encapsulation complexes formed by the mechanically locked molecular vessel will feature a significant boost in the thermodynamic and kinetic stability with respect to analogous non-locked architectures.

2. Results and Discussion

2.1. Synthesis and characterization of the calix[4]pyrrole-calix[4]pyrrole bis[2]catenane molecular capsule

The synthetic strategy to prepare this novel bis[2]catenane was similar to the one developed for the bis[2]catenane calix[4]arene – calix[4]pyrrole capsule, which was described in the previous Chapter 4. The bis[2]catenane **4** (**Scheme 1**) was obtained by metathesis reaction of the tetraurea alkenyl calix[4]pyrrole **1** using the calix[4]pyrrole bisloop **2**[8] as template and reaction partner through the heterodimeric pseudo-[2]rotaxane intermediate. In this case, 2 equivalents of the *N*-oxide were needed to induce the cone conformation of the two calix[4]pyrrole units instead of 1 equivalent used in the previous synthesis yielding the bis[2]catenane calix[4]arene – calix[4]pyrrole. The cone conformation is required for the interdigitation of the tetraurea alkenyl calix[4]pyrrole **1** through the loops of the calix[4]pyrrole **2**. The tetraurea alkenyl calix[4]pyrrole **1** was prepared by acylation of the corresponding tetraamine[9] with the activated urethane.[10] Equimolar mixtures of tetraureas **1** and **2** containing 2 equivalents of the *N*-oxide were prepared at different concentrations and analyzed by ^{1}H NMR spectroscopy in order to find the most adequate concentration to induce the quantitative formation of the heterodimer **1·2**. The quantitative formation of the heterodimer was also checked in the reaction mixture of the metathesis reaction before the addition of the Grubbs I catalyst. The progress of the metathesis reaction was monitored by ^{1}H NMR spectroscopy. After the metathesis has been completed and subsequent catalytic hydrogenation of the formed double bonds with PtO_2/H_2, the bis[2]catenane **4** was obtained as a pale grey solid in 30 % yield after column chromatography purification.

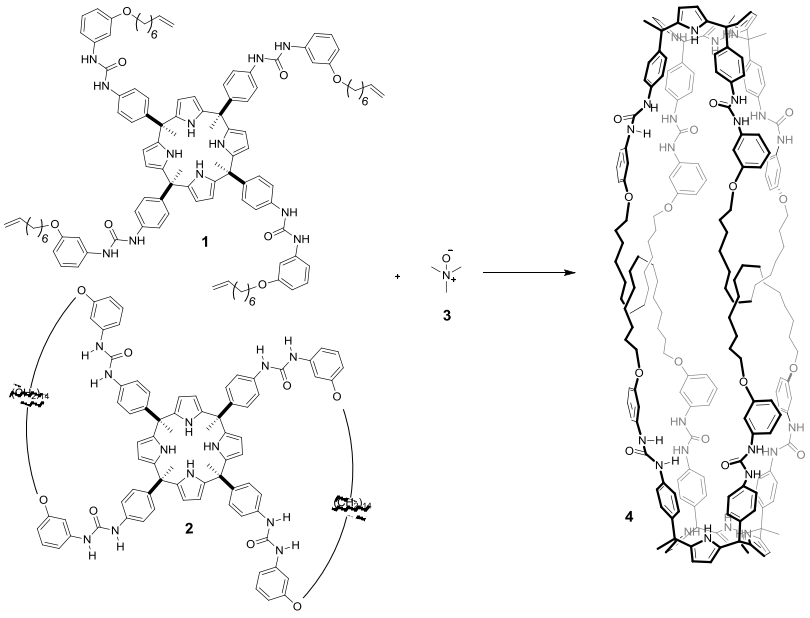

Scheme 1: Synthetic scheme of the bis[2]catenane calix[4]pyrrole - calix[4]pyrrole **4** capsule.

The ^{1}H NMR spectrum of the "free" bis[2]catenane **4** in $CDCl_3$ solution shows broad proton signals, indicating an ill-defined (collapsed) geometry. For this reason, the characterization of the compound using ^{1}H NMR spectroscopy was performed in DMSO (**Figure 1**). The broad singlet at 9.5 ppm corresponds to the pyrrolic NH protons, H_c. The broad signals at 8.5 ppm probably relate to the urea NH protons, H_g. The aromatic protons signals appear between 7.5 and 6.5 ppm. The beta-pyrrolic protons resonate at 6 ppm. The triplet at 4.2 ppm is assigned to the O-CH_2, H_n. The rest of the signals in the upfield region belong to the methylene protons of the loops.

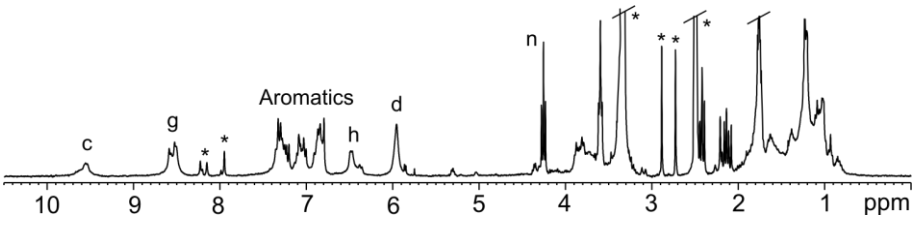

Figure 1: ^{1}H NMR spectrum of the bis[2]catenane **4** in DMSO. See **Figure 2** for proton assignments. * indicates impurities and solvent residual peaks.

Nevertheless, the ^{1}H NMR spectrum is not enough to characterize the complex molecular structure of the bis[2]catenane **4**. The results obtained in encapsulation experiments will be highly valuable to clarify the capsular structure of the compound.

2.2. Inclusion experiments

The binding studies carried out with the bis[2]catenane **4** are discussed in this section. The compounds used as guests were several *N*-oxides and one metallocene. A competitive experiment between a mono-*N*-oxide and a bis-*N*-oxide is also described in this section.

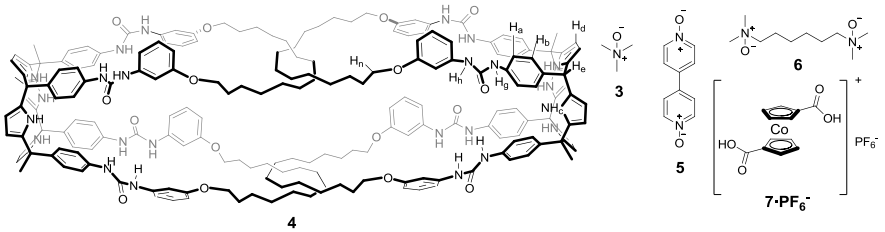

Figure 2: Bis[2]catenane **4** and molecules used as potential guests.

2.2.1. Binding experiments with single *N*-oxides

The binding studies were performed by adding one equivalent of the corresponding bis-*N*-oxide or two equivalents of the mono-*N*-oxide to a 1 mM solution of bis[2]catenane **4** in $CDCl_3$ and the encapsulation processes were studied by ^{1}H NMR spectroscopy.

Trimethylamino *N*-oxide **3** and two bis-*N*-oxides **5** and **6** were the guests of choice for the preliminary encapsulation experiments in the bis[2]catenane **4**. We have previously observed the inclusion of these *N*-oxides inside the supramolecular capsule analog to the bis[2]catenane **4** (see Chapter 2).[9,11]

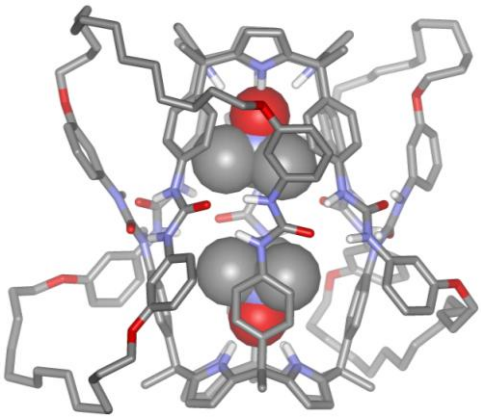

Figure 3: Energy-minimized structure of the trimethylamino *N*-oxide **3** included inside the bis[2]catenane **4**.

The diagnostic signals indicating the inclusion of the corresponding *N*-oxide in a calix[4]pyrrole-based capsular assembly are the downfield shift experience by the pyrrolic NH protons of the calix[4]pyrrole core and the significant upfiled shift detected for the protons of the included guest. As explained in previous chapters, the pyrrolic NH protons shift downfield because they are hydrogen bonded to the oxygen of the encapsulated *N*-oxide guest. In turn, the proton signals of the guest shift upfield due to the magnetic shielding exerted by the aromatic panels that shape the cavity.

The ^{1}H NMR spectra of individual solutions of **4** and the three *N*-oxides, **3**, **5** and **6**, were indicative of the quantitative encapsulation of the guests in the bis[2]catenane **4**. This results are in complete agreement with the molecular modeling studies (example of the assembly **4⊃3$_2$** in **Figure 3**) and our previous knowledge in this type of experiments. Although, in general, the proton signals were broad, we were able to assign the signals of the protons of the pyrrole NH, H_c, the urea NH, H_g, and the included guest.

Upon guest encapsulation, the pyrrolic NH proton signals of the bis[2]catenane **4** experienced a similar chemical shift in the three experiments of inclusion. They shifted from 9.2 ppm (free **4, Figure 4a**) to 9.5 ppm (**4⊃5, Figure 4d**), 10 ppm (**4⊃3$_2$, Figure 4b**) and 10.2 ppm (**4⊃6, Figure 4c**). The proton signals of the encapsulated guests **3** and

6 were easily detected: the methyl protons of the included guests trimethylamino *N*-oxide **3** and *N,N,N',N'*-tetramethylhexyl-*N,N'*-dioxide **6** resonate *ca.* at 0.6 ppm. The aromatic protons of the included 4,4'-dipyridine-*N,N'*-dioxide **5** appear at 5.9 ppm, hidden by a host signal, and 4.9 ppm, not shown in the following spectrum.

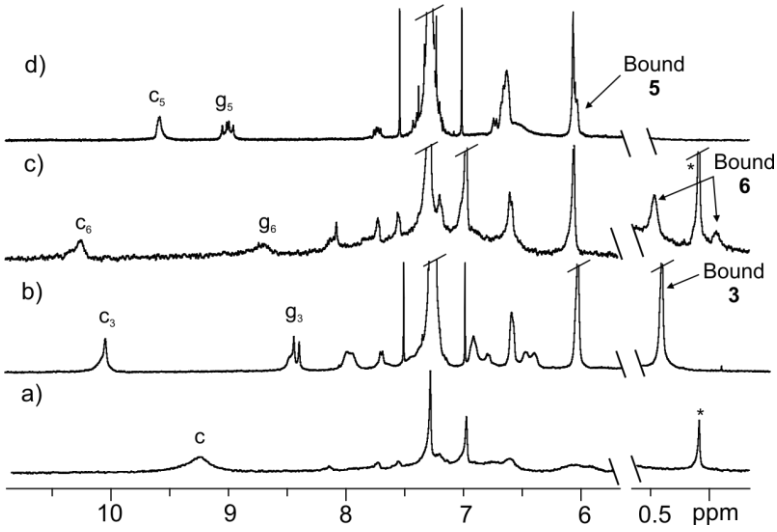

Figure 4: Selected upfield and downfield regions of the ^{1}H NMR spectra in $CDCl_3$ of: a) free catenane **4**, b) **4**⊃**3**$_2$, c) **4**⊃**6**, and d) **4**⊃**5**.

2.2.2. Binding experiment with cobaltocenium dicarboxylic acid

In this section we describe the preliminary binding studies carried out with cobaltocenium dicarboxylate. As we discussed in Chapter 4, we wanted to evaluate the electrochemical behavior of negatively charged organometallic-sandwich complexes when included in the bis[2]catenane **4**. Cobaltocenium dicarboxylic acid has an adequate size to be included in the cavity of the bis[2]catenane **4** and suitable functionalization when the two acid groups are deprotonated to carboxylates (**Figure 5**).

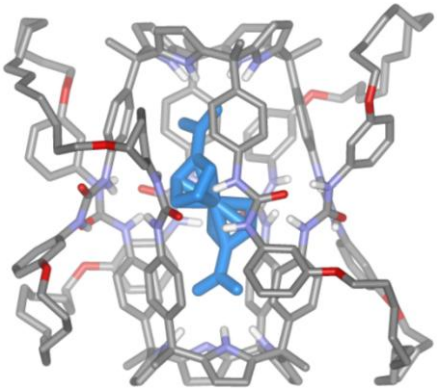

Figure 5: Energy-minimized structure of the cobaltocenium dicarboxylate **7**$^-$ included in the bis[2]catenane **4**.

The addition of one equivalent of a stock solution[12] of cobaltocenium dicarboxylate **7**$^-$ to a $CDCl_3$ solution of bis[2]catenane **4** resulted in the appearance of new protons signals in the downfield region of the spectrum at 11.5 and 11.2 ppm which we assign to the pyrrolic NH protons corresponding to the **4**⊃**7**$^-$ assembly (**Figure 6**). The broad signals resonating at 9 ppm are in agreement with the expected chemical shift values for the urea NH protons, H_g, in the capsular assembly. We expected to observe two different signals for the protons of the encapsulated guest at *ca*. 4 ppm. Probably, these signals have a very reduced in intensity and they appear buried under the signals of the protons of the host. Significantly, the most intense proton signals in this spectrum correspond to the free guest, 6 and 5.5 ppm. Guest **7**$^-$ was added in excess with respect to bis-catenane **4** to induce the complete assembly of the encapsulation complex.

We conclude that the encapsulation of cobaltocenium dicarboxylate **7**$^-$ in vessel **4** takes place, however, because the quantitative formation of the encapsulation complex required a great excess of the guest we decided that performing additional electrochemical investigations on the aggregate were not feasible.

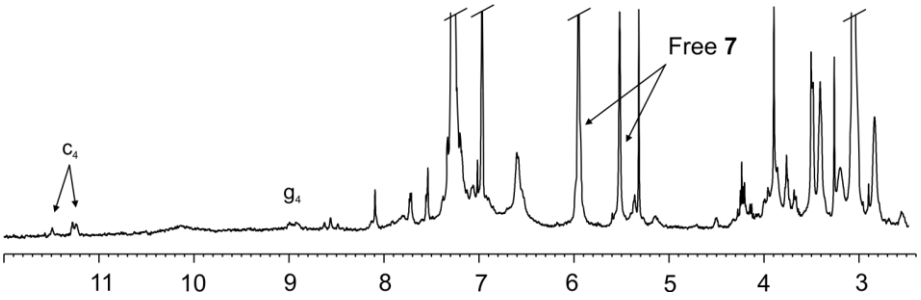

Figure 6: Selected downfield region of the ^{1}H NMR spectrum in $CDCl_3$ of the binding experiment of cobaltocenium dicarboxylate **7**$^-$ in the bis[2]catenane **4**.

2.2.3. Pairwise competitive encapsulation experiment

The results of the competitive experiment between the bis-*N*-oxide **5** and the mono-*N*-oxide **3,** comparable to the ones described in *Chapter 2* and *Chapter 4*, are explained in this section.

One equivalent of guest **5** was added to a $CDCl_3$ solution containing a preformed capsular assembly **4**⊃**3**$_2$ (**Figure 7b**). Upon addition of **5**, a new set of proton signals corresponding to the assembly **4**⊃**5** appear in the spectrum. Both assemblies, the new and the former, coexist in solution. Moreover, separate signals for the free (two doublets at 8.3 and 7.5 ppm) and bound protons of **5** are detected in the spectrum. These results indicate that the formation of the **4**⊃**5** assembly is fast and it is produced to a considerable extent, but not exclusively, in the first hours after the addition (**Figure 7c**). After two weeks, the ^{1}H NMR spectrum of the mixture reveals that the ditopic guest **5** has completely displaced the monotopic guest **3** and only signals belonging to the protons of the assembly **4**⊃**5** were visible. The signal of the protons of the free guest **3**, however, was not as intense as we expected (3.2 ppm). This is probably due to the low solubility of free **3** in chloroform solution. The encapsulation of the bis-*N*-oxide **5** produces a thermodynamically more stable assembly than the one obtained from the pairwise encapsulation, **4**⊃**3**$_2$. Since the two-particle assembly is the most thermodynamically stable, it is tempting to propose that entropy drives the exchange process of guests. The different stoichiometry of the assemblies **4**⊃**3**$_2$ and **4**⊃**5** do not

allow for a direct comparison of their stability constants. However, the result of the competition experiment gives a clear thermodynamic advantage to the two particles aggregate.

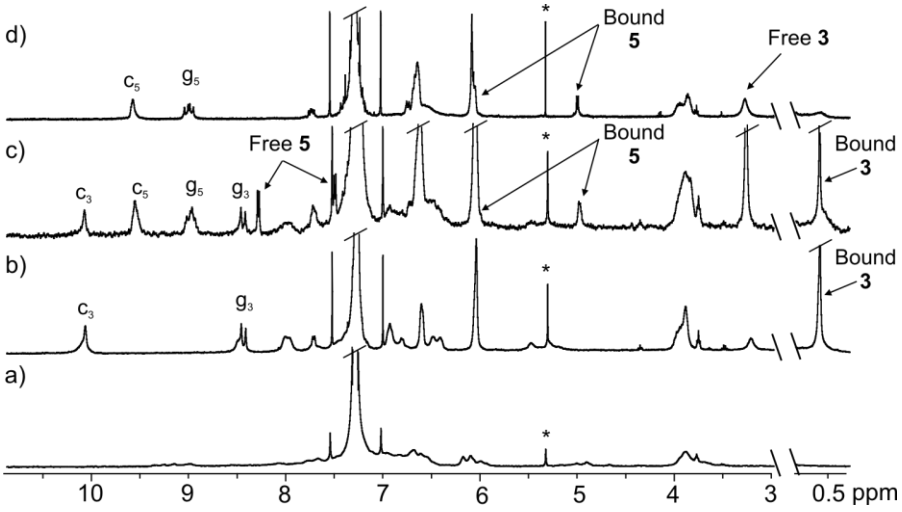

Figure 7: Selected upfield and downfield regions of the ^{1}H NMR spectra in $CDCl_3$ of the competition experiment between the bis-*N*-oxide **5** and the mono-*N*-oxide **3**. Both assemblies are present, the new and the former, but when the thermodynamic equilibrium is reached only the **4⊃5** is present. a) bis[2]catenane **4**, b) **4⊃3$_2$**, c) **4⊃3$_2$** + **4⊃5**, and d) two weeks after addition: **4⊃5.**

Related competitive experiments using the supramolecular capsule analog (self-assembled from tetraurea benzyl calix[4]pyrroles) were recently reported by our group,[11] and provided slightly different kinetic results. The complete exchange of guests was very fast, within seconds. Conversely, the complete exchange of guests for the bis[2]catenane **4** needed significantly more time (days). The difference in exchange kinetics for the two vessels lies in the mechanically locked structure of the bis[2]catenane **4**. Most likely, the rate determining step for the guest exchange is the dissociation of the initial encapsulated complex. The exchange may involve a direct displacement of guest or the intermediacy of a solvent filled capsule. Previous results support that for a given guest the mechanically locked structure of the capsule yields significantly higher thermodynamically stable complexes than the purely supramolecular counterpart, in which both hemispheres can fully dissociated at infinite

distance. Even if the formation of the encapsulation complexes with the mechanically locked architectures is not diffusion controlled, the observation of thermodynamically more stable complexes with these architectures compared to their supramolecular analogs requires than the encapsulation complexes of the former should be kinetically more stable than the ones derived of the latter. This explanation is in complete agreements with the results described above for the kinetics of the competitive experiments.

3. Conclusion

We have synthesized a novel bis[2]catenane with a polar interior containing two endohedral hydrogen-bond donor sites and constructed from two calix[4]pyrrole scaffolds. The previous knowledge developed in our group in relation to the synthesis of this type of mechanically locked architectures was very useful in the preparation of the new vessel. The bis[2]catenane **4** obtained encloses an increased volume respect to the previous calix[4]arene – calix[4]pyrrole bis[2]catenane (Chapter 4). The initial results obtained in encapsulation experiments demonstrate that, as we expected, the bis[2]catenane **4** is able to encapsulate bis-*N*-oxides, mono-*N*-oxides and metallocenes. This means that bis[2]catenane **4** presents the same binding behavior than the supramolecular capsules calix[4]pyrrole – calix[4]pyrrole analogs. The possibilities of this new molecular architecture are not exploited already, but we can predict that the bis[2]catenane **4** possesses an enhanced binding ability with respect to the supramolecular capsules based on calix[4]pyrroles, and it also provides a more thermodynamically robust system. One of the potential applications of bis[2]catenane **4** consists in its use as a molecular reactor vessel.

4. Experimental section

4.1. General information and instrumentation

Unless stated otherwise, all preparations were carried out under argon inert atmosphere and using standard techniques. All the reagents were obtained from commercial suppliers and used without further purification. Pyrrol was distilled under vacuum and freshly used. Anhydrous solvents were obtained from a solvent purification system SPS-800 from MBRAUN. HPLC grade quality solvents were obtained commercially and used without further purification. IR measurements were carried out on a Bruker Optics FTIR Alpha spectrometer equipped with a deuterated triglycine sulfate (DTGS) detector. Melting points were performed on a Mettler Toledo MP70 melting point system. Routine ^{1}H and ^{13}C NMR spectra were recorded with a Bruker Avance 400 (400 MHz) and Bruker Avance 500 (500 MHz) spectrometers with use of the solvent signals as internal reference. Flash chromatography was performed with Silica gel Scharlab60 and with Aluminium oxide 60, active basic, particle size 0.063-0.20 mm from Merck. High performance liquid chromatography analyses were performed on an Agilent 1100 series equipped with a UV-Vis detector.

4.2. Synthesis

4.2.1. Synthetic procedure for the bis[2]catenane 4

Tetraurea bisloop calix[4]pyrrole **2**[13] (163 mg, 0.098 mmol), tetraurea calix[4]pyrrole **1**[7,9] (168 mg, 0.098 mmol) and trimethylamino *N*-oxide **3** (7.3 mg, 0.098 mmol) where dissolved in dry CH_2Cl_2 (100 mL) to obtain a reaction mixture with a 1 mM concentration. The formation of the pseudo-rotaxane was checked before the addition of the catalyst. The resulting solution was degassed with argon during 30 minutes and then a solution of the Grubbs catalyst (57.3 mg, 0.068 mmol) in dry CH_2Cl_2 was added via cannula. The resulting purple reaction mixture was left stirring at room temperature for 3 hours under an argon flow. The metathesis reaction was monitored by ^{1}H NMR spectroscopy. Then, triethylamine (4 mL) was added and the solvents evaporated. The dark solid residue was purified by column chromatography (CH_2Cl_2/MeOH 98/2). The resulting grey solid was hydrogenated in dry THF (20 mL) with platinum dioxide (22.2 mg, 0.098 mmol) under hydrogen at atmospheric pressure. The reduction was monitored by ^{1}H NMR. The reaction mixture was filtered through celite, the solvent evaporated to yield a grey solid which was purified by column chromatography (CH_2Cl_2/CH_3CN 9/5).

Yield 30%. IR υ_{max} (cm^{-1}): 3370 (NH stretching), 1670 (C=O stretching); ^{1}H-NMR (DMSO, 300 MHz, 25ºC) δ (ppm) 9.5 (br s, 8H, NH), 8.6 (br s, 8H, NH), 8.5 (br s, 8H, NH), 7.3 (m, 24H), 7.1 (m, 16H), 6.9 (m, 16H), 6.5 (m, 8H), 4.2 (t, 16H). m. p.: T = 76-97ºC. In the absence of suitable guest able to fill the inner cavity of **4**, the ^{1}H NMR spectra affords broad and not well resolved proton signals. MS (MALDI^{+}) $[M+H]^{+}$ calculated for **4**: 3332.8; $[M+H]^{+}$ observed: 3332.4.

4.3. Inclusion studies

4.3.1. Binding experiments

Individual encapsulation experiments were performed by adding 1 equivalent of the ditopic guests or 2 equivalents of the monotopic guests from a stock chloroform-*d* solution to an NMR tube containing a 1 mM solution of the bis[2]catenane **4** also in chloroform-*d*. Five to ten minutes after the addition, the resulting solution was analyzed using ^{1}H NMR spectroscopy.

4.3.2. Pairwise competitive encapsulation experiments

Competitive experiments were carried out by adding 1 equivalent of the competing guest from a stock chloroform-*d* solution to an NMR tube containing a preformed capsular assembly of the guest to be displaced. The resulting solution was analyzed using ^{1}H NMR spectroscopy at different times ranging from minutes to several days.

References and notes

[1] Wasserman, E. *J. Am. Chem. Soc.* **1960**, *82*, 4433-4434.

[2] Chambron, J. C.; Sauvage, J. P. *New J. Chem.* **2013**, *37*, 49-57.

[3] Mullen, K. M.; Beer, P. D. *Chem. Soc. Rev.* **2009**, *38*, 1701-1713.

[4] Spence, G. T.; Beer, P. D. *Acc. Chem. Res.* **2013**, *46*, 571-586.

[5] Ashton, P. R.; Goodnow, T. T.; Kaifer, A. E.; Reddington, M. V.; Slawin, A. M. Z.; Spencer, N.; Stoddart, J. F.; Vicent, C.; Williams, D. J. *Angew. Chem., Int. Ed. Engl.* **1989**, *28*, 1396-1399.

[6] Fujita, M. *Acc. Chem. Res.* **1999**, *32*, 53-61.

[7] Chas, M.; Ballester, P. *Chem. Sci.* **2012**, *3*, 186-191.

[8] Synthesis described in Experimental Section of Chapter 2.

[9] Ballester, P.; Gil-Ramirez, G. *Proc. Natl. Acad. Sci.* **2009**, *106*, 10455-10459.

[10] Bogdan, A.; Vysotsky, M. O.; Ikai, T.; Okamoto, Y.; Bohmer, V. *Chem.-Eur. J.* **2004**, *10*, 3324-3330.

[11] Gil-Ramirez, G.; Chas, M.; Ballester, P. *J Am Chem Soc* **2010**, *132*, 2520-+.

[12] Bis(cyclopentadienyl) dicarboxylic acid cobalt(III) hexafluorophosphate was deprotonated with two equivalents of 1,8-Diazabicyclo[5.4.0]undec-7-ene (DBU).

[13] Synthesis described in Experimental Section of Chapter 2.

UNIVERSITAT ROVIRA I VIRGILI
REVERSIBLE MOLECULAR ENCAPSULATION IN SELF-ASSEMBLED AND MECHANICALLY LOCKED CONTAINERS WITH POLAR INTERIOR
Monica Espelt Ripoll
DL: T 1103-2014

UNIVERSITAT ROVIRA I VIRGILI
REVERSIBLE MOLECULAR ENCAPSULATION IN SELF-ASSEMBLED AND MECHANICALLY LOCKED CONTAINERS WITH POLAR INTERIOR
Monica Espelt Ripoll
DL: T 1103-2014

UNIVERSITAT ROVIRA I VIRGILI
REVERSIBLE MOLECULAR ENCAPSULATION IN SELF-ASSEMBLED AND MECHANICALLY LOCKED CONTAINERS WITH POLAR INTERIOR
Monica Espelt Ripoll
DL: T 1103-2014

UNIVERSITAT ROVIRA I VIRGILI
REVERSIBLE MOLECULAR ENCAPSULATION IN SELF-ASSEMBLED AND MECHANICALLY LOCKED CONTAINERS WITH POLAR INTERIOR
Monica Espelt Ripoll
DL: T 1103-2014